



DOC.20040922.0008

QA: QA

MDL-NBS-HS-000002 REV 03

September 2004

Seepage Model for PA Including Drift Collapse

**NOTICE OF OPEN CHANGE DOCUMENTS - THIS DOCUMENT IS
IMPACTED BY THE LISTED CHANGE DOCUMENT AND CANNOT BE USED
WITHOUT IT.**

1) ACN-001, DATED 12/01/2005

Prepared for:
U.S. Department of Energy
Office of Civilian Radioactive Waste Management
Office of Repository Development
1551 Hillshire Drive
Las Vegas, Nevada 89134-6321

Prepared by:
Bechtel SAIC Company, LLC
1180 Town Center Drive
Las Vegas, Nevada 89144

Under Contract Number
DE-AC28-01RW12101

DISCLAIMER

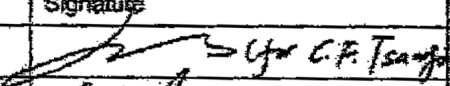
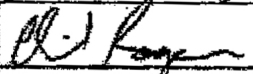
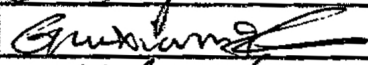
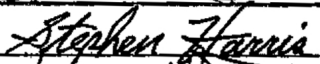
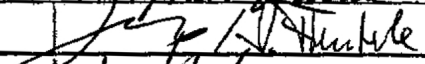
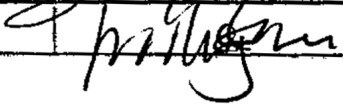
This report was prepared as an account of work sponsored by an agency of the United States Government. Neither the United States Government nor any agency thereof, nor any of their employees, nor any of their contractors, subcontractors or their employees, makes any warranty, express or implied, or assumes any legal liability or responsibility for the accuracy, completeness, or any third party's use or the results of such use of any information, apparatus, product, or process disclosed, or represents that its use would not infringe privately owned rights. Reference herein to any specific commercial product, process, or service by trade name, trademark, manufacturer, or otherwise, does not necessarily constitute or imply its endorsement, recommendation, or favoring by the United States Government or any agency thereof or its contractors or subcontractors. The views and opinions of authors expressed herein do not necessarily state or reflect those of the United States Government or any agency thereof.

QA: QA

Seepage Model for PA Including Drift Collapse

MDL-NBS-HS-000002 REV 03

September 2004

| | | | | |
|---|------------------------------|--|----------------------------------|---------------------|
| OCRWM | | MODEL SIGNATURE PAGE/CHANGE HISTORY | | Page iii |
| | | | | 1. Total Pages: 140 |
| 2. Type of Mathematical Model | | | | |
| <input checked="" type="checkbox"/> Process Model <input type="checkbox"/> Abstraction Model <input type="checkbox"/> System Model | | | | |
| Describe Intended Use of Model | | | | |
| <p>The purpose of this model report is to document the predictions and analyses performed using the Seepage Model for Performance Assessment (SMPA) for both the Topopah Spring middle nonlithophysal (Ttpm) and lower lithophysal (Ttpfl) lithostratigraphic units at Yucca Mountain, Nevada. Look-up tables of predicted seepage flow rates into intact and collapsed drifts (along with the associated prediction uncertainties) were generated by performing numerical simulations with the SMPA for many combinations of the three most important seepage-relevant parameters (permeability, capillarity, and local percolation flux). Multiple runs with different realizations of the underlying stochastic permeability field were performed. Select sensitivity analyses were performed to examine input parameters and the impact of partial drift degradation and rock bolts on seepage. A high-resolution percolation model was developed to examine flow focusing effects and to derive a distribution function of flow focusing factors. The intended purpose of the SMPA is to provide results of drift-scale seepage rates for a range of parameters and scenarios in support of the Total System Performance Assessment for License Application (TSPA-LA).</p> | | | | |
| 3. Title | | | | |
| Seepage Model for PA Including Drift Collapse | | | | |
| 4. DI (including Rev. No., if applicable): | | | | |
| MDL-NBS-HS-000002 REV03 | | | | |
| 5. Total Appendices | | | 6. No. of Pages in Each Appendix | |
| 4 | | | A-28, B-6, C-4, D-4 | |
| | Printed Name | Signature | Date | |
| 7. Originator | Chin-Fu Tsang |  | 9/22/04 | |
| 8. Independent Technical Reviewer | Phillip Rogers |  | 9/22/04 | |
| 9. Checker | Geoxing Zhang |  | 9/22/04 | |
| 10. QER | Stephen Harris |  | 9/22/04 | |
| 11. Responsible Manager/Lead | Hui-Hai Liu/Stefan Finsterle |  | 9/22/04 | |
| 12. Responsible Manager | Ming Zhu |  | 9/22/04 | |
| 13. Remarks | | | | |
| Block 7: Additional contributors to this model report are G. Li (all sections), J. Rutqvist (Section 6.7), Q. Zhou (Sections 6.8, 6.9.2, and 7.2) | | | | |
| Change History | | | | |
| 14. Revision No. | | 15. Description of Change | | |
| REV00 | | Initial issue | | |
| REV01 | | Revision to include updated parameter sets from the Seepage Calibration Model (MDL-NBS-HS-000004 REV01, CRWMS M&O 2001 [DIRS 153045]). | | |
| REV02 | | Revision to include updated parameter sets from the Seepage Calibration Model (MDL-NBS-HS-000004 REV02, BSC 2003 [DIRS 162267]). | | |
| REV03 | | Revision to increase transparency in response to the regulatory-focused evaluation performed by the Regulatory Integration Team. Entire model documentation was revised. Side bars are not used because the changes were too extensive to use Step 5.8f(1) per AP-SIH.10Q Revision 02, ICN 07. | | |

INTENTIONALLY LEFT BLANK

CONTENTS

| | Page |
|---|-------------|
| ACRONYMS AND ABBREVIATIONS | xii |
| 1. PURPOSE | 1-1 |
| 2. QUALITY ASSURANCE | 2-1 |
| 3. USE OF SOFTWARE | 3-1 |
| 4. INPUTS | 4-1 |
| 4.1 DIRECT INPUT | 4-1 |
| 4.2 ACCEPTANCE CRITERIA | 4-3 |
| 4.3 CODES, STANDARDS, AND REGULATIONS | 4-7 |
| 5. ASSUMPTIONS | 5-1 |
| 6. MODEL DISCUSSION | 6-1 |
| 6.1 MODEL OBJECTIVES | 6-1 |
| 6.2 SEEPAGE-RELATED PROCESSES | 6-2 |
| 6.2.1 Flow and Seepage Processes Considered | 6-2 |
| 6.2.2 Features, Events, and Processes | 6-3 |
| 6.3 THE SMPA AND SELECTION OF PARAMETER RANGES | 6-4 |
| 6.3.1 Drift Geometry and Grid Design | 6-6 |
| 6.3.2 Fracture Continuum Permeability k_{FC} | 6-8 |
| 6.3.3 Standard Deviation of $\log k_{FC}$ | 6-9 |
| 6.3.4 van Genuchten Parameters | 6-10 |
| 6.3.5 Spatial Correlation Length λ of k_{FC} | 6-10 |
| 6.3.6 Percolation Flux, Q_p | 6-10 |
| 6.3.7 Summary on Parameter Ranges | 6-11 |
| 6.4 IMPACT OF DRIFT DEGRADATION ON SEEPAGE | 6-11 |
| 6.5 EFFECTS OF ROCK BOLTS ON SEEPAGE | 6-13 |
| 6.6 RESULTS | 6-15 |
| 6.6.1 Seepage over (k_{FC} , $1/\alpha$, Q_p) Space | 6-16 |
| 6.6.2 Sensitivity to λ and σ | 6-22 |
| 6.6.3 Results for Degraded-Drift Scenario | 6-23 |
| 6.6.4 Results for the Effect of Rock Bolts | 6-32 |
| 6.7 COMMENT ON LONG-TERM THERMAL-HYDROLOGICAL-CHEMICAL AND THERMAL-HYDROLOGICAL-MECHANICAL EFFECTS ON SEEPAGE | 6-33 |
| 6.8 FLOW FOCUSING | 6-34 |
| 6.8.1 Model Development for Calculating Flow Focusing Factors | 6-35 |
| 6.8.2 Results and Sensitivity Analyses | 6-36 |

CONTENTS (Continued)

| | Page |
|--|-------------|
| 6.9 ALTERNATIVE CONCEPTUAL MODELS AND SENSITIVITY ANALYSIS | 6-41 |
| 6.9.1 Alternative Seepage Prediction Models..... | 6-41 |
| 6.9.2 Alternative Flow Focusing Model..... | 6-42 |
| 7. VALIDATION..... | 7-1 |
| 7.1 CONFIDENCE BUILDING DURING MODEL DEVELOPMENT TO ESTABLISH SCIENTIFIC BASIS AND ACCURACY FOR INTENDED USE..... | 7-1 |
| 7.2 CONFIDENCE BUILDING AFTER MODEL DEVELOPMENT TO SUPPORT THE SCIENTIFIC BASIS OF THE MODEL..... | 7-2 |
| 7.3 VALIDATION OF SEEPAGE MODEL FOR PERFORMANCE ASSESSMENT | 7-2 |
| 7.4 VALIDATION OF FLOW FOCUSING MODEL..... | 7-4 |
| 7.5 PUBLICATION IN PEER REVIEWED JOURNALS..... | 7-5 |
| 7.6 SUMMARY..... | 7- 6 |
| 8. CONCLUSIONS..... | 8-1 |
| 8.1 SUMMARY..... | 8-1 |
| 8.2 LIMITATIONS..... | 8-1 |
| 8.3 RECOMMENDATIONS..... | 8-2 |
| 8.4 HOW THE ACCEPTANCE CRITERIA ARE ADDRESSED..... | 8-2 |
| 8.5 OUTPUT DTNS | 8-7 |
| 9. INPUTS AND REFERENCES..... | 9-1 |
| 9.1 DOCUMENTS CITED..... | 9-1 |
| 9.2 CODES, STANDARDS, REGULATIONS, AND PROCEDURES..... | 9-5 |
| 9.3 SOURCE DATA, LISTED BY DATA TRACKING NUMBER | 9-5 |
| 9.4 OUTPUT DATA, LISTED BY DATA TRACKING NUMBER | 9-6 |
| 9.5 SOFTWARE CODES..... | 9-6 |
| APPENDIX A – LIST OF COMPUTER FILES SUBMITTED WITH THIS MODEL REPORT UNDER OUTPUT DTNS : LB0304SMDCREV2.001; LB0304SMDCREV2.002; LB0304SMDCREV2.003; LB0304SMDCREV2.004; LB0307SEEPDRCL.001; LB0307SEEPDRCL.002; LB0406U0075FCS.001; AND LB0406U0075FCS.002 | A-1 |
| APPENDIX B – DATA REDUCTION STEPS FOR <i>RESPONSESURFACESMPA.DOC</i> | B-1 |
| APPENDIX C – DATA REDUCTION STEPS FOR FIGURES 6-9 TO 6-11 | C-1 |
| APPENDIX D – DATA REDUCTION STEPS FOR FIGURES OF ROCKFALL | D-1 |

FIGURES

| | Page |
|---|-------------|
| 6-1. Model Domain and Mesh Design. The Point Shown at ($z = 0$ and $x = 0$) Indicates the Axis of the Drift..... | 6-7 |
| 6-2. Model to Evaluate Impact of Rock Bolt. Note That the Radius of the Spherical Drift Is Taken to be 5.5 m, Making Its Curvature Equal to That of a Cylindrical Drift with a Radius of 2.75 m. The Rock Bolt Hole Is at the Crown of the Drift with Length of 3 m..... | 6-14 |
| 6-3. Grout Parameter Combinations | 6-15 |
| 6-4. Distribution of Mean (a) and Standard Deviation (b) of Seepage Rate as a Function of Permeability, van Genuchten $1/\alpha$, and Percolation Flux..... | 6-17 |
| 6-5. Trend of the Mean of Seepage Percentage as a Function of Permeability, van Genuchten $1/\alpha$, and Percolation Flux | 6-18 |
| 6-6. The Mean of Seepage Percentage on Vertical Planes of van Genuchten $1/\alpha = 200, 400, 600, 800,$ and $1,000$ Pa Respectively | 6-18 |
| 6-7. The Mean of Seepage Percentage on Vertical Planes of Permeability Field for $\log_{10}(k_{FC} [m^2]) = -14, -13, -12, -11,$ and -10 | 6-19 |
| 6-8. The Mean of Seepage Percentage on Horizontal Planes of Percolation Flux for $Q_p = 1, 10, 50, 200, 400, 600, 800,$ and $1,000$ mm/year..... | 6-19 |
| 6-9. Seepage Percentage as a Function of van Genuchten $1/\alpha$ (P_a), with $\log_{10}(k_{FC} [m^2]) = -12, Q_p = 200$ mm/year..... | 6-20 |
| 6-10. Seepage Percentage as a Function of Percolation Flux, with $\log_{10}(k_{FC} [m^2]) = -12, 1/\alpha = 400$ Pa | 6-21 |
| 6-11. Seepage Percentage as a Function of Mean Permeability, with $Q_p = 200$ mm/year, $1/\alpha = 400$ Pa | 6-21 |
| 6-12. Seepage Percentage as a Function of Correlation Length, with $\log_{10}(k_{FC} [m^2]) = -12, Q_p = 200$ mm/year, $1/\alpha = 600$ Pa..... | 6-22 |
| 6-13. Seepage Percentage as a Function of Standard Deviation σ , with $\log_{10} K_{FC} = -12, Q_p = 200$ mm/year, $1/\alpha = 600$ Pa | 6-23 |
| 6-14. Liquid Saturation (S_{liq}) Distribution for the 75 Percentile Case Profile in Tptpmn Unit (left) and No-Degradation Base Case (right) [$\log_{10}(k_{FC} [m^2]) = -11.86, Q_p = 200$ mm/year, $1/\alpha = 600$ Pa]..... | 6-26 |
| 6-15. Seepage Percentage as a Function of Percolation Flux for the 75 Percentile Case Profile in Tptpmn Unit [$\log_{10}(k_{FC} [m^2]) = -11.86, 1/\alpha = 600$ Pa]. Red Open Squares Are Results for 10 Realizations. The Mean Seepage Percentages Are Shown as Black Open Circles (See Text). For Comparison, the Mean over 10 Realizations for No-Degradation Case (Base Case) Is Shown as Blue Filled Circles | 6-27 |
| 6-16. Liquid Saturation (S_{liq}) Distribution for the Worst-Case Profile in Tptpmn Unit (left) and No-Degradation Base Case (right) [$\log_{10}(k_{FC} [m^2]) = -11.86, Q_p = 200$ mm/year, $1/\alpha = 600$ Pa]..... | 6-28 |

FIGURES (Continued)

| | Page |
|--|-------------|
| 6-17. Seepage Percentage as a Function of Percolation Flux for the Worst-Case Profile Case in Tptpmn Unit [$\log_{10}(k_{FC} [m^2]) = -11.86$, $1/\alpha = 600$ Pa]. Red Open Squares Are the Results for 10 Realizations, with Their Mean Shown as Black Open Circles. For Comparison, the Mean over 10 Realizations for the No-Degradation Case (Base Case) Is Shown as Blue Filled Circles..... | 6-28 |
| 6-18. Mean Seepage Percentage for the Collapsed Drift Scenario as a Function of Capillary-Strength Parameter and Mean Permeability for a Percolation Flux of 5 mm/year..... | 6-30 |
| 6-19. Mean Seepage Percentage for the Collapsed Drift Scenario as a Function of Capillary-Strength Parameter and Mean Permeability for a Percolation Flux of 50 mm/year..... | 6-31 |
| 6-20. Mean Seepage Percentage for the Collapsed Drift Scenario as a Function of Capillary-Strength Parameter and Mean Permeability for a Percolation Flux of 200 mm/year..... | 6-31 |
| 6-21. Mean Seepage Percentage as a Function of Capillary-Strength Parameter and Mean Permeability for a Percolation Flux of 500 mm/year..... | 6-32 |
| 6-22. Seepage Percentage (Expressed in Fraction) Is Shown as a Function of Percolation Flux for Permeability Fields around the Drift after Excavation and Also at 10,000 Years, Accounting for THM Effects..... | 6-34 |
| 6-23. Generated Random Fields of Log Fracture-Permeability Modifier in Three Cases: (a) 1 m Correlation Length, Realization 1 (Field 1); (b) 1 m Correlation Length, Realization 2 (Field 2); and (c) 3 m Correlation Length (Field 3)..... | 6-36 |
| 6-24. Distributions of Flow Focusing Factor within the Two-Dimensional Model Domain, Simulated Using (a) Field 1 and (b) Field 3 of Fracture-Permeability, with 5 mm/year Uniform Infiltration on the Top Boundary..... | 6-37 |
| 6-25. (a) Spatial Variability (0.25 m Horizontal Resolution) and (b) Frequency and Cumulative Frequency of Flow Focusing Factor at the Bottom Boundary for the Base-Case Scenario, as well as Cumulative Frequency Curve for the Entire Model Domain..... | 6-38 |
| 6-26. Generalized Cumulative Frequency Curve of Flow Focusing Factor at the Bottom Boundary (“Fitted”), Data Points from 15 Different Study Cases (Symbols), and the Generalized CFC Obtained by Bodvarsson et al. (2003 [DIRS 163443], Figure 13) (“Previous”)..... | 6-39 |
| 6-27. Sensitivity Analysis of Cumulative Frequency Curve of Flow Focusing Factor on the Bottom Boundary with Respect to (a) Mean Infiltration Rate, (b) Infiltration Distribution along the Top Boundary, and (c) Different Fracture-Permeability Fields..... | 6-40 |
| 6-28. Cumulative Frequency Curves of Flow Focusing Factor, Averaged over 5 m Horizontal Width, on the Bottom Boundary for the 15 Different Study Cases, Obtained for the 2003 Calibrated Fracture Property Set, as well as the Generalized CFCs for a Gridblock Width of 0.25 m..... | 6-43 |

TABLES

| | Page |
|---|-------------|
| 3-1. Qualified Software Programs Used in This Report | 3-1 |
| 3-2. Software Products Exempt from Software Qualification | 3-2 |
| 4-1. Hydrogeologic Input Parameters | 4-1 |
| 4-2. Geometric Parameters Used..... | 4-1 |
| 4-3. Parameters Used in THM Study | 4-2 |
| 4-4. Data and Information Used in This Report for Establishing Parameter Ranges | 4-2 |
| 4-5. Parameter Used in Flow Focusing Study..... | 4-3 |
| 4-6. Project Requirements and Yucca Mountain Review Plan Acceptance Criteria Applicable to This Report..... | 4-3 |
| 6-1. Scientific Notebooks..... | 6-1 |
| 6-2. Included FEPs Addressed in This Report..... | 6-3 |
| 6-3. Ranges of Key Parameters..... | 6-11 |
| 6-4. Results on Seepage Enhancement Factor Due to a Rock Bolt in Drift Ceiling..... | 6-33 |
| 6-5. The 2003 Set of Fracture Properties Used in Alternative Flow Focusing Modeling Study..... | 6-43 |
| 7-1. Comparison between Mean Seepage Percentages of the SMPA (20 Realizations) and the SCM (10 Realizations)..... | 7-4 |
| 8-1. Output DTNs | 8-7 |
| A-1. File Name and Description for Numerical Simulations DTN: LB0304SMDCREV2.001 (All Occurred During 2003) | A-1 |
| A-2. File for Figures and Tables in This Model Report DTN: LB0304SMDCREV2.002..... | A-17 |
| A-3. Files for the Impact of Thermal-Hydrologic-Mechanical Effects on Seepage DTN: LB0304SMDCREV2.003..... | A-17 |
| A-4. Files for Plotting Results of the Impact of Thermal-Hydrologic-Mechanical Effects on Seepage; DTN: LB0304SMDCREV2.004 | A-19 |
| A-5. File Listing for DTN: LB0307SEEPDRCL.001 | A-19 |
| A-6. File Listing for DTN: LB0307SEEPDRCL.002..... | A-20 |
| A-7. File Listing for DTN: LB0406U0075FCS.001 | A-21 |
| A-8. File Listing for DTN: LB0406U0075FCS.002..... | A-26 |
| B-1. Portion of the EXCEL Spreadsheet <i>ResponseSurfaceSMPA.DAT</i> | B-2 |
| C-1. Portion of the EXCEL Spreadsheet <i>fig6-10_1</i> | C-2 |
| C-2. Portion of the EXCEL Spreadsheet <i>fig6-10_2</i> | C-2 |
| D-1. Portion of the EXCEL Spreadsheet <i>fig6-17_1</i> | D-2 |
| D-2. Portion of the EXCEL Spreadsheet <i>fig6-17_2</i> | D-2 |

INTENTIONALLY LEFT BLANK

ACRONYMS AND ABBREVIATIONS

| | |
|----------|---|
| CFC | cumulative frequency curve |
| DFNM | discrete fracture network model |
| DRKBA | Discrete Region Key Block Analysis |
| FEP | feature, event, and process |
| FFF | flow focusing factor |
| LA | license application |
| PA | performance assessment |
| PTn | Paintbrush nonwelded unit |
| QA | quality assurance |
| SCM | seepage calibration model |
| SMPA | seepage model for performance assessment |
| TDMS | Technical Data Management System |
| THC | thermal-hydrological-chemical |
| THM | thermal-hydrological-mechanical |
| Tptpll | lower lithophysal zone of Topopah Spring Tuff |
| Tptpmn | middle nonlithophysal zone of Topopah Spring Tuff |
| TSPA | Total System Performance Assessment |
| TSw | Topopah Spring welded |
| TWP | technical work plan |
| UZ | unsaturated zone |
| UZ Model | unsaturated zone flow and transport model |

INTENTIONALLY LEFT BLANK

1. PURPOSE

The purpose of this report is to document the predictions and analyses performed using the seepage model for performance assessment (SMPA) for both the Topopah Spring middle nonlithophysal (Tptpmn) and lower lithophysal (Tptpll) lithostratigraphic units at Yucca Mountain, Nevada. Look-up tables of seepage flow rates into a drift (and their uncertainty) are generated by performing numerical simulations with the seepage model for many combinations of the three most important seepage-relevant parameters: the fracture permeability, the capillary-strength parameter $1/\alpha$, and the percolation flux. The percolation flux values chosen take into account flow focusing effects, which are evaluated based on a flow-focusing model. Moreover, multiple realizations of the underlying stochastic permeability field are conducted. Selected sensitivity studies are performed, including the effects of an alternative drift geometry representing a partially collapsed drift from an independent drift-degradation analysis (BSC 2004 [DIRS 166107]). The intended purpose of the seepage model is to provide results of drift-scale seepage rates under a series of parameters and scenarios in support of the Total System Performance Assessment for License Application (TSPA-LA). The SMPA is intended for the evaluation of drift-scale seepage rates under the full range of parameter values for three parameters found to be key (fracture permeability, the van Genuchten $1/\alpha$ parameter, and percolation flux) and drift degradation shape scenarios in support of the TSPA-LA during the period of compliance for postclosure performance [*Technical Work Plan for: Performance Assessment Unsaturated Zone* (BSC 2002 [DIRS 160819], Section I-4-2-1)]. The flow-focusing model in the Topopah Spring welded (TSw) unit is intended to provide an estimate of flow focusing factors (FFFs) that (1) bridge the gap between the mountain-scale and drift-scale models, and (2) account for variability in local percolation flux due to stochastic hydrologic properties and flow processes.

The SMPA serves as a link between the seepage calibration model (SCM) (BSC 2004 [DIRS 170034]) and the *Abstraction of Drift Seepage* (BSC 2004 [DIRS 169131]). The SCM evaluates available field data from air-injection and liquid-release tests performed in niches and the Enhanced Characterization of Repository Block Cross-Drift, uses an equivalent fracture continuum model, and calibrates parameter values to reproduce the observed seepage-rate data. The SMPA then adopts the same conceptual framework from the SCM to systematically evaluate seepage into waste emplacement drifts by performing flow simulations with multiple realizations of the permeability field around the drift, using a wide range of values for three parameters that were found to be key in estimating seepage. Sensitivity analyses are performed, in which the three-dimensional flow of water in the fractured host rock and potential seepage into emplacement drifts are simulated for a variety of hydrogeologic conditions. In particular, a disturbed-drift seepage case evaluates the sensitivity of seepage results to the effects of partial drift collapse as well as of ground support using rock bolts. However, the effects of potential igneous disruptive events and enhanced drift degradation resulting from the loss of rock cohesive strength are not included in the present report. They are addressed in *Abstraction of Drift Seepage* (BSC 2004 [DIRS 169131]). The main results from the SMPA are in the form of calculated seepage rates as a function of fracture medium permeability k_{FC} , the van Genuchten $1/\alpha$ parameter, and percolation flux Q_p . The seepage rates are presented as mean values and standard deviations over statistical realizations at each combination of the parameter set. These are then fed into the *Abstraction of Drift Seepage* (BSC 2004 [DIRS 169131]) to eventually be used for the TSPA-LA.

The work scope of this report is based on the technical work plan (TWP) (BSC 2004 [DIRS 169654], Section 2), which includes the following tasks:

- (1) Incorporate model description and results of seepage into collapsed drift, and create output DTN of corresponding look-up tables as well as input and output files.
- (2) Clarify validation methodology; justify applicability of Seepage Calibration Model (SCM) parameters for ambient seepage predictions.
- (3) Respond to CR 2051 (explain non-convergence in simulations).
- (4) Improve transparency and clarity by responding to key RIT evaluation comments (justify use of superseded information exchange drawings; justify data not used; remove future work; remove references to grout).
- (5) Justify the use of historic technical product output within the report per AP-SIII.10Q using information from *Seepage Calibration Model and Testing Data*.
- (6) Remove reference to FEP 2.2.07.21.0A, *Drift shadow forms below repository*.
- (7) Rerun the calculation of flow focusing factors using qualified software and revised model grid.

The work scope of the previous version of this model report was based on the *Technical Work Plan for: Performance Assessment Unsaturated Zone* (BSC 2002 [DIRS 160819]). It is carried out through the following steps:

- (1) Develop the SMPA, which is a process model simulating unsaturated flow and seepage into a segment of a waste emplacement drift.
- (2) Review the parameter sets covering both Ttpmn and Ttpml units developed in the SCM and the percolation flux predictions from the unsaturated zone (UZ) site scale flow and transport model (UZ model) to derive ranges of permeability as well as van Genuchten capillary-strength parameters and percolation fluxes to be examined by the SMPA.
- (3) Design a set of simulations for evaluating drift seepage using a model structure consistent with that of the SCM.
- (4) Perform multiple realizations of the heterogeneous permeability field, and, subsequently, simulate drift seepage using the SMPA.
- (5) Review information from existing drift collapse models presented in report *Drift Degradation Analysis* (BSC 2004 [DIRS 166107]) and develop a representation of the geometry of a partially collapsed drift.
- (6) Perform simulations using the degraded drift profiles.
- (7) Use the SMPA to evaluate the impact of the presence of a rock bolt used for ground support.

- (8) Provide technical basis for features, events, and processes (FEPs) screening concerning certain seepage-related FEPs; see Section 6.2.1.

The primary caveats and limitations on the results from the SMPA are that its basis is limited to the available site data, and upstream models. This includes the drift configuration defined by the current design and analysis, available hydrological properties data from the site, and limitations identified in reports directly supporting this report. Some discussions of these effects on long-term hydrological properties, especially those resulting from irreversible processes, are discussed in Section 6.7. Furthermore, the model is based on, and consistent with, the conceptualization of the SCM; it, therefore, considers the same features and seepage mechanisms.

Note that the purpose of this report is to document the predictions from the SMPA and not to draw conclusions about final performance assessment (PA) predictions. It forms the link between field data, calibrated-model parameters, and the PA effort. Developed results of the SMPA are summarized in the following Output DTNs: LB0304SMDCREV2.001, LB0304SMDCREV2.002, LB0304SMDCREV2.003, LB0304SMDCREV2.004, LB0307SEEPDRCL.001, LB0307SEEPDRCL.002, LB0406U0075FCS.001, and LB0406U0075FCS.002 (see Appendix A).

The technical scope, content, and management of this report are controlled by the TWP (BSC 2004 [DIRS 169654]). There were no deviations from the TWP, except for an editorial correction in one of the acceptance criteria, where the words “Waste Packages” have been replaced by “Engineered Barriers” (Table 4-6, right column).

This report is supported by input from the following analysis and reports:

- *Seepage Calibration Model and Seepage Testing Data* (BSC 2004 [DIRS 170034]): provides conceptual model and seepage-related parameters.
- *Drift Scale THM Model* (BSC 2004 [DIRS 169864]): provides estimates of property changes induced by coupled thermal-hydrologic-mechanical (THM) effects.
- *Drift-Scale THC Seepage Model* (BSC 2004 [DIRS 169856]): provides estimates of property changes induced by coupled thermal-hydrologic-chemical (THC) effects.
- *Analysis of Hydrologic Properties Data* (BSC 2004 [DIRS 170038]): provides hydrogeologic parameters.
- *Calibrated Properties Model* (BSC 2004 [DIRS 169857]): provides hydrogeologic parameters.
- *UZ Flow Models and Submodels* (CRWMS M&O 2000 [DIRS 122797] and BSC 2004 [DIRS 169861]): provides percolation fluxes.

- *Drift Degradation Analysis* (BSC 2004 [DIRS 166107]): provides shapes of degraded and collapsed waste emplacement drifts.
- *Seismic Consequence Abstraction* (BSC 2004 [DIRS 169183]): provides drift collapse scenarios.

In addition to providing seepage rates and seepage-rate uncertainties to the Model Report *Abstraction of Drift Seepage*, this report also provides output and supports the following reports:

- *Screening Analysis for Criticality Features, Events, and Processes for License Application*: provides FEPs screening arguments.
- *Features, Events, and Processes in UZ Flow and Transport*: provides FEPs screening arguments.

2. QUALITY ASSURANCE

Development of this report and the supporting modeling activities are subject to the Yucca Mountain Project's quality assurance (QA) program, as indicated in *Technical Work Plan for: Unsaturated Zone Flow Analysis and Model Report Integration* (BSC 2004 [DIRS 169654], Section 8.1). The model validation activities and acceptance criteria presented in Section 7 follow those of the TWP (BSC 2004 [DIRS 160819], Attachment I, Section I-4-2-1; BSC 2004 [DIRS 169654], Section 2.2.1.4). Approved QA procedures identified in the TWP (BSC 2004 [DIRS 169654], Section 4) have been used to conduct and document the activities described in this report. The TWP also identifies the methods used at Lawrence Berkeley National Laboratory to control the electronic management of data (BSC 2004 [DIRS 169654], Section 8.4) during the modeling and documentation activities.

This report examines certain characteristics of an identified natural barrier classified in the *Q-List* (BSC 2004 [DIRS 168361]) as "Safety Category" because they are important to waste isolation, as defined in AP-2.22Q, *Classification Analyses and Maintenance of the Q-List*. The report contributes to the analysis and modeling data used to support PA. The conclusions of this report do not affect the repository design or engineered features important to safety, as defined in AP-2.22Q.

INTENTIONALLY LEFT BLANK

3. USE OF SOFTWARE

The software programs used in this study are listed in Table 3-1. These are appropriate for the intended application and were used only within the range of validation. They are obtained from Software Configuration Management and they are all run in the versions of operating system and platforms listed in Table 3-1.

Table 3-1. Qualified Software Programs Used in This Report

| Software Name | Version | Software Tracking Number | Platform | Operating System | Reference |
|---------------|-----------------|--------------------------|----------------|------------------|-------------------------|
| iTOUGH2 | 5.0 | 10003-5.0-00 | Sun UltraSparc | SunOS 5.5.1 | LBNL 2002 [DIRS 160106] |
| GSLIB | V1.0SISIMV1.204 | 10397-1.0SISIMV1.204-00 | Sun UltraSparc | SunOS 5.5.1 | LBNL 2000 [DIRS 153100] |
| MoveMesh | 1.0 | 10358-1.0-00 | Sun UltraSparc | SunOS 5.5.1 | LBNL 2000 [DIRS 152824] |
| AddBound | 1.0 | 10357-1.0-00 | Sun UltraSparc | SunOS 5.5.1 | LBNL 2000 [DIRS 152823] |
| Perm2Mesh | 1.0 | 10359-1.0-00 | Sun UltraSparc | SunOS 5.5.1 | LBNL 2000 [DIRS 152826] |
| CutDrift | 1.0 | 10375-1.0-00 | Sun UltraSparc | SunOS 5.5.1 | LBNL 2000 [DIRS 152816] |
| TOUGH2 | 1.4 | 10007-1.4-01 | Sun UltraSparc | SunOS 5.5.1 | LBNL 2000 [DIRS 146496] |
| TOUGH2 | 1.6 | 10007-1.6-01 | PC | Windows 98 | LBNL 2003 [DIRS 161491] |
| EXT | 1.0 | 10047-1.0-00 | Sun UltraSparc | SunOS 5.5.1 | LBNL 1999 [DIRS 134141] |
| CutNiche | 1.3 | 10402-1.3-00 | Sun UltraSparc | SunOS 5.5.1 | LBNL 2000 [DIRS 152828] |

The uses of the software programs are all within their ranges of use described in Section 6.3, and no limitations on output are imposed because of the selected software. Their use in Table 3-1 is documented in Section 6 and in the supporting Scientific Notebooks (Table 6-1). The selection of these softwares is specific to the objectives of this report, including the need of being consistent with the SCM (BSC 2004 [DIRS 170034]). No other software or methods are more suitable. A summary description of the programs and their use is given below.

The program iTOUGH2 V5.0 (LBNL 2002 [DIRS 160106]) has—among other features—the capability to perform extensive parameter sensitivity analyses based on the TOUGH2 simulator (BSC 2002 [DIRS 161067], Section 1.2). The program is used in this report for predicting seepage rates and for the flow focusing study of Section 6.8.

The GSLIB V1.0SISIM1.204 (LBNL 2000 [DIRS 153100]) generates three-dimensional, spatially correlated random fields by means of sequential indicator simulations. It is used in this report to generate spatially correlated fields of log-permeability modifiers. The TOUGH2 V1.4 (LBNL 2000 [DIRS 146496]) is used for a fine-grid analysis of the rock bolt problem.

The program TOUGH2 V1.6 (LBNL 2003 [DIRS 161491]) is used to evaluate the effect of permeability changes due to coupled THM processes near a drift.

The following utility programs support the generation of computational meshes. The software program MoveMesh V1.0 (LBNL 2000 [DIRS 152824]) adds a constant to the coordinates of a mesh file translating the coordinate system. This allows the relabeling of a subdomain of the mesh file to be used for detailed calculations. The software program AddBound V1.0

(LBNL 2000 [DIRS 152823]) adds boundary elements to a mesh file. The software program Perm2Mesh V1.0 (LBNL 2000 [DIRS 152826]) maps a field of log-permeability modifiers onto a mesh file. The software program CutDrift V1.0 (LBNL 2000 [DIRS 152816]) cuts a drift portion with a diameter of 5.5 m from the mesh domain. The software program CutNiche V1.3 (LBNL 2000 [DIRS 152828]) cuts a rock-fall volume above the drift in the mesh domain. The software program EXT V1.0 (LBNL 1999 [DIRS 134141]) generates three-dimensional Tecplot formatted data from iTOUGH2 output files. Table 3-2 summarizes the commercial, off-the-shelf software used in support of this report. These software products are exempt from software qualification.

Table 3-2. Software Products Exempt from Software Qualification

| Software Name | Version | Platform Information | Use |
|----------------------|------------------------------|---|---|
| MS EXCEL | 2000 (9.0.3821 SR-1) | PC, Windows 98 PC, Windows 2000 Professional | Data reduction, computation, graphical representation of output in all figures in Section 6.6, and in Table 7-1. Details given in Appendices B–D. |
| Tecplot | 8.0-0-6, 9.0-0-9 and 9.0-3-0 | PC, Windows 98 PC, Windows 2000 Professional | Technical three-dimensional figures (Figures 6-1, 6-4 to 6-8, 6-14, 6-16, 6-18, and 6-20) |

4. INPUTS

4.1 DIRECT INPUT

This report presents calculated potential seepage rates over ranges of parameter values. The PA abstraction and evaluation will be presented in a separate report in which probability weighting factors will be discussed for parameter values and scenarios that are appropriate to the repository horizon at Yucca Mountain (see BSC 2004 [DIRS 169131]). Hence, for this report, while some data are used as direct input to model calculations, other data are used mainly to establish the limits of the parameter ranges to be used. Also, information on rockfall scenarios is taken to design special cases to study their potential impact on the seepage results. Tables 4-1 through 4-3 and Table 4-5 present direct-input data, and Table 4-4 presents data used to establish parameter ranges and scenarios used in the current report. These data are also considered to be direct-input data. Discussions of parameter ranges, scenarios, and uncertainties are given in Section 6. No unqualified project data are qualified under this report.

First, the hydrologic parameters used as direct input are the van Genuchten parameter m , residual liquid saturation S_{lr} in the fracture continuum, and saturated saturation S_{ls} . These values and their sources are given in Table 4-1.

Table 4-1. Hydrogeologic Input Parameters

| Description | Input Source | Value | Units |
|---|----------------------------------|-------|-----------------|
| Fracture Properties for Tptpmn Unit, tsw34 | | | |
| van Genuchten Parameter, m | LB0208UZDSCPMI.002 [DIRS 161243] | 0.633 | [dimensionless] |
| Residual Liquid Saturation, S_{lr} | LB0208UZDSCPMI.002 [DIRS 161243] | 0.01 | [dimensionless] |
| Saturated Saturation S_{ls} | LB0208UZDSCPMI.002 [DIRS 161243] | 1.0 | [dimensionless] |
| Fracture Properties for Tptpll Unit, tsw35 | | | |
| van Genuchten Parameter, m | LB0208UZDSCPMI.002 [DIRS 161243] | 0.633 | [dimensionless] |
| Residual Liquid Saturation, S_{lr} | LB0208UZDSCPMI.002 [DIRS 161243] | 0.01 | [dimensionless] |
| Saturated Saturation S_{ls} | LB0208UZDSCPMI.002 [DIRS 161243] | 1.0 | [dimensionless] |

Note that the parameter values for Tptpmn and Tptpll are the same. Geometric parameters used in the present report are given in Table 4-2.

Table 4-2. Geometric Parameters Used

| Description | Input Source | Value | Units |
|---|--|-------|--------|
| Emplacement Drift Diameter | 800-IED-MGRO-00201-000-00B (BSC 2004 [DIRS 168489]) | 5.5 | meters |
| Waste Package Length (average over 44-BWR, 24-BWR, 12-PWR, and 21-PWR packages) | 800-IED-WISO-00205-000-00C (BSC 2004 [DIRS 167758]) | 5.1 | meters |

In Section 6.7, a sensitivity study of the THM effect on seepage is conducted. Input data required for this study are listed in Table 4-3.

Table 4-3. Parameters Used in THM Study

| Description | Input Source | Value/Results |
|-------------------------------------|--|---|
| van Genuchten Parameter, $1/\alpha$ | LB0302SCMREV02.002 [DIRS 162273] | 604.3 Pa |
| Fracture Permeability Field | LB0306DRSCLTHM.001 [DIRS 169733], File <i>tmn1_10ky.out</i> | Figures 6.5.1-1, 6.5.4-3 (d), and 6.5.4-4 (d) of BSC 2004 (DIRS 169864) |

Information and data used in this report for establishing parameter ranges are given in Table 4-4. The appropriateness of the data is discussed in Section 6.3.

Table 4-4. Data and Information Used in This Report for Establishing Parameter Ranges

| Description | Input Source | Comments |
|---|---|---|
| Results from Seepage Calibration Model: K_{FC} , $1/\alpha$ | DTN: LB0302SCMREV02.002 [DIRS 162273] | Statistics of postexcavation air permeabilities and calibrated $1/\alpha$ parameter for niches and systematic testing boreholes in both Ttpmn and Ttpll units. |
| Air-Permeability Data: K_{FC} | DTN: LB0012AIRKTEST.001 [DIRS 154586] | Pre-excavation air-permeability data from Niche 1620 in the Ttpll unit (also referred to as Niche 5). |
| | DTN: LB980901233124.101 [DIRS 136593] | Pre-excavation air-permeability data from Niches 3107 (Niche 3) and 4788 (Niche 4) in the Ttpmn unit. |
| | DTN: LB0011AIRKTEST.001 [DIRS 153155] | Pre-excavation air-permeability data from Niche 3650 (Niche 2) and 3566 (Niche 1) in the Ttpmn unit. |
| | DTN: LB0205REVUZPRP.001 [DIRS 159525] | Air permeability analysis. |
| Flow Field Simulations for Infiltration Scenarios: Q_p | DTN: LB0302PTNTSW9I.001 [DIRS 162277] | Present-day, monsoon, and glacial transition low-, median-, and high-infiltration flow fields from unsaturated zone model. Fluxes are given at the PTn/TSw interface. |
| Degraded Drift Profiles | DTN: MO0306MWDDPPDR.000 [DIRS 164736] | Degraded drift profiles for Ttpmn and Ttpll units. |
| Collapsed Drift Diameter | BSC (2004 [DIRS 166107], Figures 6-112, 6-113, 6-114, 6-115, 6-116, 6-128, 6-154, S-46) | Simulated drift geometry after postclosure seismic event |

PTn=Paintbrush nonwelded unit; Ttpll=lower lithophysal zone of Topopah Spring Tuff; Ttpmn=middle nonlithophysal zone of Topopah Spring Tuff; TSw= Topopah Spring welded unit

Fracture hydrologic properties used for the flow focusing study discussed in Section 6.8 are listed in Table 4-5.

Table 4-5. Parameter Used in Flow Focusing Study

| Model Layer | Permeability | van Genuchten Parameters | | Porosity | Residual Saturation |
|-------------|--------------|--------------------------|----------------------|----------|---------------------|
| | | K_F (m^2) | α_F (1/Pa) | | |
| TSw31 | 3.21E-11 | 2.49E-4 | 0.566 | 5.5E-3 | 0.01 |
| TSw32 | 3.56E-11 | 1.27E-3 | 0.608 | 9.5E-3 | 0.01 |
| TSw33 | 3.86E-11 | 1.46E-3 | 0.608 | 6.6E-3 | 0.01 |
| TSw34 | 1.70E-11 | 5.16E-4 | 0.608 | 1.0E-2 | 0.01 |
| TSw35 | 4.51E-11 | 7.39E-4 | 0.611 | 1.2E-2 | 0.01 |

Source: DTN: LB991121233129.001 [DIRS 147328].

NOTE: The superceded parameters of DTN: LB991121233129.001 [DIRS 147328] (which is a qualified product output from a previous version of model report *UZ Flow Model and Submodels*) are suitable for their intended use within this report. These parameter values have been used in previous analyses of unsaturated flow for the same units and are considered pertinent to the property of interest. As shown in Figure 6-28 and Section 6.9.2 of this report, the superceded parameter set gives more conservative results corresponding to a large degree of flow focusing [compared with the superceding values (Table 6-5)]. The discussion of the use of flow focusing calculation is presented in BSC 2004 [DIRS 169131]. The parameter values were superceded because the numerical grid for the UZ flow model was modified and a new model calibration methodology was employed.

4.2 ACCEPTANCE CRITERIA

The general requirements to be satisfied by the TSPA-LA are stated in 10 CFR 63 [DIRS 156605], Section 63.114. Technical requirements to be satisfied by the TSPA-LA are identified in the *Yucca Mountain Project Requirements Document* (Canori and Leitner 2003 [DIRS 166275]). The acceptance criteria that will be used by the U.S. Nuclear Regulatory Commission to determine whether the technical requirements have been met are identified in *Yucca Mountain Review Plan, Final Report* (YMRP) (NRC 2003 [DIRS 163274]). Pertinent requirements and criteria for this report are summarized in Table 4-6 and described below.

Table 4-6. Project Requirements and Yucca Mountain Review Plan Acceptance Criteria Applicable to This Report

| Requirement Number ^a | Requirement Title ^a | 10 CFR 63 Link | YMRP Acceptance Criteria ^{b,c} |
|---------------------------------|---|-----------------------------|--|
| PRD-002/T-015 | Requirements for Performance Assessment | 10 CFR 63.114 [DIRS 156605] | Criteria 1 to 4 for <i>Quantity and Chemistry of Water Contacting Engineered Barriers and Waste Forms</i> ^b |
| | | | Criteria 1 to 3 for <i>Flow Paths in the Unsaturated Zone</i> ^c |

^a Source: Canori and Leitner 2003 ([DIRS 166275]).

^b Source: NRC 2003 [DIRS 163274], Section 2.2.1.3.3.3.

^c Source: NRC 2003 [DIRS 163274], Section 2.2.1.3.6.3.

YMRP=Yucca Mountain Review Plan

The acceptance criteria identified in Sections 2.2.1.3.3.3 and 2.2.1.3.6.3 of the Yucca Mountain Review Plan (NRC 2003 [DIRS 163274]), as applicable to the present report, are given below. Statements on how these criteria are met are given in Section 8.4. The applicable subsidiary criteria are included below.

Acceptance Criteria from Section 2.2.1.3.3.3, *Quantity and Chemistry of Water Contacting Engineered Barriers and Waste Forms*

- **Acceptance Criterion 1: *System Description and Model Integration Are Adequate.***

- (1) Total system performance assessment adequately incorporates important design features, physical phenomena, and couplings, and uses consistent and appropriate assumptions throughout the quantity and chemistry of water contacting engineered barriers and waste forms abstraction process;
- (2) The abstraction of the quantity and chemistry of water contacting engineered barriers and waste forms uses assumptions, technical bases, data, and models that are appropriate and consistent with other related U.S. Department of Energy abstractions. For example, the assumptions used for the quantity and chemistry of water contacting engineered barriers and waste forms are consistent with the abstractions of “Degradation of Engineered Barriers” (Section 2.2.1.3.1); “Mechanical Disruption of Engineered Barriers (Section 2.2.1.3.2); “Radionuclide Release Rates and Solubility Limits” (Section 2.2.1.3.4); “Climate and Infiltration” (Section 2.2.1.3.5); and “Flow Paths in the Unsaturated Zone (Section 2.2.1.3.6). The descriptions and technical bases provide transparent and traceable support for the abstraction of quantity and chemistry of water contacting engineered barriers and waste forms:
- (4) Spatial and temporal abstractions appropriately address physical couplings (thermal-hydrologic-mechanical-chemical). For example, the U.S. Department of Energy evaluates the potential for focusing of water flow into drifts, caused by coupled thermal-hydrologic-mechanical-chemical processes;
- (5) Sufficient technical bases and justification are provided for total system performance assessment assumptions and approximations for modeling coupled thermal-hydrologic-mechanical-chemical effects on seepage and flow, the waste package chemical environment, and the chemical environment for radionuclide release. The effects of distribution of flow on the amount of water contacting the engineered barriers and waste forms are consistently addressed, in all relevant abstractions;
- (8) Adequate technical bases are provided, including activities such as independent modeling, laboratory or field data, or sensitivity studies for inclusion of any thermal-hydrologic-mechanical-chemical couplings and features, events, and processes;

- **Acceptance Criterion 2: *Data are Sufficient for Model Justification.***
 - (1) Geological, hydrological, and geochemical values used in the license application are adequately justified. Adequate description of how the data were used, interpreted, and appropriately synthesized into the parameters is provided;
 - (2) Sufficient data were collected on the characteristics of the natural system and engineered materials to establish initial and boundary conditions for conceptual models of thermal-hydrologic-mechanical-chemical coupled processes that affect seepage and flow and the engineered barrier chemical environment;

- **Acceptance Criterion 3: *Data Uncertainty is Characterized and Propagated Through the Model Abstraction.***
 - (1) Models use parameter values, assumed ranges, probability distributions, and bounding assumptions that are technically defensible, reasonably account for uncertainties and variabilities, and do not result in an under-representation of the risk estimate;
 - (4) Adequate representation of uncertainties in the characteristics of the natural system and engineered materials is provided in parameter development for conceptual models, process-level models, and alternative conceptual models. The U.S. Department of Energy may constrain these uncertainties using sensitivity analyses or conservative limits. For example, the U.S. Department of Energy demonstrates how parameters used to describe flow through the engineered barrier system bound the effects of backfill and excavation-induced changes;

- **Acceptance Criterion 4: *Model Uncertainty is Characterized and Propagated Through the Model Abstraction.***
 - (1) Alternative modeling approaches of features, events, and processes are considered and are consistent with available data and current scientific understanding, and the results and limitations are appropriately considered in the abstraction;
 - (2) Alternative modeling approaches are considered and the selected modeling approach is consistent with available data and current scientific understanding. A description that includes a discussion of alternative modeling approaches not considered in the final analysis and the limitations and uncertainties of the chosen model is provided;
 - (3) Consideration of conceptual model uncertainty is consistent with available site characterization data, laboratory experiments, field measurements, natural analog information, and process-level modeling studies; and the treatment of conceptual model uncertainty does not result in an under-representation of the risk estimate;
 - (4) Adequate consideration is given to effects of thermal-hydrologic-mechanical-chemical coupled processes in the assessment of alternative conceptual models.

These effects may include: (i) thermal-hydrologic effects on gas, water, and mineral chemistry; (ii) effects of microbial processes on the engineered barrier chemical environment and the chemical environment for radionuclide release; (iii) changes in water chemistry that may result from the release of corrosion products from the engineered barriers and interactions between engineered materials and ground water; and (iv) changes in boundary conditions (e.g., drift shape and size) and hydrologic properties relating to the response of the geomechanical system to thermal loading;

Acceptance Criteria from Section 2.2.1.3.6.3, *Flow Paths in the Unsaturated Zone*

- **Acceptance Criterion 1: *System Description and Model Integration Are Adequate.***

- (1) Total system performance assessment adequately incorporates, or bounds, important design features, physical phenomena, and couplings, and uses consistent and appropriate assumptions throughout the flow paths in the unsaturated zone abstraction process. Couplings include thermal-hydrologic-mechanical-chemical effects as appropriate;
- (2) The aspects of geology, hydrology, geochemistry, physical phenomena, and couplings that may affect flow paths in the unsaturated zone are adequately considered. Conditions and assumptions in the abstraction of flow paths in the unsaturated zone are readily identified and consistent with the body of data presented in the description;
- (6) Adequate spatial and temporal variability of model parameters and boundary conditions are employed in process-level models to estimate flow paths in the unsaturated zone, percolation flux, and seepage flux.
- (7) Average parameter estimates used in process-level models are representative of the temporal and spatial discretizations considered in the model.

- **Acceptance Criterion 2: *Data Are Sufficient for Model Justification.***

- (1) Hydrological and thermal-hydrological-mechanical-chemical values used in the license application are adequately justified. Adequate descriptions of how the data were used, interpreted, and appropriately synthesized into the parameters are provided;
- (2) The data on the geology, hydrology, and geochemistry of the unsaturated zone are collected using acceptable techniques;
- (5) Sensitivity or uncertainty analyses are performed to assess data sufficiency, and verify the possible need for additional data;

- (6) Accepted and well-documented procedures are used to construct and calibrate the numerical models;
 - (7) Reasonably complete process-level conceptual and mathematical models are used in the analyses. In particular: (I) mathematical models are provided that are consistent with conceptual models and site characteristics; and (ii) the robustness of results from different mathematical models is compared;
- **Acceptance Criterion 3: *Data Uncertainty Is Characterized and Propagated through the Model Abstraction.***
 - (1) Models use parameter values, assumed ranges, provability distributions, and bounding assumptions that are technically defensible, reasonably account for uncertainties and variabilities, and do not result in an under-representation of the risk estimate;
 - (4) The initial conditions, boundary conditions, and computational domain used in sensitivity analyses and/or similar analyses are consistent with available data. Parameter values are consistent with the initial and boundary conditions and the assumptions of the conceptual models for the Yucca Mountain site;
 - (5) Coupled processes are adequately represented;
 - (6) Uncertainties in the characteristics of the natural system and engineered materials are considered.

This work is done consistent with the activities performed as part of the *Technical Work Plan for: Regulatory Integration Evaluation of Analysis and Model Reports Supporting the TSPA-LA* (BSC 2004 [DIRS 169653]) and fulfills a portion of the Phase 2 work identified in that plan. No requirement of the Corrective Action Program has been applied to this particular Model Report.

No boundary condition in this work is established in related process models or interface exchange drawings.

4.3 CODES, STANDARDS, AND REGULATIONS

No codes, standards, or regulations other than those referenced in Section 4.2 apply to this modeling activity.

INTENTIONALLY LEFT BLANK

5. ASSUMPTIONS

Assumption: The rubble material in collapsed drifts is assumed to have a capillary strength (van Genuchten parameter $1/\alpha$) of 100 Pa.

Rationale: The bulk porosity of the rubble material in the drift is much greater than the porosity of intact rock, because it includes large voids between chunks of fragmented rock. The chunks of fragmented rock are expected to have sizes on the order of centimeters to decimeters (BSC 2004 [DIRS 166107], Section 8.1). The voids are similar in size to the chunks of rubble and have almost-zero capillary strength. The resulting capillary strength of the rubble-filled drift is, therefore, much weaker than that of the intact surrounding rock. The value of 100 Pa is, thereby, chosen as a conservative value to represent the effective capillary strength of the rubble-filled drift with an air gap forming at the ceiling. This assumption, which is used in Section 6.6.3, is considered adequate and requires no further confirmation.

Assumption: The effective, seepage-relevant capillary-strength parameter is assumed to be spatially uniform on the drift scale and, thus, not correlate to the small-scale heterogeneous permeability field.

Rationale: The capillary-strength parameter to be estimated by calibration of the model against seepage-rate data is considered an *effective* parameter that includes a number of seepage-relevant features and processes, such as (1) the continuum capillarity of a network of rough-walled fractures, (2) capillary rise within finite fracture segments intersected by the underground opening, (3) small-scale drift-wall roughness (including effects of lithophysal cavities), and (4) capillary adsorption of water along drift wall leading to film flow.

The capillary strength of the fracture system is correlated to the fracture aperture distribution. Similarly, permeability may be correlated to aperture, suggesting that capillarity and permeability are (negatively) correlated. However, given that these parameters describe continuum properties of a fracture network (rather than those of a single fracture), it should be noted that an increase in permeability might be associated with an increase in fracture density (rather than an increase in aperture). An increase in fracture density does not affect capillarity. Consequently, capillarity and permeability are not necessarily correlated.

Items (2) through (4) are features and processes related to capillarity and are, thus, well represented by a capillary-strength parameter; however, they are not related to permeability. Finally, since capillary strength is an effective parameter estimated by inverse modeling for a given conceptual model, its value is appropriate for use in a prediction model that has the same model structure, i.e., that uses the same assumption regarding the uniformity of these parameters.

Given that (1) capillarity and permeability are not necessarily correlated, (2) seepage-relevant features and processes not related to permeability are represented by the capillary-strength parameter, and (3) the effective parameter is estimated and used within a suite of conceptually consistent models, it is appropriate to consider the capillary-strength parameter uniform on the drift scale and not correlated to the small-scale heterogeneous permeability field. This assumption, which is used throughout Sections 6 and 7, does not require further confirmation.

Additional assumptions specific to the model are discussed in Section 6.

INTENTIONALLY LEFT BLANK

6. MODEL DISCUSSION

6.1 MODEL OBJECTIVES

The objectives of the SMPA are to calculate potential drift seepage under long-term, steady-state conditions for a range of percolation-flux values at the depth of the drift as a function of the fracture continuum permeability and van Genuchten $1/\alpha$ parameter. The results are presented as look-up tables of seepage rates and their uncertainties to be used as input to PA. Furthermore, the effects on seepage resulting from excavation-induced drift degradation (i.e., drift collapse) and the presence of rock bolts are also calculated.

This section first discusses the processes and features involved in the SMPA. Then, the geometry used and the ranges of parameters will be described, and the choice of conditions presented and rationalized. Finally, results are given with a discussion of alternative models. Key scientific notebooks (with relevant page numbers) used for modeling activities described in this report are listed in Table 6-1.

Table 6-1. Scientific Notebooks

| LBNL Scientific Notebook Identification Number | Citation | M&O Scientific Notebook Register Identification Number | Page Numbers |
|---|-------------------------|---|---------------------|
| YMP-LBNL-CFT-GL-2 | Wang 2003 [DIRS 162319] | SN-LBNL-SCI-189-V1 | 136–146, 148–151 |
| YMP-LBNL-SAF-3 | Wang 2003 [DIRS 162319] | SN-LBNL-SCI-228-V1 | 38–41, 46–54 |
| YMP-LBNL-SAF-3 | Wang 2004 [DIRS 170511] | SN-LBNL-SCI-228-V1 | 64–83 |
| YMP-LBNL-JR-2 | Wang 2003 [DIRS 162319] | SN-LBNL-SCI-204-V2 | 149–163 |

LBNL=Lawrence Berkeley National Laboratory; M&O=management and operating contractor

According to the TWP (BSC 2004 [DIRS 169654]), this Model Report contains a new discussion of a process model developed to study flow-focusing effects (see Sections 6.8 and 7.4). Also note that the seepage results in the current report (Revision 03) are different from those of Revision 01 (CRWMS M&O 2000 [DIRS 153314]), because the later results made use of information from the revised SCM (BSC 2004 [DIRS 170034], Sections 5 and 6). In addition, the following changes were adopted:

- (1) The SMPA uses the same conceptual framework as in the SCM, with the same level of grid-design refinement. Thus, the SMPA is consistent with the SCM, enabling the SMPA to take full advantage of the SCM, which has been calibrated to account for features not explicitly modeled, such as surface roughness of the drift walls.
- (2) New calibrated parameters from the SCM (DTN: LB0302SCMREV02.002 [DIRS 162273]) are used with other information to guide the selection of parameter ranges.
- (3) Twenty realizations of the heterogeneous permeability fields are used for each case in the main simulations as a function of mean fracture permeability, inverse van Genuchten α parameter, and percolation flux, thus, allowing an estimate of the spread of results from a geostatistical representation of the site. For supplementary sensitivity studies, 10 realizations are used for each case.

6.2 SEEPAGE-RELATED PROCESSES

6.2.1 Flow and Seepage Processes Considered

The SMPA builds on the SCM (BSC 2004 [DIRS 170034]), and is also described in Birkholzer et al. (1999 [DIRS 105170], pp. 358 to 362). The SCM provides the scientific and technical background for this report. The conceptual model is a drift opening in a heterogeneous permeability field representing the fracture continuum, generated with parameters discussed below using the SISIM module of the GSLIB package (LBNL 2000 [DIRS 153100]).

Water that penetrates the ground surface and reaches a depth that is unaffected by evapotranspiration percolates downwards under gravity and capillary forces. The detailed flow paths are determined by the degree of fracturing, fracture geometry, orientation, and connectivity, as well as the hydrogeologic properties of the fractures and the matrix. Depending on these factors, the continuous water phase in the unsaturated fracture network will either disperse or focus along flow paths or channels. Tilted contacts between hydrogeologic units (especially between welded and nonwelded tuffs) may affect the overall flow pattern and lead to a change in the frequency and spacing of flow channels. Flow focusing and dispersion of flow paths also happens *within* a rough-walled fracture, where asperity contacts and locally larger fracture openings lead to small-scale redistribution of water within the fracture. A general discussion of channeling effects under unsaturated flow conditions can be found in Birkholzer and Tsang (1997 [DIRS 119397]). Flow focusing is important for seepage, because seepage depends on the local percolation flux at the approximate scale of the average fracture spacing.

As water approaches a waste emplacement drift (one to several meters from the drift ceiling), conditions change in several ways, all affecting the amount of water that will eventually seep into the opening. The water may first encounter a dryout zone caused by drift ventilation. The dryout zone may also develop as a result of increased temperature, in which case it is referred to as a boiling zone. Under these thermal conditions, the dryout zone may be surrounded by a two-phase zone in which heat-pipe effects determine water, vapor, heat fluxes, and a condensation zone with increased saturation.

In addition, formation properties around the openings are likely to be altered as a result of stress redistribution during drift excavation (see discussion in Section 6.3.2). This alteration leads to local opening or partial closing of fractures and, potentially, the creation of new fractures. Thermal expansion of the rock matrix may also induce changes in apertures (see discussion in Section 6.7). Finally, the local chemical environment, which is altered by evaporation and thermal effects, may lead to dissolution and precipitation of minerals, again affecting porosity, permeability, and capillarity of the fracture system as well as fracture-matrix interaction (see discussion in Section 6.7). All these conditions lead to a flow pattern in the vicinity of a waste emplacement drift different from that in the undisturbed formation under ambient conditions.

Assuming that liquid water reaches the immediate vicinity of the drift wall, where (at least under ambient conditions) a layer of increased saturation is expected to develop as a result of the capillary barrier effect of the drift opening (Philip 1989 [DIRS 152651]), the water is prevented from seeping into the drift because of capillary suction, which retains the wetting fluid in the pore space of the rock. This barrier effect leads to a local saturation build-up in the rock next to

the interface between the geologic formation and the drift. If the permeability as well as the capillarity of the fracture network within this layer is sufficiently high, all or a portion of the water is diverted around the drift under partially saturated conditions. Locally, however, the water potential in the formation may be higher than that in the drift, and then water exits the formation and enters the drift.

6.2.2 Features, Events, and Processes

The FEPs listed in Table 6-2 are addressed in the present report. They are taken from the LA FEP List (DTN: MO0407SEPFEPPLA.000 [DIRS 170760]). The cross-reference for each FEP to the relevant section (or sections) of this report is also given below. The UZ Department's documentation for the FEPs listed in Table 6-2 is compiled from this and other reports, and can be found in the UZ FEPs report as listed in BSC (2004 [DIRS 169654], Table 2.1.5-1).

Table 6-2. Included FEPs Addressed in This Report

| FEP No. | FEP Name | Relevant Sections of This Report |
|--------------|--|--|
| 1.2.02.01.0A | Fractures | Fracture properties are taken from postexcavation air-permeability data and through calibrated seepage-relevant fracture continuum capillary-strength parameter. See Sections 6.3.2–6.3.4. |
| 1.3.01.00.0A | Climate change | The change in percolation flux at the repository level due to climatic change is accounted for by a choice in the range of flux values to cover those changes. See Section 6.3.6 |
| 1.4.01.01.0A | Climate modification increases recharge | The change in percolation flux at the repository level due to climatic change is accounted for by a choice in the range of flux values to cover those changes. See Section 6.3.6. |
| 2.1.08.01.0A | Water influx at the repository | An increase in the unsaturated water flux at the repository affects thermal, hydrological, chemical, and mechanical behavior of the system. Increases in flux could result from climate change, and increasing flux will increase probability of seepage. See Section 6.3.6. |
| 2.1.08.02.0A | Enhanced influx at the repository | The impact of an underground opening on the unsaturated flow field (including dryout from evaporation, capillary barrier effect, and flow diversion around the drift) is captured in the seepage process model by solving the equations governing unsaturated flow in fractured porous media and by specifying appropriate boundary conditions at the drift wall. It leads to reduced (not enhanced) influx. See Sections 6.2.1, 6.3.1, and 6.3.6. |
| 2.2.01.01.0A | Mechanical effects of excavation/ construction in the near field | Excavation effects are taken into account through the use of postexcavation air-permeability data and the estimation of a capillary-strength parameter determined from seepage data that reflect seepage from an excavation-disturbed zone around a drift. See Sections 6.3.2 and 6.4. |

Table 6-2. Included FEPs Addressed in This Report (Continued)

| FEP No. | FEP Name | Relevant Sections of This Report |
|--------------|---|---|
| 2.2.03.01.0A | Stratigraphy | Stratigraphic information is necessary information for the performance assessment. For seepage into drift, the Tptpmn and Tptpll units at the repository level are considered. See Sections 6.3.2–6.3.4. |
| 2.2.03.02.0A | Rock properties of host rock and other units | Location-specific rock properties are taken (1) from UZ Model, (2) from local air-permeability data (including measures of heterogeneity and spatial correlation), and (3) from inverse modeling. Variability is accounted for on various scales. See Sections 4.1, 6.3.2–6.3.4. |
| 2.2.07.02.0A | Unsaturated groundwater flow in the geosphere | Unsaturated flow processes are accounted for in the conceptual and mathematical model. See Section 6.2.1, 2nd and 4th paragraphs, and Section 6.3, 4th paragraph. |
| 2.2.07.04.0A | Focusing of unsaturated flow (fingers, weeps) | Explicitly modeled heterogeneity induces flow focusing. Impact of small-scale flow focusing effects on seepage is included in effective parameters. See Sections 6.2.1, 6.3.3, 6.3.5, and 6.8. |
| 2.2.07.08.0A | Fracture flow in the UZ | Liquid flow through unsaturated fractures is simulated using site-specific fracture properties; explicit inclusion of heterogeneity leads to flow channeling. See Sections 6.3.2–6.3.3 |
| 2.2.07.09.0A | Matrix imbibition in the UZ | Matrix imbibition is considered small under steady seepage conditions and is therefore neglected. See Section 6.3, 5th paragraph. |
| 2.2.07.18.0A | Film flow into the repository | Water entering waste emplacement drifts occurs by a film flow process. This differs from the traditional view of a flow in a capillary network where the wetting phase exclusively occupies capillaries with apertures smaller than some level defined by the capillary pressure. As a result, a film flow process could allow water to enter a waste emplacement drift at nonzero capillary pressure. Dripping into the drifts could also occur through collection of the film flow on the local minima of surface roughness features along the crown of the drift. For seepage evaluation, this effect is implicitly accounted for through calibration of the SCM against field data. See Section 6.3, 4th paragraph. |
| 2.2.07.20.0A | Flow diversion around repository drifts | The impact of an underground opening on the unsaturated flow field (including capillary barrier effect and flow diversion around the drift) is captured in the seepage process model by solving the equations governing unsaturated flow in fractured porous media and by specifying appropriate boundary conditions at the drift wall. See Section 6.2.1, 5th paragraph and also Sections 6.3.2 and 6.7. |

FEP=feature, event, and process; SCM=seepage calibration model; Tptpll=lower lithophysal zone of Topopah Spring Tuff; Tptpmn=middle nonlithophysal zone of Topopah Spring Tuff; UZ=unsaturated zone

6.3 THE SMPA AND SELECTION OF PARAMETER RANGES

Similar to the SCM (BSC 2004 [DIRS 170034]), the continuum approach is used in the SMPA to calculate percolation flux and drift seepage at Yucca Mountain. It is considered appropriate for seepage studies since it is capable of predicting seepage rates for a drift in the fractured formation at Yucca Mountain. Though water flow and seepage from the tuff formation at Yucca Mountain occurs predominantly through the fracture network, it is important to recognize that

flow diversion around the drift opening occurs *within* the fracture plane. As flow within the fracture plane encounters the drift opening, which acts as a capillary barrier, it is diverted around it, as described by Philip et al. (1989 [DIRS 105743]). This process is appropriately captured by a two-dimensional, heterogeneous fracture continuum model even for a single fracture. In-plane flow from multiple fractures can be readily combined into a three-dimensional fracture continuum. The need to engage multiple fractures arises only if the flow path within the fracture plane is insufficient for flow diversion around the drift.

At Yucca Mountain, the formation at the repository horizon has a high fracture density, and these fractures form a well-connected three-dimensional system at all scales. The appropriateness of the continuum approach to simulate flow through fractured rock was studied by Jackson et al. (2000 [DIRS 141523]) using synthetic and actual field data. They concluded that heterogeneous continuum representations of fractured media are self-consistent, i.e., appropriately estimated effective continuum parameters are able to represent the underlying fracture-network characteristics.

Furthermore, Finsterle (2000 [DIRS 151875]) demonstrated that simulating seepage into underground openings excavated from a fractured formation could be performed using a continuum model, provided that the model is calibrated against seepage-relevant data (such as data from liquid-release tests). Synthetically generated data from a model that exhibits discrete flow and seepage behavior were used to calibrate a simplified fracture continuum model. The calibrated continuum model was used to predict average seepage rates into a sufficiently large section of an underground opening under low percolation flux conditions. Thus, the study corresponds to the extrapolation from the calibration runs against high-rate liquid-release tests performed with the SCM to the predictive simulations that are performed by the SMPA. As discussed in Finsterle (2000 [DIRS 151875]), the extrapolated seepage predictions performed with the continuum model were consistent with the synthetically generated data from the discrete fracture model under low percolation conditions. This demonstrates that (1) the calibrated continuum model and discrete fracture model yield consistent estimates of average seepage rates, and (2) that the continuum approach is appropriate for performing seepage predictions even if extrapolated to percolation fluxes that are significantly lower than the injection rates of the liquid-release tests used for model calibration.

Within the continuum approach, relative permeability and capillary pressure are described as continuous functions of effective liquid saturation, following the expressions given by the van Genuchten-Mualem model (van Genuchten 1980 [DIRS 100610], pp. 892 to 893) as implemented in the iTOUGH2 code (BSC 2002 [DIRS 161066], Section 4.3.2). Capillary strength (represented by the $1/\alpha$ parameter) and permeability are not correlated, because the functional relationship describing the potential correlation between permeability and capillary strength is unknown for a fractured medium. A large permeability value may be attributed to larger fracture apertures (which would reduce capillary strength) or to a larger value in fracture density (which would not affect capillary strength). Thus, the capillary-strength parameter $1/\alpha$ is taken to be constant for a given test bed, and its value is to be estimated through calibration. In this, the SMPA has the same formulation as the SCM; the consistent conceptualization in the SMPA and the SCM make this a valid approach. The SMPA provides results on seepage for a wide range of permeability and capillary-strength values. However, the use of the results should center on the SCM calibrated values and explore variations from them. This will avoid a

combination of extreme choices of these two parameters that may represent a nonphysical condition.

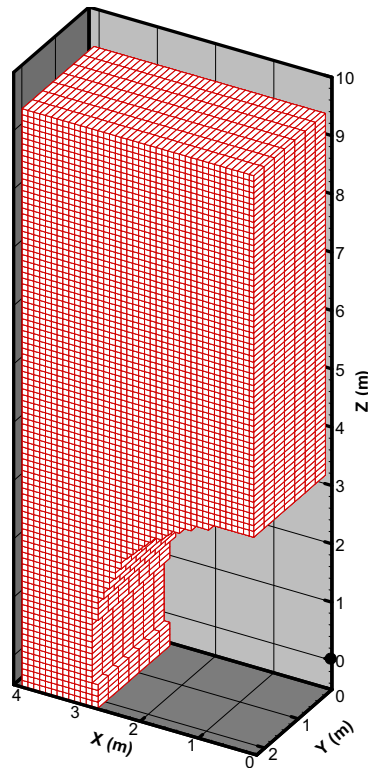
Within the SMPA, the flux exchange between fractures and matrix in a steady-state fracture-matrix system is negligible and does not need to be modeled explicitly in the SMPA. In general, matrix permeability is low, and the potential for imbibition of substantial amounts of water into the matrix is limited because of its relatively low porosity and relatively high initial liquid saturation. In a fracture-matrix system, the transient flow between fracture and matrix is restricted to intermediate times; i.e., they are insignificant (1) for a short-term liquid-release test with insufficient time for matrix imbibition, and (2) for a long-term seepage experiment, in which near-steady late-time data are no longer affected by matrix imbibition. The ability of a single fracture-continuum model to reproduce and predict average seepage from a discrete fracture-matrix system has been demonstrated by Finsterle (2000 [DIRS 151875]) using synthetic data.

Also within the SMPA, the effect of lithophysal cavities on seepage is represented through the use of an effective capillary-strength parameter, without the explicit inclusion of lithophysal cavities into the process model. This approach is considered appropriate for the following reasons: (1) the effect of lithophysal cavities is included by the SCM (BSC 2004 [DIRS 170034], Section 5.7) in the calibration conditioned to data from Tptpl testing; (2) because of capillary effects, flow will be mainly through fractures rather than the cavities; and (3) omitting lithophysal cavities is consistent with the SCM, and consistency between the calibration model (the SCM) and the prediction model (the SMPA) removes the impact of a potential bias.

6.3.1 Drift Geometry and Grid Design

As provided in design drawings 800-IED-MGR0-00201-000-00B (BSC 2004 [DIRS 168489]) and 800-IED-WIS0-00205-000-00C (BSC 2004 [DIRS 167758]) respectively, the drift diameter is 5.5 m and the waste package length is 5.1 m. The three-dimensional calculational domain for this report is chosen to be 10 m high, 4 m wide, and 2.4384 m long, covering the upper left-hand half of the drift with a diameter of 5.5 m (See Figure 6-1). Thus, a vertical plane through the axis of the drift forms the right-hand boundary, and the drift axis is 0.5 m above the lower boundary. The length along the drift axis is chosen to be 8 ft (2.4384 m), which is 8 grid cells of 1 foot (0.3048 m) length. Thus, the calculated seepage will be over an area of half the drift (cut along its axis) and the length of 2.4384 m, which amounts to an area of $(5.5/2) \times 2.4384 = 6.706 \text{ m}^2$. On the other hand, the cross-sectional area of the drift containing one waste package is $5.1 \times 5.5 = 28.05 \text{ m}^2$. Consequently, the seepage rate at steady state calculated in the simulation domain needs to be scaled-up by a factor of $(28.05/6.706 = 4.183)$ to obtain the seepage rate for the full drift per waste package, expressed as m^3 of water per year per waste package ($\text{m}^3/\text{year}/\text{wp}$). Seepage percentage is defined as this seepage rate divided by the product of percolation flux (m/year), the diameter of the drift (5.5 m), and the length of the waste package (5.1 m). This product is the amount of percolation water incident on the footprint of the drift section with one waste package. The calculation of seepage percentage does not require consideration of the scale-up factor of 4.183 if the calculated seepage from this model is divided by the total percolation water incident on the model area of 6.706 m^2 .

The grid cells in the plane normal to the drift axis are 0.1×0.1 m. The limited size of the calculational domain was chosen to allow the use of a fine mesh at the same refinement level as the SCM, and yet contain a reasonable number of grid cells so as not to make the computational time too long. The left-hand boundary is placed at $(4-2.75) = 1.25$ m beyond the left-hand limit of the drift to capture the main flow feature, i.e., flow diversion around the drift (Philip et al. 1989 [DIRS 105743], p. 21, Figure 1). The side boundary conditions are no-flow, and the lower boundary condition is gravity drainage, implemented by setting the capillary pressure gradient to zero across the bottom connections. The upper boundary surface is simulated by an extra grid cell with constant percolation flux connected to all the grid cells in the first row. Flow is, thus, free to move into these cells according to local property parameters. Since all calculations were run to steady state, the initial conditions are not important and are set to zero saturation over the domain.



Output DTN: LB0304SMDCREV2.002.

NOTE: As shown, the lines are drawn through the centers of grid cells and not the sides, so that n lines shown represent n cells and not $(n-1)$ cells.

Figure 6-1. Model Domain and Mesh Design. The Point Shown at $(z = 0$ and $x = 0)$ Indicates the Axis of the Drift

In regards to the no-flow boundary condition on the two planes normal to the drift axis and on the right-hand vertical boundary, for a homogeneous, constant-property medium, these planes are symmetry planes, and a no-flow boundary condition is justified. For a heterogeneous system, the issue is the length of the flow domain versus the spatial correlation length λ . Except for the cases used in a sensitivity study of the spatial correlation length, the spatial correlation length λ is chosen to be 0.3 m (see Section 6.3.5 below). Thus, the length of flow domain in the direction

of the drift axis is 8 times the spatial correlation length, and its width is 13 times the correlation length. Given this setup, no-flow boundaries should not have a significant effect on flow results.

At the drift wall, the nodal distance between the drift surface and the grid cell representing the drift is set to be very small, so that the boundary condition can be applied directly at the drift wall. The length of the last vertical connection between the drift wall and the neighboring gridblocks representing the formation is set equal to 0.05 m to make this model consistent with the SCM (BSC 2004 [DIRS 170034]). The choice of this 0.05 m vertical connection to the drift wall implies a direct gravity-controlled vertical flow with no horizontal diversion over this 0.05 m distance.

Flow calculation was performed using iTOUGH2 V5.0 (LBNL 2002 [DIRS 160106]). The selection of this software is specific to the objectives of this report including the need of being consistent with the SCM (BSC 2004 [DIRS 170034]). Other comparable codes are not used because they are not used in the SCM and the originators are not familiar with them. The selection of parameter ranges and particular cases to be modeled is based on available relevant data and is presented below along with the rationale for the selection. Much information and data are available for the Tptpmn (UZ model layer tsw34, lithostratigraphic unit Tptpmn). However, additional data from the lower lithophysal unit have also been analyzed in the SCM (BSC 2004 [DIRS 170034]); the parameter values for this unit are also covered by the selected range of parameters. The parameters most likely to affect drift seepage are fracture continuum permeability k_{FC} , van Genuchten $1/\alpha$ value, and the percolation flux Q_p . For each combination of these three parameters (i.e., at each grid point in three-dimensional parameter space), seepage model calculations will be made for 20 realizations of the generated heterogeneous permeability field.

Though the choices of parameter ranges for which seepage calculations are performed are based on a review of available relevant data, these data are not directly used as input to the model to produce seepage results, but rather as references to establish parameter ranges.

6.3.2 Fracture Continuum Permeability k_{FC}

For the SMPA, a range of k_{FC} values needs to be established that, when coupled with other parameters, forms a set of cases. Potential seepage rates as a function of percolation flux on top of the simulation domain are then calculated for each case. The k_{FC} range has been selected based on a review of the available site data at Yucca Mountain (see below) and *Abstraction of Drift Seepage* (BSC 2004 [DIRS 169131]). The series of k_{FC} values in terms of $\log_{10}(k_{FC} [\text{m}^2])$ are initially chosen to be from -12.5 to -10.5 , but later expanded to the range from -14 to -10 at steps of 0.25. Data and information leading to the selection of this group of k_{FC} values are described below.

A number of air-permeability measurements have been made in the Tptpmn. BSC (2004 [DIRS 170038]) presents a systematic study of these data, and Table 6-5 of BSC (2004 [DIRS 170038]) indicates that the mean $\log_{10}(k_{FC} [\text{m}^2])$ values for Tptpmn (tsw34) unit without the effect of excavation are about -12.81 to -12.48 . For drift seepage simulations, the postexcavation data are probably more suitable, as they account for stress release due to the excavation, resulting in a change in fracture permeabilities in the rock near the drift wall.

BSC (2004 [DIRS 170034], Section 6.5.2) presents an analysis of postexcavation data and gives the mean $\log_{10}(k_{FC} [m^2])$ for Tptpmn unit as -12.14 to -11.66 (Niches 3107, 3650, and 4788 in the Table (also referred to as Niches 3, 2, and 4 respectively)) $\log_{10}(k_{FC} [m^2])$ with a mean of -11.86 (DTN: LB0302SCMREV02.002 [DIRS 162273]). Thus, there is an increase of about 1.2 to 0.3 in \log_{10} compared with the preexcavation values. BSC (2004 [DIRS 169864]) conducted a coupled THM analysis of rock permeability changes on the drift scale. This analysis shows (BSC 2004 [DIRS 169864], Figure 6.5.1-1) that drift excavation induces a change in vertical permeability, averaged over 1 drift radius above the crown of the drift, of about 1.3 (\log_{10} change of 0.11), and a change in horizontal permeability in the same region of about 10 (\log_{10} change of 1.0). For drift seepage, a larger increase in horizontal permeability and a small increase in vertical permeability near the drift crown will facilitate the flow of water laterally around the drift and, hence, reduce seepage probability. Also, note that the flow diversion effect of the capillary barrier, as presented by the drift, acts in a rock layer very close to the drift wall. The thickness of this rock layer depends on the capillary strength. For a van Genuchten $1/\alpha$ parameter of 600 Pa, this thickness is less than 20 cm. BSC (2004 [DIRS 169864]) shows a horizontal permeability increase of 10 or more extending about 0.5 m into the rock above the crown of the drift. Further discussions on excavation enhanced k_{FC} values are given in Section 6.7 as well as in BSC (2004 [DIRS 169864]).

For the Tptpll unit, there are much less data. They are found from measurements in Niche 1620 (also referred to as Niche 5) and the Borehole SYBT-ECRB-LA#2. Generally the air permeability values are an order of magnitude larger than those of the Tptpmn unit. BSC (2004 [DIRS 170034], Section 6.5.2) presents an analysis of the data and gives the mean $\log_{10}(k_{FC} [m^2])$ from Niche 5 data as -10.95 and from SYBT-ECRB-LA#2 as -10.73 , with an average of -10.84 (DTN: LB0302SCMREV02.002 [DIRS 162273]). These numbers are within the range chosen for the $\log_{10}(k_{FC} [m^2])$ parameter, -14 to -10 .

Note that the range is chosen to bracket the data; however, no effort is taken to ensure it brackets data symmetrically. The choices for the limits of the ranges are influenced by the knowledge that larger values will result in less seepage than lower values. Thus, the range limits are selected to de-emphasize the side of no-seepage and to cover more of the side where seepage may occur. Also, a range was initially chosen from -12.5 to -10.5 , but later was expanded to -14.0 to -10 to allow for the study of the effect of a wider range of permeability values.

6.3.3 Standard Deviation of $\log k_{FC}$

For the three niches (Niches 3, 2, and 4) in the middle nonlithophysal zone, the SCM (BSC 2004 [DIRS 170034], Section 6.5.2) gives values for the standard deviation σ of fracture continuum permeability in log base 10, which vary from 0.72 to 0.84 (DTN: LB0302SCMREV02.002 [DIRS 162273]). For the lower lithophysal unit, the same source gives a log base 10 standard deviation of 0.21 for the Enhanced Characterization of Repository Block test and 1.31 for the niche test (DTN: LB0302SCMREV02.002 [DIRS 162273]).

In a numerical study of seepage from a heterogeneous fracture continuum into a drift, Birkholzer et al. (1999 [DIRS 105170], p. 371, Figure 14) found that drift seepage tracks the probability for finding local ponding in the heterogeneous field and, further, that the ponding probability is smaller for smaller permeability standard deviations (Birkholzer et al. 1999 [DIRS 105170],

p. 375, Figure 17). Hence, less seepage is expected for smaller σ values. Based on this, this report uses $\sigma = 1.0$ as the base case. Then, a sensitive study on seepage rates will be made for $\sigma = 0.5$ and 2.0 , and the results compared with those of $\sigma = 1$. It is shown (Section 6.6.2) that while the calculated seepage percentage is sensitive to σ for low σ values, it does not vary much for $\sigma = 1$ to 2 . Since these results show that lower seepage occurs for lower σ values, we have not tried to consider $\sigma = 0.21$ indicated by one data set, but have used $\sigma = 1.0$ as the base case.

6.3.4 van Genuchten Parameters

It is a conclusion from the SCM analysis (BSC 2004 [DIRS 170034], Section 6.6.3.1) that seepage is not sensitive to the van Genuchten parameter n . Therefore, in this analysis, n is not varied, but set to 2.55 (corresponding to the van Genuchten parameter $m = (n-1)/n = 0.6$). This is consistent with the approach in the SCM (BSC 2004 [DIRS 170034]). This value of m is used for both the Tptpmn and Tptpll units. Table 4-1 gives m values to be 0.633 ; the 5 percent change of this parameter will have negligible impact on simulation results of this report.

The $1/\alpha$ values calibrated with the SCM mean of 582 Pa in the lower lithophysal unit, with a standard deviation of 105 Pa (DTN: LB0302SCMREV02.002 [DIRS 162273]). For the middle nonlithophysal zone, the SCM gives a calibrated mean for $(1/\alpha)$ as 604 Pa, with the standard deviation of 131 Pa (DTN: LB0302SCMREV02.002 [DIRS 162273]). Initially we chose a range from 300 to 1000 Pa, but later we expanded the lower limit down to 100 since seepage is larger for lower $1/\alpha$. In this report, ten $1/\alpha$ values, namely 100 to 1000 Pa at 100 Pa steps, are chosen to cover well beyond these numbers.

6.3.5 Spatial Correlation Length λ of k_{FC}

In general, this is a difficult parameter to determine in the field. As indicated by the SCM (BSC 2004 [DIRS 170034], Section 6.6.2.1), the analysis of air-injection tests shows that “the permeability is random without a noticeable or significant spatial correlation” for the middle nonlithophysal zone. These results can be taken to indicate a spatially uncorrelated structure. Thus, for the main set of calculations covered in this report, the spatial correlation length is set equal to grid size in the direction of the drift axis (i.e., 0.3 m), also applying this to the plane normal of the drift axis. Since grid size in the normal plane is 0.1 m, this correlation length is equal to 3 grid lengths in this plane.

Since λ is not an easily determined parameter in situ, cases with alternative λ values were calculated to investigate its sensitivity. Cases with $\lambda = 1$ m and $\lambda = 2$ m are calculated, and ten realizations of the heterogeneous field are considered for each of these cases.

6.3.6 Percolation Flux, Q_p

For the SMPA calculations, 15 values of Q_p are used, ranging from 1 to $1,000$ mm/year; or, more specifically, $Q_p = 1, 5, 10, 20, 50$, and then 100 to 1000 mm/year at 100 mm/year steps. The range is chosen to cover various estimates of percolation fluxes. Wu et al. (1999 [DIRS 117161], p. 210) calculated the percolation flux expected at the repository level based on a three-dimensional UZ of Yucca Mountain. They obtained an average fracture flow of 4 to 5 mm/year at the repository level under present climate conditions. Ritcey and Wu (1999

[DIRS 139174], p. 262) found that under a climate scenario simulating the most recent glacial period, the percolation flux at the repository level ranges from 0 to 120 mm/year, with the peak of the probability distribution to be around 20 mm/year. More recent predictions of percolation flux have been summarized in DTN: LB0302PTNTSW9I.001 [DIRS 162277]. These are reviewed to arrive at the parameter range used in this report. In particular, the upper limit of Q_p is chosen to accommodate potential flow focusing in the geologic layers above the drift (see discussion in Sections 6.8 and 6.9.2) and to safely bracket a large uncertainty range. Note that the choice of the range is not made to bracket known data symmetrically because we expect low seepage for low Q_p values and, thus, the focus is on the upper bound of the Q_p range.

6.3.7 Summary on Parameter Ranges

Table 6-3 shows parameter values for simulations in two categories. The first category is an extensive set of systematic calculations conducted for all combinations of $\log_{10}(k_{FC} [m^2])$, $1/\alpha$ (Pa) and Q_p (mm/year) values shown in the table. Standard deviations of seepage rates over 20 realizations of the heterogeneous permeability field are also evaluated. Second, sensitivity studies are made for σ of $\log_{10}(k_{FC} [m^2])$ and λ , with 10 realizations for each case.

Table 6-3. Ranges of Key Parameters

| Parameter | Values |
|---|--|
| Systematic Simulations (20 Realizations) | |
| $\log_{10} k_{FC} (m^2)$ | -14.0 to -10.0 (steps of 0.25) |
| $1/\alpha$ (Pa) | 100 to 1000 (steps of 100) |
| Q_p (mm/year) | 1, 5, 10, 20, 50, 100 to 1000 (steps of 100) |
| Sensitivity Studies: $\log_{10} k_{FC} (m^2) = -12$; $1/\alpha = 600$ Pa; $Q_p = 200$ mm/year (10 realizations) | |
| σ of $\log_{10} k_{FC} (m^2)$ | 0.5, 1.0 (Base Case), 2.0 |
| λ (m) | 0.3 (Base Case), 1.0, 2.0 |

Output DTN: LB0304SMDCREV2.001.

6.4 IMPACT OF DRIFT DEGRADATION ON SEEPAGE

Because of excavation, stress is redistributed and fractures are generally expected to dilate near the crown of the drift. Such fracture dilation depends on the orientation of the fracture set and generally occurs within one drift radius (Brekke et al. 1999 [DIRS 119404], Figures E-5, E-11 and E-13). An increase in fracture aperture generally causes an increase in fracture permeability and a decrease in $1/\alpha$ value. The measured increase in permeability from the preexcavation to the postexcavation values (Wang et al. 1999 [DIRS 106146], p. 328; DTN: LB0011AIRKTEST.001 [DIRS 153155]) is a result of this effect. Calibrated parameters from calculations based on in situ postexcavation data, as presented by the SCM (BSC 2004 [DIRS 170034]), have already taken this into account. This means that the rock properties already represent the total effect of the near-field disturbed zone and the far field, and no additional calculations are necessary.

The possibility exists that new fractures may be formed due to the excavation or subcritical crack growth over time. In general, an increase in k_{FC} could result from either an increase in the number of fractures or an increase in apertures. It is only in the latter case that $1/\alpha$ will decrease.

The part of increase in k_{FC} resulting from the creation of new fractures will be accompanied by no decrease in $1/\alpha$ values. This scenario is, however, not studied because it would lead to less seepage.

Over time, extended rock failure may also occur at the roof of the drift. Kaiser (Brekke et al. 1999 [DIRS 119404], pp. D-11, D-12) estimated the failure at the roof to be 0.1–1 m in depth, and 0.4–1.2 m in depth if seismic effects were included. Generally, Kaiser expected stress-induced failure at the drift crown to occur over a distance of 1/2 drift radius, i.e., approximately 1.375 m.

More detailed studies of drift profile shape changes as a possible result of thermal stress and joint cohesion degradation, as well as seismic motion, have been evaluated in different revisions of the report *Drift Degradation Analysis* [Revision 01: BSC (2001 [DIRS 156304]); Revision 02: BSC 2003 [DIRS 162711]; Revision 03: BSC (2004 [DIRS 166107])]. Revision 01 of the report *Drift Degradation Analysis* (BSC 2001 [DIRS 156304]) was based on a Discrete Region Key Block Analysis (DRKBA) to determine the potential rockfall at the repository horizon. Key blocks are critical rock blocks in the surrounding rock mass of an excavation which are removable and oriented in an unsafe manner so that they are likely to fall into the opening unless ground support is provided. It was later recognized, however, that the DRKBA analysis presented in BSC (2001 [DIRS 156304]) needed improvement in several areas. For example, the DRKBA could not be used to explicitly apply dynamic loads (due to seismic ground motion) or thermal stresses. The DRKBA analysis, which determines structurally controlled key-block failure, was also not applicable to lithophysal units, where failure is essentially stress controlled (BSC 2004 [DIRS 166107], Section 1.1). Therefore, an improved degradation analysis was presented in later revisions of the report *Drift Degradation Analysis*. In particular, BSC (2004 [DIRS 166107]) used additional approaches such as two-dimensional and three-dimensional discontinuum analysis with explicit representation of seismic and thermal loads, and time-dependent degradation in rock strength. Results from this revised analysis indicate more drastic drift shape changes in the lithophysal rocks compared to the earlier revision, including cases with partial or complete collapse of drifts. Lithophysal (Tptpl and Tptpl units) and nonlithophysal (Tptpmn and Tptpln units) repository units were evaluated with different simulation approaches because the two types of rocks have fundamentally different failure modes under dynamic loading. The nonlithophysal units comprise hard, strong, jointed rock masses, while the lithophysal rocks are relatively deformable with lower compressive strength (BSC 2004 [DIRS 166107]).

The calculated drift profiles and the fall-off rock volumes are used to construct three-dimensional cases for seepage calculations. This was done first by taking away rock grid cells in a plane normal to drift axis to approximately match the profile in that plane, and then by taking away grid cells along the drift axis to approximately match the fall-off rock volume. Note that since the calculational domain represents only part of the drift (Section 6.3.1 and Figure 6.1), if the rock-fall is across the model boundary, the rock-fall volume is factored accordingly. Now, on these discretized drift profiles, seepage was calculated with 10 realizations of the heterogeneous permeability field. Calculations were carried out for both the Tptpmn and the Tptpl units. No-degradation results with the same parameter values were also calculated for comparison to study the impact of drift degradation on seepage.

6.5 EFFECTS OF ROCK BOLTS ON SEEPAGE

Using rock bolts is one proposed method of ground support for emplacement drifts at Yucca Mountain (BSC 2001 [DIRS 155187]). Rock bolts are steel rods emplaced into a borehole drilled normal to the drift wall. Typically they are 3 m long (BSC 2001 [DIRS 155187], Section 6.5.1.2.2) with a diameter of 1 inch (0.0254 m) and an open annulus thickness of ¼ inch (0.00635 m) (BSC 2001 [DIRS 155187], Table 4-10). Rock bolts pose a concern with respect to seepage because they provide a direct flow conduit to the drift wall and may increase the likelihood of seepage into drifts.

A refined model has been prepared that includes a range of properties for the formation as well as a range of percolation rates. Figure 6-2 shows a sketch of the model. The model uses a two-dimensional, radially symmetric grid with a vertical symmetry axis generated using the software TOUGH2 V1.4 (LBNL 2000 [DIRS 146496]). Grid size is 10 cm, with finer discretization (down to 0.1 mm) in the region between the rock bolt and the surrounding rock. Because this is a radially symmetric grid, the drift opening, created using the routines MoveMesh V1.0 (LBNL 2000 [DIRS 152824]) and CutNiche V1.3 (LBNL 2000 [DIRS 152828]), is spherical instead of cylindrical. Knight et al. (1989 [DIRS 154293], p. 37) find that seepage exclusion from a cylindrical cavity is similar to that of a spherical cavity of twice the radius. This is explained by relating the seepage exclusion potential of an opening to the total curvature of the boundary of the opening. For a cylindrical cavity, the radius of curvature is infinite along the axis of the cylinder and finite perpendicular to the axis. For a spherical cavity, the radius of curvature is finite and equal in any direction. As a result, to have the same curvature, the equivalent radius of the spherical “drift” in the model is twice that of the design drift radius. This relationship is used in the calculation of seepage enhancement owing to the presence of rock bolts.

The main reason that the “equivalent spherical drift” is used to simulate the seepage result of a rock bolt in the ceiling of a cylindrical drift is that the latter is intrinsically a three-dimensional problem, which, in a scoping evaluation, has been found to be very computationally intensive. The “equivalent spherical model,” being radially symmetric, has allowed us to use very fine mesh and many more elements in the simulation.

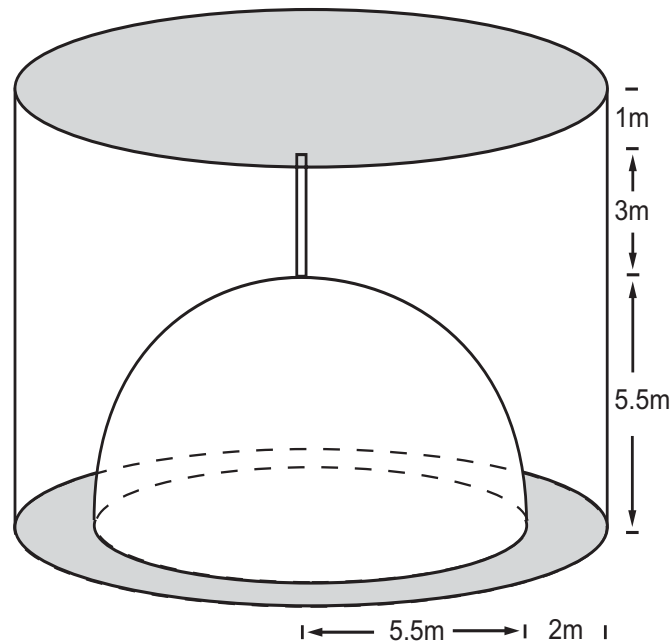


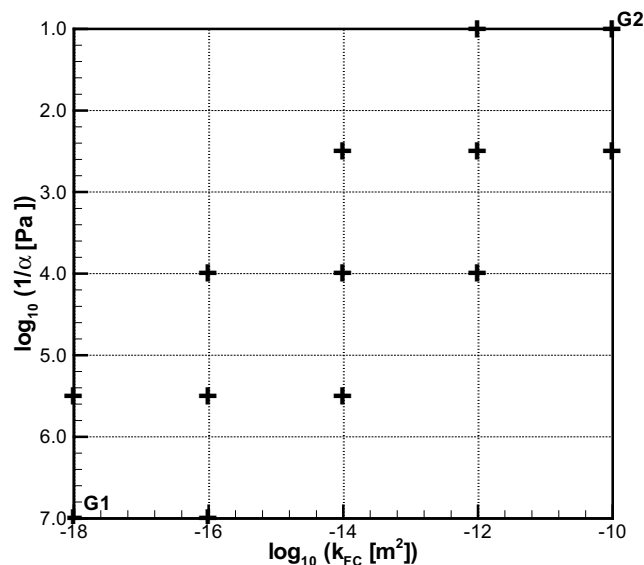
Figure 6-2. Model to Evaluate Impact of Rock Bolt. Note That the Radius of the Spherical Drift Is Taken to be 5.5 m, Making Its Curvature Equal to That of a Cylindrical Drift with a Radius of 2.75 m. The Rock Bolt Hole Is at the Crown of the Drift with Length of 3 m

As a base case, seepage into the opening without any rock bolts is modeled. Since this is treated as a sensitivity study, the low and high percolation rates of 5 and 500 mm/year are applied uniformly to the upper model boundary. A constant zero capillary pressure is specified at the drift wall boundary, a gravity-drainage condition at the lower boundary (assigned in the grid using the routine AddBound V1.0 (LBNL 2000 [DIRS 152823])), and a no-flow condition on the lateral boundary. The fracture-continuum permeability is chosen to be the mean of data for the Tptpmn unit, i.e., $\log(k_{FC} [m^2]) = -11.86$ (see Section 6.4). The mean value for the Tptpll unit is -10.84 (see Section 6.4), which would allow for more water diversion and less seepage, and, therefore, is not calculated. The $1/\alpha$ values of 200 and 400 Pa are used for the rock. An additional calculation with $1/\alpha = 589$ Pa [a number in between the calibrated values for Tptpmn and Tptpll units (BSC 2004 [DIRS 170034], Table 8-1)] was also made, as part of the sensitivity analysis.

To investigate the impact of a rock bolt on seepage, only the case of a rock bolt borehole extending vertically upward from the crown of the drift is modeled. If there is negligible effect, then this case is sufficient to resolve the question of impact on seepage caused by the presence of the rock bolt borehole. If the borehole is not vertical, flow will be in contact with the neighboring rock, with the probability of flowing into the rock matrix. Thus, vertical borehole represents a condition for higher seepage. Three slightly different grids are prepared to explore diversion capacity away from the rock bolt borehole: (1) Case 1 allows flow between the rock bolt borehole and the surrounding rock along the entire length of the rock bolt hole, (2) Case 2 prevents flow between the rock bolt borehole and the surrounding rock for 10 cm above the crown of the drift, and (3) Case 3 restricts flow between the rock bolt borehole and the

surrounding rock for 50 cm above the crown of the drift. Cases 2 and 3 represent scenarios in which the first feature capable of carrying flow away from the rock bolt borehole is found 10 cm or 50 cm, respectively, into the borehole. A 1-inch (0.0254 m) radius rock bolt borehole with a ½-inch (0.0127 m) radius rock bolt and a ½-inch (0.0127 m) annular thickness is modeled. The modeled annular thickness is chosen to be larger than the design value (BSC 2001 [DIRS 155187], Table 4-10), so as to reduce demand for numerical computation. This configuration results in a conservative model, because the modeled bolt hole has less potential as a capillary barrier to exclude in-flow, but a larger surface area to intercept flow, thus, allowing a greater opportunity to conduct flow to the drift wall.

Though the current design for rock bolt calls for no grout around the rock bolt, as a sensitivity study we have assumed a grouted rock bolt with grout properties ranging from no-grout, open rock bolt condition to a slightly degraded grout condition. Figure 6-3 shows the combinations of grout properties evaluated. In particular, shown in the lower left is a combination (case G1), where the grout permeability equals 10^{-18} m^2 and $1/\alpha$ equals 10^7 Pa , corresponding to a slightly degraded grout. The upper right shows a combination (case G2) in which the grout permeability equals 10^{-10} m^2 and $1/\alpha$ equals 10 Pa , which essentially corresponds to an open rock bolt borehole. Thus, the G2 case particularly corresponds to the case of an open, mechanically anchored bolt design.



Output DTN: LB0304SMDCREV2.002.

Figure 6-3. Grout Parameter Combinations

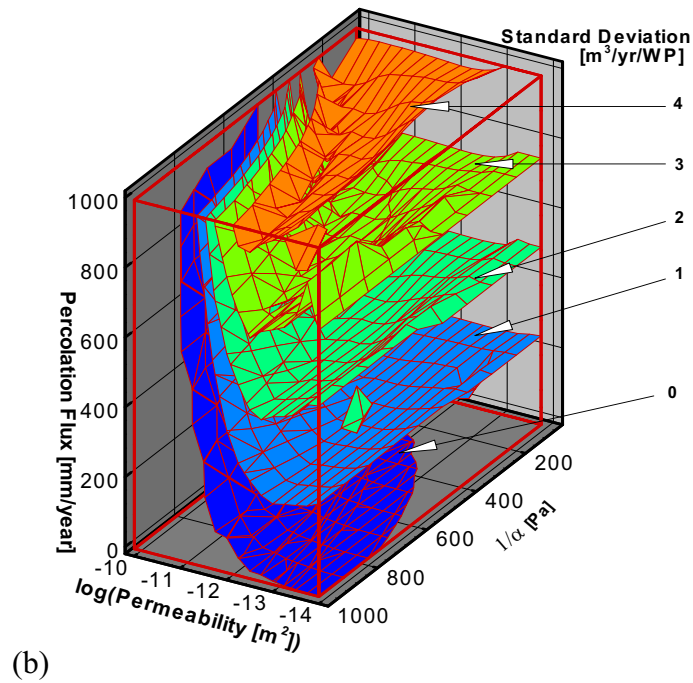
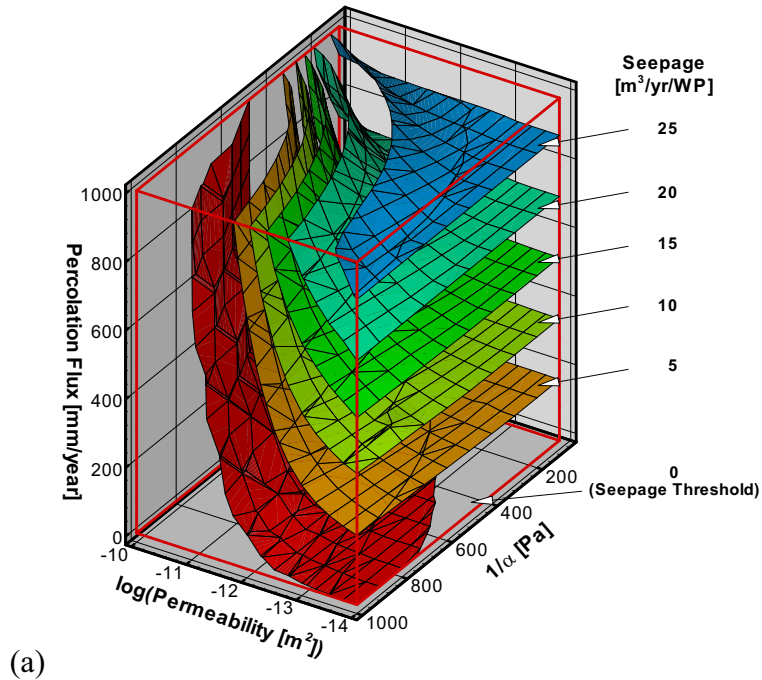
6.6 RESULTS

Seepage percentage is defined as the ratio of the seepage rate into a drift section to the percolation rate applied to the top of the model over the projected cross-sectional area of that drift section.

6.6.1 Seepage over (k_{FC} , $1/\alpha$, Q_p) Space

This section provides insights into the range of results obtained from the model by describing and discussing seepage calculated over the expected range of seepage-relevant parameters. For each parameter combination, 20 realizations of the underlying permeability field are evaluated to assess the impact of small-scale heterogeneity on seepage. Figure 6-4a gives the calculated seepage rate in cubic meters of water per year per waste package ($m^3/year/wp$) as contour sheets in a space spanned by $\log_{10}(k_{FC} [m^2])$, $1/\alpha$ (Pa), and Q_p . This corresponds to simulated total seepage rates into a drift of 5.5 m diameter and 5.1 m length (length of a waste canister). The contour sheets are labeled by the seepage rates averaged over 20 realizations of the generated heterogeneous permeability field. Thus, to get the seepage rate for a particular set of $\log_{10}k_{FC}$, $1/\alpha$ and Q_p values, the corresponding point in three-dimensional space is located and interpolated between sheets of seepage rate values. In practice, detailed seepage results for all 20 realizations are provided for every combination of k_{FC} , $1/\alpha$, and Q_p values in the form of look-up tables, and are submitted to the Technical Data Management System (TDMS) (Output DTN: LB0304SMDCREV2.002). As one would expect, seepage is large for large Q_p , small $1/\alpha$, and small k_{FC} values. The threshold for seepage is shown as the lowest sheet (red) in the figure. The parameter space below this sheet represents cases in which no seepage is expected to occur.

Figure 6-4b shows the standard deviation over the 20 seepage results for the 20 realizations. The arrangement is the same as in Figure 6-4a. Thus, for any particular set of $\log_{10}k_{FC}$, $1/\alpha$, and Q_p parameter values, one can go to Figure 6-4a to obtain the mean seepage rate and then go to Figure 6-4b to obtain the corresponding standard deviation over 20 realizations for this particular case. The results indicate that the geostatistical spread is larger for large seepage rates, and it is generally less than approximately 20 percent.

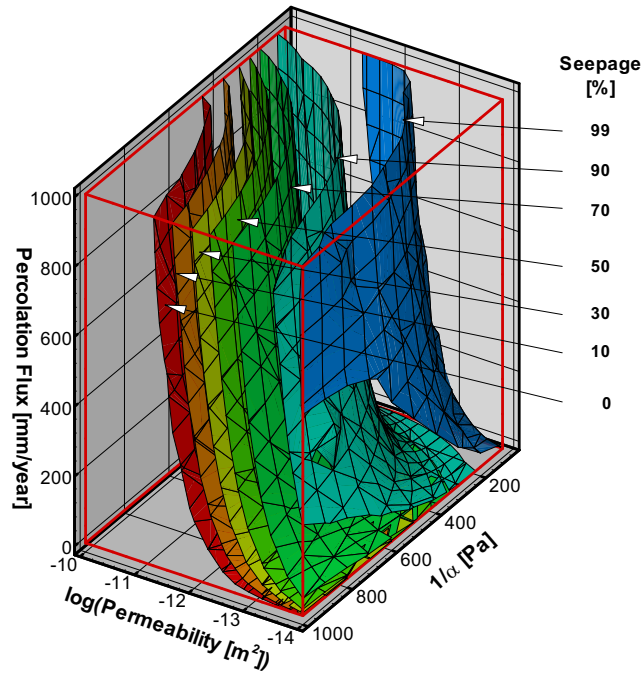


Output DTN: LB0304SMDCREV2.002.

Figure 6-4. Distribution of Mean (a) and Standard Deviation (b) of Seepage Rate as a Function of Permeability, van Genuchten $1/\alpha$, and Percolation Flux

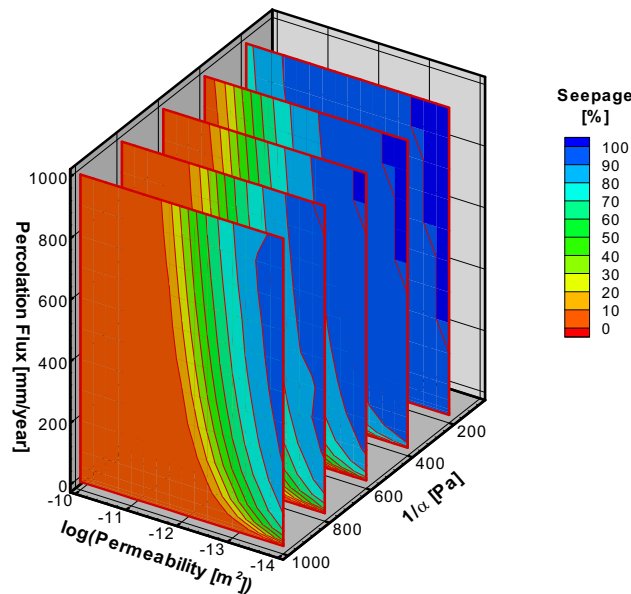
Figure 6-5 corresponds to Figure 6-4a, but expresses the results as seepage percentage. Figures 6-6 to 6-8 show the same results as Figure 6-5, but as mean seepage-percentage contours on planes representing two out of the three parameters. Thus, the calculated results from

Figure 6-5 are projected on planes corresponding to constant values for one of the three parameters.



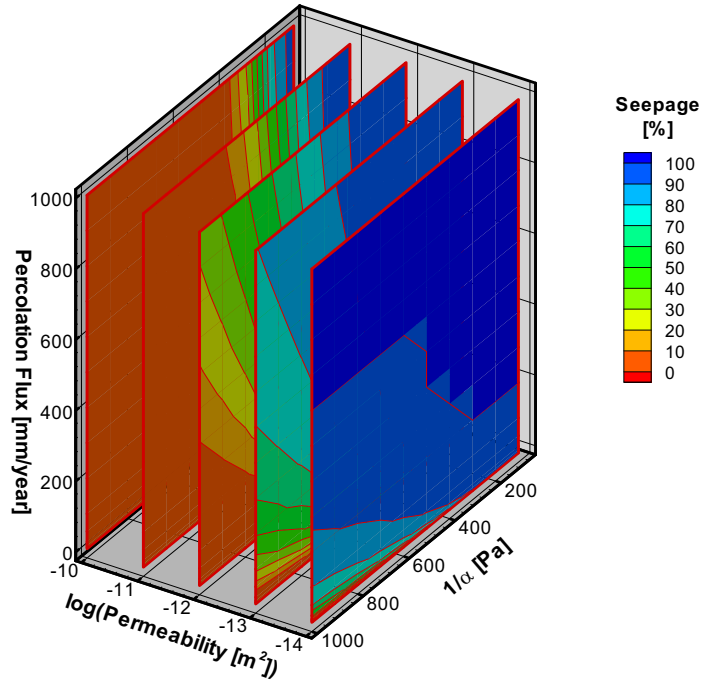
Output DTN: LB0304SMDCREV2.002.

Figure 6-5. Trend of the Mean of Seepage Percentage as a Function of Permeability, van Genuchten $1/\alpha$, and Percolation Flux



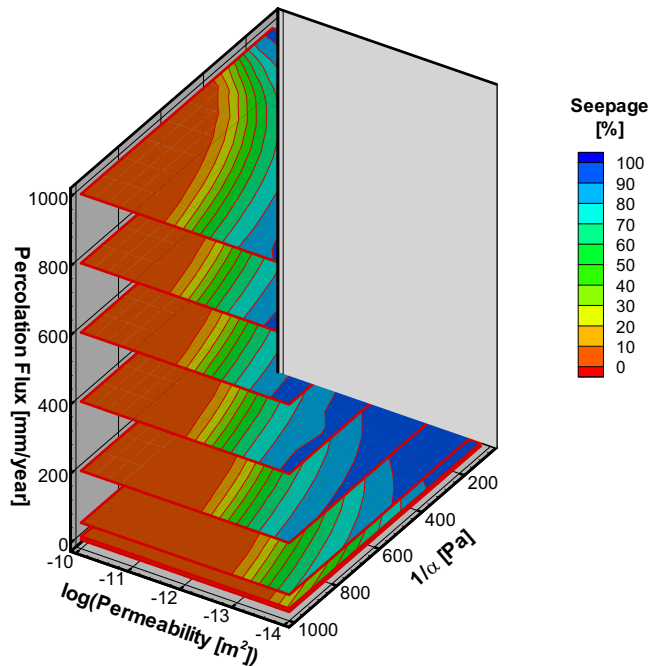
Output DTN: LB0304SMDCREV2.002.

Figure 6-6. The Mean of Seepage Percentage on Vertical Planes of van Genuchten $1/\alpha = 200, 400, 600, 800,$ and $1,000$ Pa Respectively



Output DTN: LB0304SMDCREV2.002.

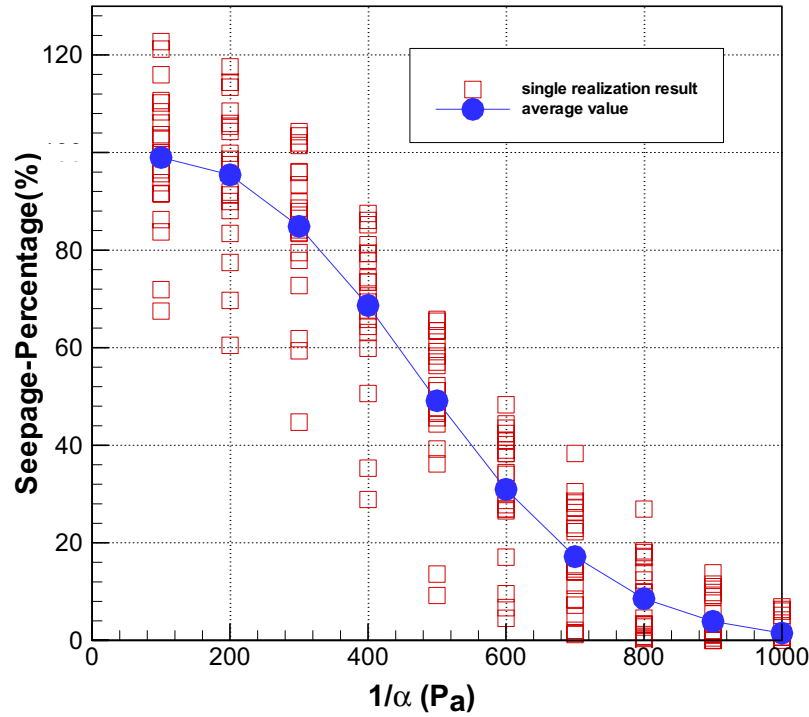
Figure 6-7. The Mean of Seepage Percentage on Vertical Planes of Permeability Field for $\log_{10}(k_{FC} [m^2]) = -14, -13, -12, -11, \text{ and } -10$



Output DTN: LB0304SMDCREV2.002.

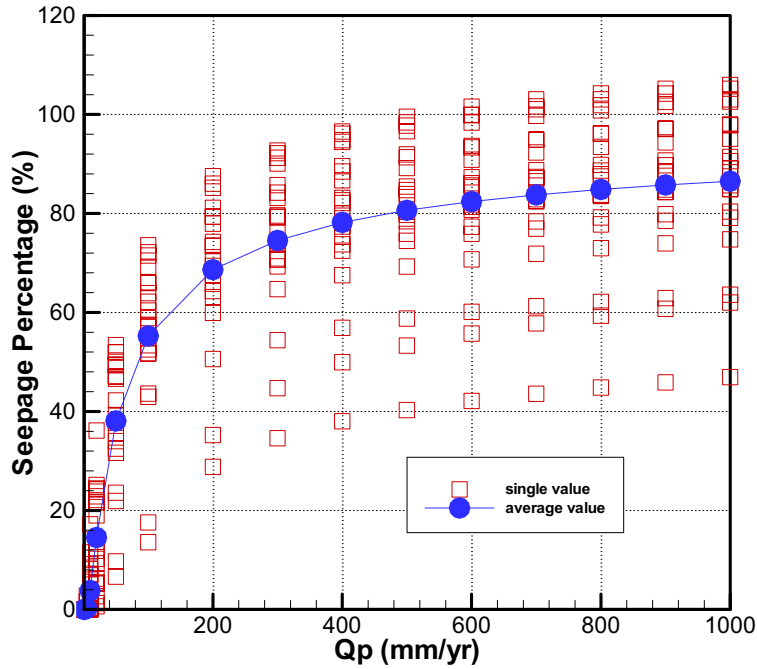
Figure 6-8. The Mean of Seepage Percentage on Horizontal Planes of Percolation Flux for $Q_p = 1, 10, 50, 200, 400, 600, 800, \text{ and } 1,000$ mm/year

As a further illustration, dependence of seepage percentage on one of the three parameters (k_{FC} , $1/\alpha$, Q_p), one at a time, is shown in Figures 6-9 to 6-11. In these figures, the red squares show results for each of the 20 realizations, and the blue-filled dots give their average values. These figures demonstrate clearly that seepage decreases with larger k_{FC} and $1/\alpha$, and increases with larger Q_p . They also show that the geostatistical spread is quite large.



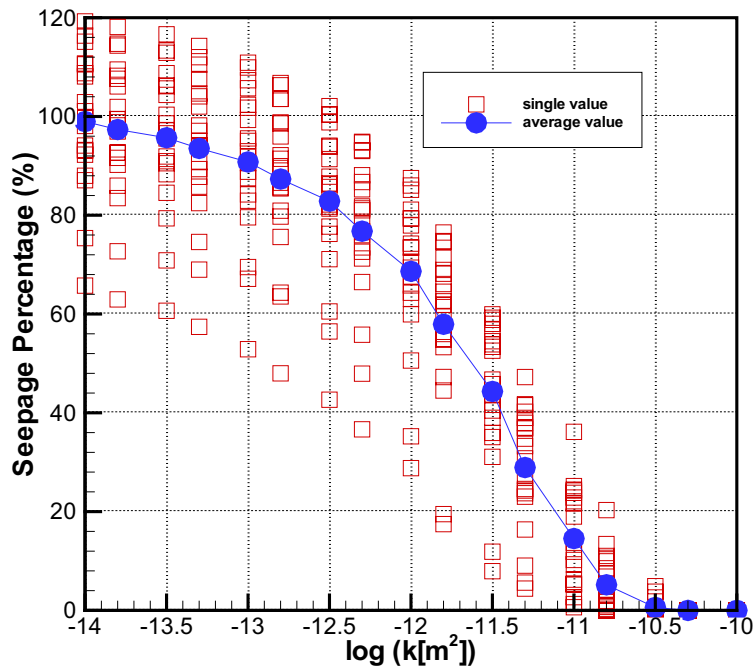
Output DTN: LB0304SMDCREV2.002.

Figure 6-9. Seepage Percentage as a Function of van Genuchten $1/\alpha$ (Pa), with $\log_{10}(k_{FC} [m^2]) = -12$, $Q_p = 200$ mm/year



Output DTN: LB0304SMDCREV2.002.

Figure 6-10. Seepage Percentage as a Function of Percolation Flux, with $\log_{10}(k_{FC} [m^2]) = -12$, $1/\alpha = 400$ Pa



Output DTN: LB0304SMDCREV2.002.

Figure 6-11. Seepage Percentage as a Function of Mean Permeability, with $Q_p = 200$ mm/year, $1/\alpha = 400$ Pa

6.6.2 Sensitivity to λ and σ

The sensitivities of calculated seepage rates to λ and σ values are calculated for one particular combination of parameters, namely:

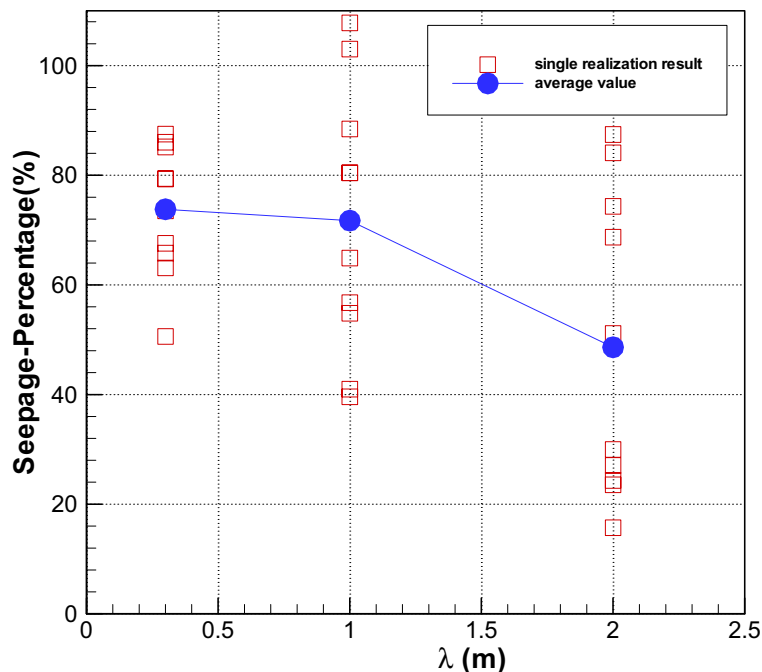
$$\begin{aligned}\log_{10}(k_{FC} [\text{m}^2]) &= -12.0 \\ 1/\alpha &= 600 \text{ Pa} \\ Q_p &= 200 \text{ mm/year}\end{aligned}$$

This parameter set is chosen to be approximately at the center of the $[\log_{10}(k_{FC}), 1/\alpha]$ plane, having a large, but not extremely large, percolation flux rate of 200 mm/year. In this analysis, 10 realizations of the heterogeneous permeability fields are used.

Figure 6-12 shows the results for three values of λ :

$$\begin{aligned}\lambda &= 0.3 \text{ m (base case)} \\ \lambda &= 1 \text{ m} \\ \lambda &= 2 \text{ m}\end{aligned}$$

The red squares give results for individual realizations, and the blue-filled circles give the average over the 10 realizations for each case. As can be expected, the geostatistical spread results from the multiple realizations increases with λ .



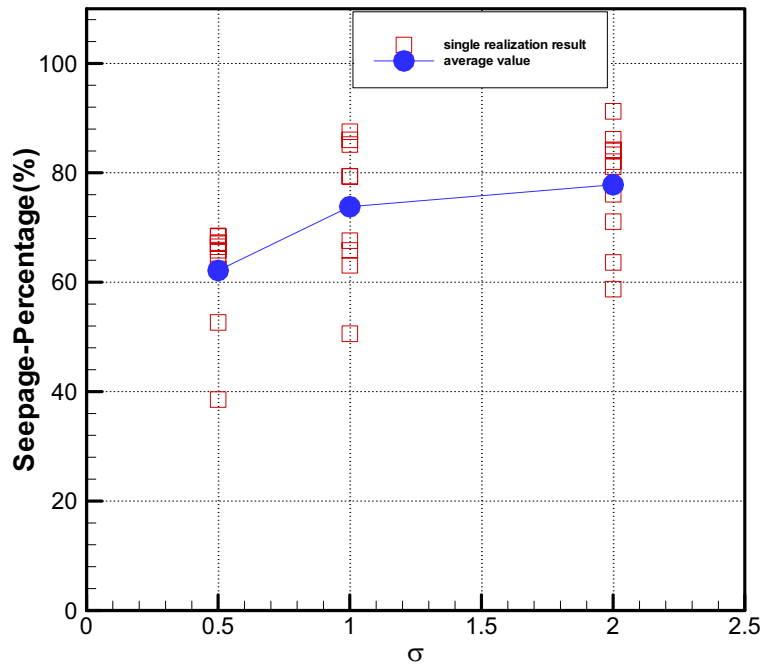
Output DTN: LB0304SMDCREV2.002.

Figure 6-12. Seepage Percentage as a Function of Correlation Length, with $\log_{10}(k_{FC} [\text{m}^2]) = -12$, $Q_p = 200 \text{ mm/year}$, $1/\alpha = 600 \text{ Pa}$

Figure 6-13 presents the results of sensitivity to the standard deviation, σ , in $\log k_{FC}$ of the heterogeneous permeability field, using the same notation as before. Three values were used:

$$\begin{aligned}\sigma &= 0.5 \\ \sigma &= 1 \text{ (base case)} \\ \sigma &= 2\end{aligned}$$

The Figure shows that results for the base case are comparable to those for $\sigma = 2$, but are higher (thus more conservative) than those for $\sigma = 0.5$.



Output DTN: LB0304SMDCREV2.002.

Figure 6-13. Seepage Percentage as a Function of Standard Deviation σ , with $\log_{10}(k_{FC} [\text{m}^2]) = -12$, $Q_p = 200 \text{ mm/year}$, $1/\alpha = 600 \text{ Pa}$

6.6.3 Results for Degraded-Drift Scenario

Results on seepage based on calculated degraded drift profiles are discussed in this section firstly for the nonlithophysal and then for the lithophysal rocks. Drift degradation in the hard, strong, jointed rock of the nonlithophysal units is mostly limited to local gravitational drop of rock blocks (wedge-type rockfall) at the drift ceiling. As summarized in BSC (2004 [DIRS 166107], Section 8.1), minor damage due to wedge-type rockfall (i.e., controlled by the geological structure) is expected in nonlithophysal units from (1) all seismic events (BSC 2004 [DIRS 166107], Section 6.3.1.2), (2) thermal stress (BSC 2004 [DIRS 166107], Section 6.3.1.3), and (3) time-dependent strength degradation (BSC 2004 [DIRS 166107], Section 6.3.1.5). Except for local wedge-type rockfall, the drifts in nonlithophysal units remain intact openings with the horizontal extent essentially unchanged (BSC 2004 [DIRS 166107], Figures 6-112

through 6-116), similar to the results obtained in the earlier Revision 01 of the report *Drift Degradation Analysis* (BSC 2001 [DIRS 156304], compare with profiles in Figures 39 and 40). Note that some of the extreme seismic cases lead to very high stresses that may exceed the compressive strength of the intact rock mass in the nonlithophysal units (BSC 2004 [DIRS 166107], Section 6.3.1.6.4). In such cases, severe spalling or even drift collapse would occur, as the intact rock blocks would essentially be crushed. However, as such extreme events are extremely unlikely, given the 11-million-year lifetime of the Yucca Mountain, the *Seismic Consequences Abstraction* (BSC 2004 [DIRS 169183], Section 6.8.1) determines that complete collapse of drifts in nonlithophysal units is not to be considered in the TSPA-LA. The effect of wedge-type rockfall in nonlithophysal units, on the other hand, is implicitly accounted for in the TSPA-LA.

More significant drift degradation than in the nonlithophysal units is predicted for the relatively deformable lithophysal rock. In lithophysal units, all seismic events with peak ground motions greater than about 2 m/s lead to complete collapse of emplacement drifts, as discussed in BSC (2004 [DIRS 166107], Sections 6.4.2.2). Peak ground motions larger than 2 m/s occur, for example, in some of the 1×10^{-5} seismic hazard levels and in all 1×10^{-6} and the 1×10^{-7} seismic hazard levels. As discussed in Section 6.4.2.4.2, complete collapse of emplacement drifts leads to a significant increase in seepage compared to nondegraded or slightly degraded drifts. For all other seismic events with smaller peak ground motions, the extent of drift damage in lithophysal rocks is less significant. For example, according to Figure 6-128 in BSC (2004 [DIRS 166107]), partial drift collapse will occur for a peak ground motion of 1.04 m/s for low-strength rock of Category 1, while only minor damage is expected for all other rock strength categories at the same peak ground motion. Independent of the rock category, no or very minor rock damage from local rockfall is predicted for the seismic cases with annual occurrence of 5×10^{-4} and the 1×10^{-4} , with the drifts remaining essentially intact. Based on these results (and other considerations), the *Seismic Consequences Abstraction* (BSC 2004 [DIRS 169183], Section 6.8.1) recommends for the TSPA-LA that all peak ground motions equal or greater than 0.384 m/s should be considered large enough to collapse the drift in the lithophysal zones. This threshold value for collapse includes all seismic events with annual occurrence probability equal to or lower than 1×10^{-4} .

In contrast to the impact of seismic events, thermal effects and time-dependent rock strength degradation result in minor drift damage in the lithophysal units, limited to small breakouts in the wall and the crown (BSC 2004 [DIRS 166107], Sections 6.4.2.4, 8.1 and Appendix S3.4.2, Figures S-41 through S-43). Over a 20,000-year time span, the reduction in rock strength is estimated on the order of 40 percent from the initial cohesive strength. This reduction is not significant enough to allow for major damage or even complete collapse (see also profiles predicted from quasistatic simulations for 40 percent cohesion reduction in Appendix R of BSC (2004 [DIRS 166107])). More damage is expected from a combination of seismic, thermal, and time-dependent effects. As shown for the 1×10^{-4} seismic hazard level in Appendix S3.4.3 of BSC (2004 [DIRS 166107]), the extent of rockfall is affected by the timing of the seismic event (effects are stronger at later stages when cohesive strength has reduced) and by the rock category (effects are stronger for low-quality rock). The most significant damage for these cases is predicted for rock of Categories 1 and 2 (about 10 percent of the rock mass in the Ttptll unit) and the seismic event occurring after 10,000 years (Figures 6-154 and Figure S-46 in BSC 2004 [DIRS 166107]), with partial wall breakouts and a 50 percent diameter increase.

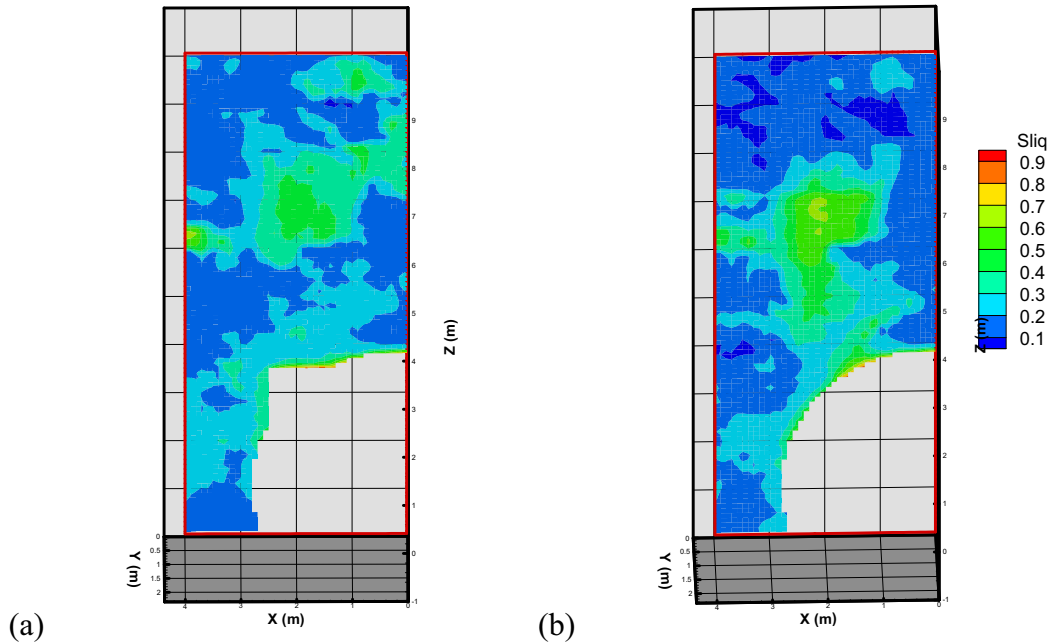
In seepage calculations for degraded drifts in this report, two profile scenarios have been considered that cover most of the degradation results discussed above. The first profile scenario is for drifts with local wedge-type rockfall along the crown or the wall, as seen in the nonlithophysal rocks. Otherwise, the drifts remain intact openings with the horizontal extent essentially unchanged. Note that this profile scenario is also representative for the seepage conditions in lithophysal units with minor drift damage from rockfall, as predicted for all nonseismic cases and the moderate seismic events. The second scenario considers seepage into completely collapsed drifts, as expected in lithophysal rocks as a result of severe seismic events.

For Scenario 1 (seepage into intact drifts with local rockfall), the SMPA seepage calculations were conducted for two selected drift profiles representative of the degradation conditions in the nonlithophysal rocks (Figures 6-14(a) and 6-16(a)). These two profiles were based on model results from the earlier Revision 01 of the drift degradation analysis (BSC 2001 [DIRS 156304]), but are similar to those in the recent revision of this report (BSC 2004 [DIRS 166107]). The selected profiles were the 75 percentile profile and the worst-case profile of the seismic Level 3 case for both geological units, as presented in BSC (2001 [DIRS 156304], Figures 39 and 40, Table 43). The 75 percentile profile for a particular unit and seismic event indicates that 75 percent of the drift length within that unit will have less (or no) drift profile deterioration. The worst-case profile represents the most severely degraded profile of the probabilistic analysis.

On the drift profiles, seepage was calculated with 10 realizations of the heterogeneous permeability field, using the same methodology as employed for nondegraded drifts. (Note that the seepage calculations for nondegraded drifts were carried out with 20 realizations. The degraded drift analysis was conducted with fewer realizations in order to limit the computational load of the predictive simulations. The results are expected to be close to the ones obtained from 20 realizations. This assessment is based on the comparison of selected simulation cases conducted with 10 vs. 20 realizations, which indicated differences of 2 percent or less in the mean seepage rates (see below, Table 7-1).) Seepage simulations were conducted for selected parameter cases using a capillary strength of 600 Pa and a percolation flux of 200 mm/year. No-degradation results with the same parameter values were also calculated for comparison to study the impact of drift degradation on seepage.

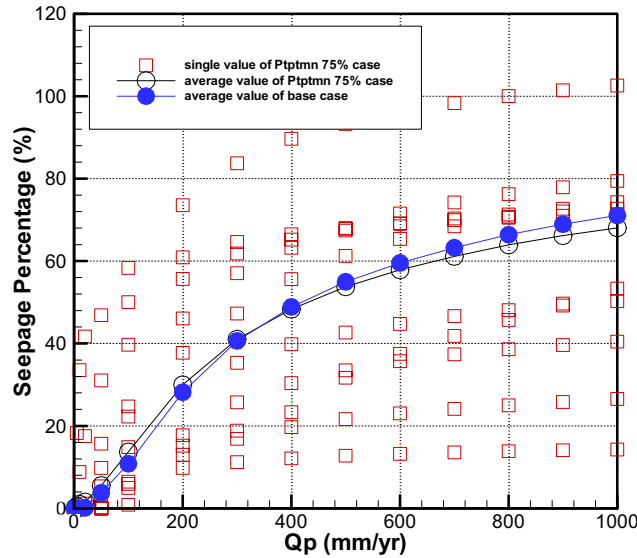
These calculations were performed using a $\log_{10}(k_{FC} \text{ [m}^2\text{)})$ value of -11.86 , which is the mean of the values found at the three niche locations (-12.14 , -11.66 , -11.79) (DTN: LB0302SCMREV02.002 [DIRS 162273]). The normal drift profile without degradation is shown in Figures 6-14(b) and 6-15(b) for comparison. The color contours in Figure 6-14 show the calculated liquid saturation distribution for $Q_p = 200$ mm/year. Degradation created a more square-like profile (left profile in Figure 6-14a), which creates less flow diversion than a smooth circular profile. One can, therefore, see a slightly larger area of high saturation near this location. Figure 6-15 presents the seepage rates for a range of Q_p for this case. Results of seepage percentage for ten realizations of the degraded drift for the model (with cross-sectional area of 6.706 m^2 , see Section 6.3.1, first paragraph) are shown as red squares in the figure. Note that the rock-fall is at about the middle of this model domain. To obtain the mean seepage over the drift containing one waste canister (with area of 28.05 m^2 , see Section 6.3.1, first paragraph), one needs to recognize that the extra area $28.05 - 6.706 = 21.344 \text{ m}^2$ (i.e., the area of drift minus the area of the part of the drift containing the rock-fall) does not contain rock-fall. Since the mean seepage without drift degradation has been calculated (blue filled circles in Figure 6-15),

one can calculate the mean seepage with degradation by combining the calculated seepage with and without degradation in the ratio of 6.706 to 21.344. The results are shown as black open circles in Figure 6-15. It turns out that the mean for the degraded case has actually slightly less seepage, though the geostatistical spread is quite large.



Output DTN: LB0304SMDCREV2.002.

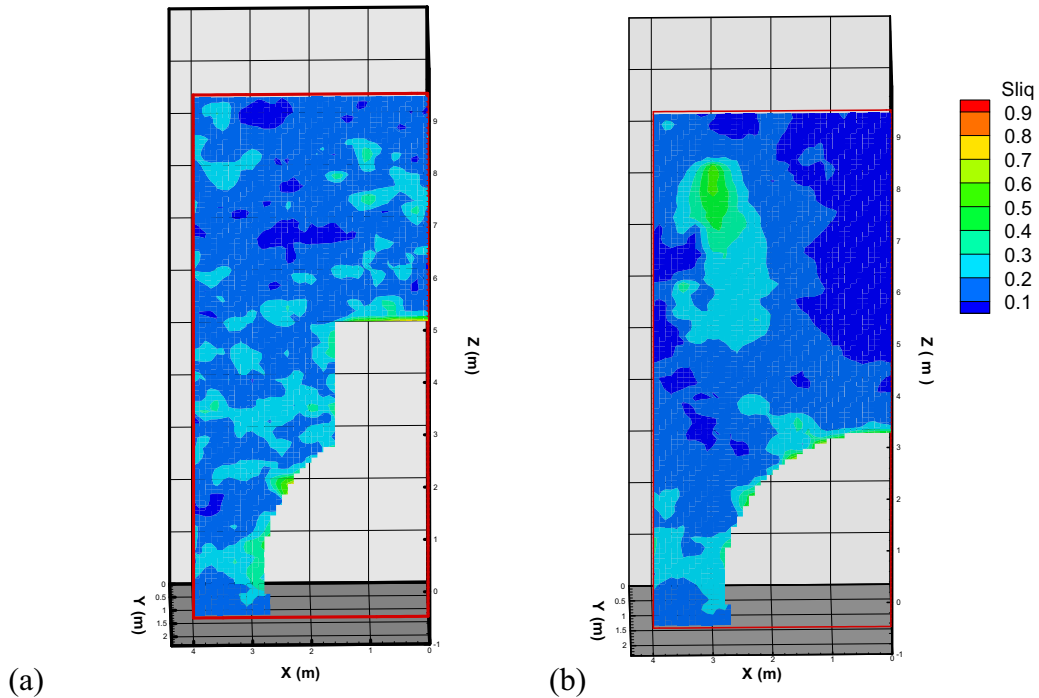
Figure 6-14. Liquid Saturation (Sliq) Distribution for the 75 Percentile Case Profile in Tptpmn Unit (left) and No-Degradation Base Case (right) [$\log_{10}(k_{FC} [m^2]) = -11.86$, $Q_p = 200$ mm/year, $1/\alpha = 600$ Pa]



Output DTN: LB0304SMDCREV2.002.

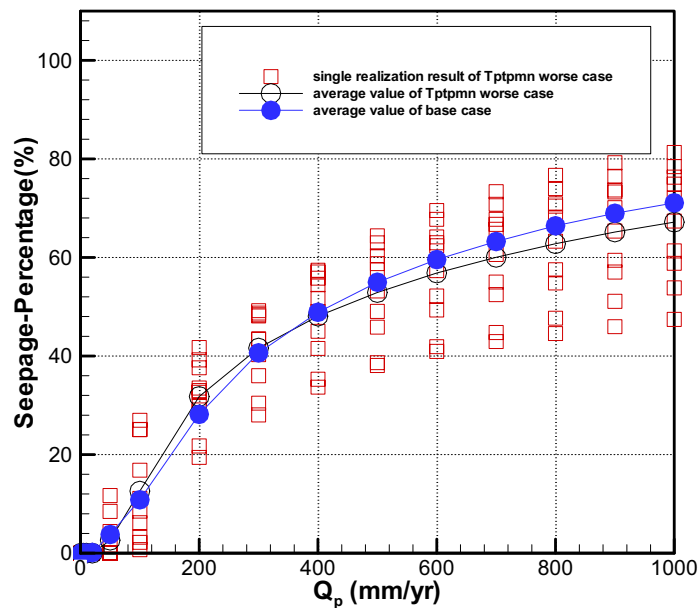
Figure 6-15. Seepage Percentage as a Function of Percolation Flux for the 75 Percentile Case Profile in Tptpmn Unit [$\log_{10}(k_{FC} [m^2]) = -11.86$, $1/\alpha = 600$ Pa]. Red Open Squares Are Results for 10 Realizations. The Mean Seepage Percentages Are Shown as Black Open Circles (See Text). For Comparison, the Mean over 10 Realizations for No-Degradation Case (Base Case) Is Shown as Blue Filled Circles

Similar results for the worst-case drift-degradation profile are shown in Figures 6-16 and 6-17. In this case, however, the rockfall is extensive and is located at the center above the drift crown, thus, cutting across the model boundary. The rockfall volume is scaled accordingly, so that the mean seepage does not need to be scaled as in the case of Figure 6-15. The results of mean seepage percentages for degraded cases are shown as black open circles in Figure 6-17. They show small changes in seepage percentage (Figure 6-17) compared to the geostatistical spread due to multiple realizations.



Output DTN: LB0304SMDCREV2.002.

Figure 6-16. Liquid Saturation (S_{liq}) Distribution for the Worst-Case Profile in Tptpmn Unit (left) and No-Degradation Base Case (right) [$\log_{10}(k_{FC} [m^2]) = -11.86$, $Q_p = 200$ mm/year, $1/\alpha = 600$ Pa]



Output DTN: LB0304SMDCREV2.002.

Figure 6-17. Seepage Percentage as a Function of Percolation Flux for the Worst-Case Profile Case in Tptpmn Unit [$\log_{10}(k_{FC} [m^2]) = -11.86$, $1/\alpha = 600$ Pa]. Red Open Squares Are the Results for 10 Realizations, with Their Mean Shown as Black Open Circles. For Comparison, the Mean over 10 Realizations for the No-Degradation Case (Base Case) Is Shown as Blue Filled Circles

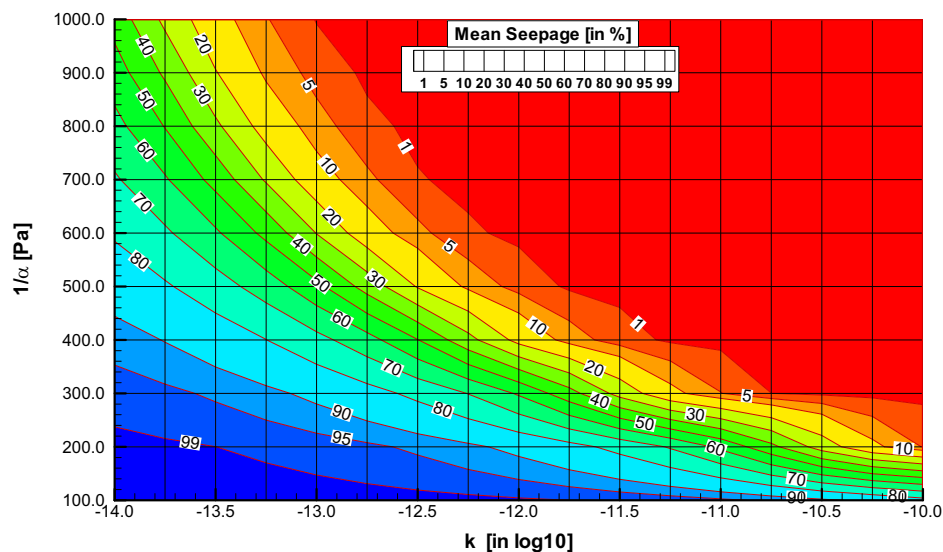
Scenario 2 involves seepage into completely collapsed drifts in the lithophysal rocks. During collapse, either sudden or gradual, the rock mass above an underground opening disintegrates into a number of fragments that fall down and begin to fill the open space. Because there are large voids between the rock fragments, the bulk porosity of the fragmented rubble is much larger than the intact rock. As a result, the open space of the original excavation plus the collapsed portion of rock above are completely filled with rubble at a certain stage. When this occurs, the broken rock provides backpressure, which prevents further collapse of the rock mass (BSC 2004 [DIRS 166107], Section 6.4.2.5). The final situation after complete drift collapse can be categorized as follows: the original opening has increased in size, but is filled with fragmented rubble with large voids. The solid wall rock surrounding the rubble-filled opening is intact, but may have increased permeability and reduced capillary strength because of the dynamic motion and the stress redistribution (see Section 6.4.4.1.2). For convenience, we refer to the rubble-filled opening as a “collapsed drift”, although technically there is no drift after collapse. The size and the shape of a collapsed drift mainly depend on the porosity of the rubble material and on the type of caving mechanism as collapse occurs. The collapsed drift profiles provided in DTN: MO0306MWDDPPDR.000 [DIRS 164736] are all similar, independent of the event leading to collapse. (Note that these profiles are also depicted in Appendix R of BSC (2004 [DIRS 166107])). In this reference, collapsed drifts are shown for Scenarios 2 through 5, 11, 12, 17, 18, 23, 24, 28, 29, and 30.) All drifts remain approximately circular after complete collapse. However, the size of the collapsed drifts increases considerably, with the largest drifts having a diameter of approximately 11 m after collapse.

Though complete drift collapse may lead to significantly different seepage behavior, capillary barrier effects still give rise to considerable flow diversion at the interface between the solid rock and the rubble-filled drift opening. This is because of the large scattered voids between the rock fragments (block sizes on the order of centimeters and decimeters (BSC 2004 [DIRS 166107], Section 8.1)), suggesting that the capillary strength parameter in the rubble filled drift is very small, most likely close to the zero capillary strength of an air-filled opening. Also, a small gap can be expected between the solid rock at the ceiling and the collapsed rubble material as a result of consolidation. Therefore, capillary-driven flow diversion remains an important mechanism in reducing seepage in collapsed drifts, which should be included in the seepage abstraction model. Additional simulation cases were conducted with the SMPA to study seepage into collapsed drifts. A worst-case drift profile for seepage was selected as representative of the complete drift collapse scenarios depicted in MO0306MWDDPPDR.000 [DIRS 164736] (see also Appendix R of BSC (2004 [DIRS 166107])). The chosen profile has a circular shape with a diameter of 11 m, which is the largest diameter predicted. The larger the drift size, the more seepage can be expected because (1) the total amount of percolation flux arriving at the drift increases with the horizontal size, and (2) flow diversion is less effective for a larger drift. A capillary strength parameter of 100 Pa was used for the fragmented rock material within the collapsed drift (Section 5). This value is considered a conservative choice for seepage calculations, because the capillary strength of the rubble material is most likely smaller.

Systematic seepage simulations for the collapsed drift case were conducted for the full set of parameter combinations, with capillary strength values ranging from 100 Pa to 1,000 Pa, mean permeability values ranging from -14 to -10 (in \log_{10}), and percolation flux values ranging from 1 mm/year to 1,000 mm/year. (These are the same parameter cases as simulated for the nondegraded drift in Section 6.4.2.3). The resulting seepage values are provided in a seepage

look-up table for the collapsed drift scenario (Output DTN: LB0307SEEPDRCL.002). The format of this look-up table is identical to the nondegraded drift case in Section 6.4.2.3. Thus, to account for collapsed drifts, the seepage abstraction model would simply sample from this second look-up table without changing the basic abstraction methodology (see Section 6.5.1.5). The collapsed drift look-up table in Output DTN: LB0307SEEPDRCL.002 is based on results from 10 realizations. (As mentioned before, the seepage calculations for nondegraded drifts were carried out with 20 realizations. The collapsed drift analysis was conducted with fewer realizations on order to limit the computational load. The results are expected to be close to the ones obtained from 20 realizations. This assessment is based on the comparison of selected simulation cases conducted with 10 vs. 20 realizations, which indicated differences of 2 percent or less in the mean seepage rates.)

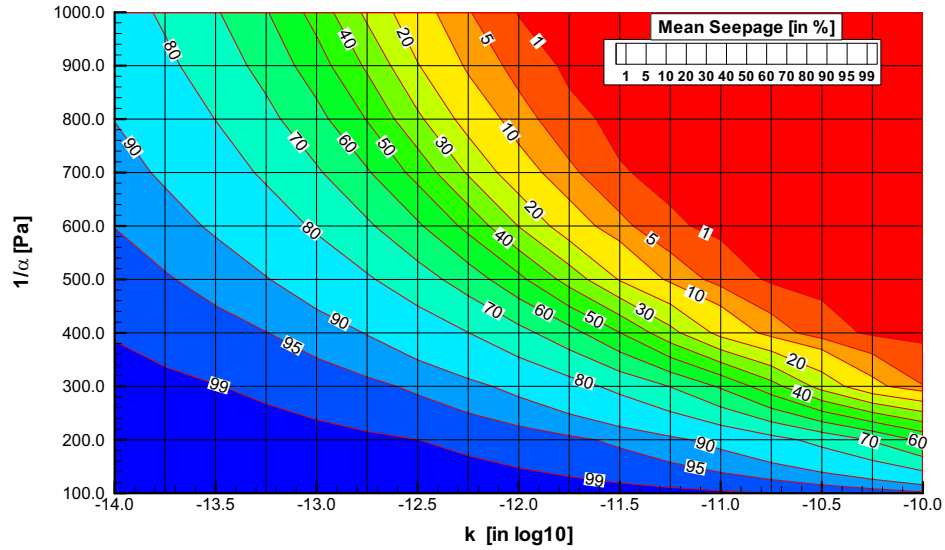
Example seepage results for the collapsed drift scenario are illustrated in Figures 6-18 through 6-21, showing contours of simulated seepage percentage. Comparison with results from the nondegraded drift scenario (Section 6.6.1) indicates a considerable increase in seepage percentage, caused by the larger size of the collapsed drift (reducing the effectiveness of flow diversion around the drift) and by the nonzero capillary strength in the drift (reducing the effectiveness of the capillary barrier). Nevertheless, the simulation results demonstrate that most of the percolation flux is still diverted around the collapsed drift for most of the considered parameter range. Note that the related seepage rates for the collapsed drift scenario are much larger than for nondegraded drifts because the footprint of the drifts has doubled in size, thereby, doubling the amount of percolation flux arriving at the collapsed drift.



Output DTN: LB0307SEEPDRCL.002.

NOTE: Horizontal and vertical lines indicate simulated parameter cases.

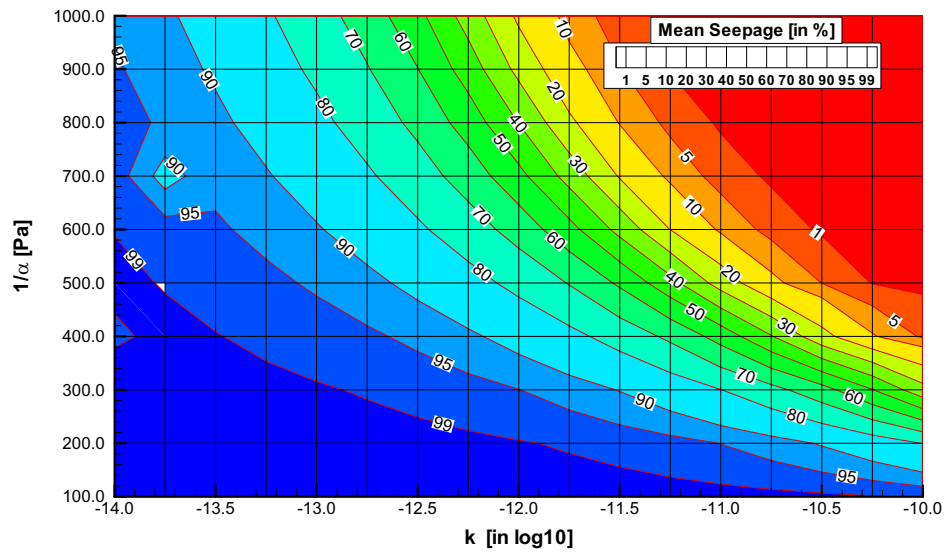
Figure 6-18. Mean Seepage Percentage for the Collapsed Drift Scenario as a Function of Capillary-Strength Parameter and Mean Permeability for a Percolation Flux of 5 mm/year



Output DTN: LB0307SEEPDRCL.002.

NOTE: Horizontal and vertical lines indicate simulated parameter cases.

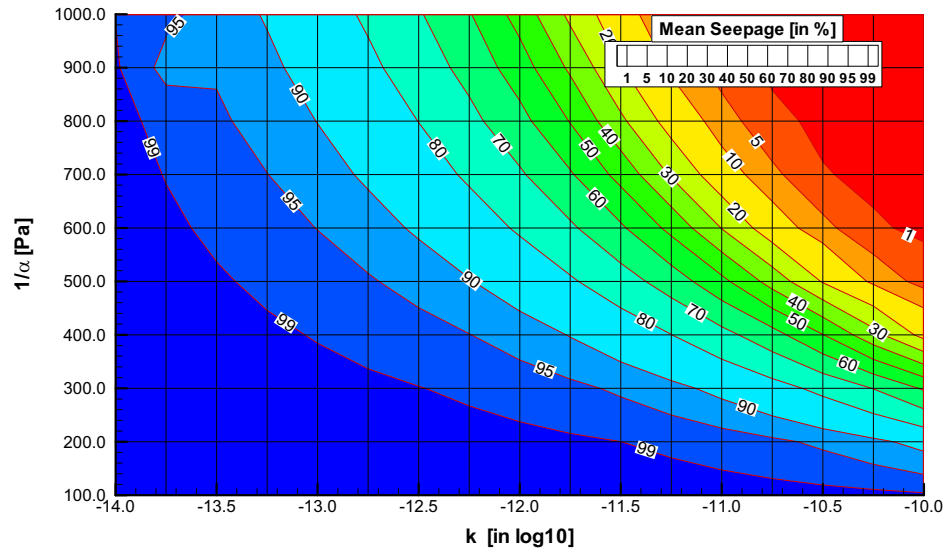
Figure 6-19. Mean Seepage Percentage for the Collapsed Drift Scenario as a Function of Capillary-Strength Parameter and Mean Permeability for a Percolation Flux of 50 mm/year



Output DTN: LB0307SEEPDRCL.002.

NOTE: Horizontal and vertical lines indicate simulated parameter cases.

Figure 6-20. Mean Seepage Percentage for the Collapsed Drift Scenario as a Function of Capillary-Strength Parameter and Mean Permeability for a Percolation Flux of 200 mm/year



Output DTN: LB0307SEEPDRCL.002.

Figure 6-21. Mean Seepage Percentage as a Function of Capillary-Strength Parameter and Mean Permeability for a Percolation Flux of 500 mm/year

6.6.4 Results for the Effect of Rock Bolts

Modeling results for seepage enhancement caused by the presence of a vertical rock bolt are shown in Table 6-4. Here, a seepage enhancement factor is defined as:

$$\text{Enhancement Factor} = 1 - \frac{\text{SeepageWithTheRockbolts}}{\text{SeepageWithoutTheRockbolts}} \quad (\text{Eq. 6-1})$$

Thus, the enhancement factor is negative if the seepage increases because of the presence of a rock bolt and is positive if it decreases. Table 6-2 shows results only for $Q_p = 500$ mm/year because, with $Q_p = 5$ mm/year, seepage rates in all cases are zero, and enhancements are also found to be zero. In Table 6-2, Cases C1, C2, and C3 represent three variations in mesh design for accounting connections between rock bolt borehole and the rock, and Cases G1 and G2 represent, respectively, the properties of grout being slightly degraded from original values and being very degraded, so that the rock bolt hole is essentially open.

From the table, one can see that seepage enhancement is negligible for the presence of the rock bolt for the two limiting cases G1 and G2. This result is understandable, considering that the cross-sectional area of the rock bolt borehole, onto which flow may be incident, is small, and the borehole can exchange moisture with the rock along its length. For a vertical rock bolt, if only the horizontal surface is considered, the area is only about 0.002 m^2 . For a nonvertical rock bolt, while the area of rock bolt projected onto a horizontal plane is larger, the potential for flow from the rock bolt borehole to the rock matrix around it is also increased.

Also note that the results are not sensitive to the alternative mesh design, C1, C2, and C3. Further, since the changes are so small, even the presence of five or six rock bolts will not change seepage significantly.

Table 6-4. Results on Seepage Enhancement Factor Due to a Rock Bolt in Drift Ceiling

| $1/\alpha$ (Rock) Pa | Seepage Percentage (without rock bolt) | Seepage Enhancement Factor, Eq. (6-1) (with rock bolt) | | |
|-------------------------|--|---|---|---|
| | | | Case G1 $\log(k_{\text{grout}} [\text{m}^2]) = -18$ $1/\alpha_{\text{grout}} = 10^7 \text{ Pa}$ | Case G2 $\log(k_{\text{grout}} [\text{m}^2]) = -10$ $1/\alpha_{\text{grout}} = 10 \text{ Pa}$ |
| 200 | 100% | C1 | 0 | 0 |
| | | C2 | 0 | 0 |
| | | C3 | 0 | 0 |
| 400 | 53% | C1 | 0 | 0 |
| | | C2 | 0 | 0 |
| | | C3 | 0 | 0 |
| 589 | 0.034% | C1 | -0.0033 | -0.0034 |
| | | C2 | -0.0113 | -0.0113 |
| | | C3 | -0.0156 | -0.0156 |

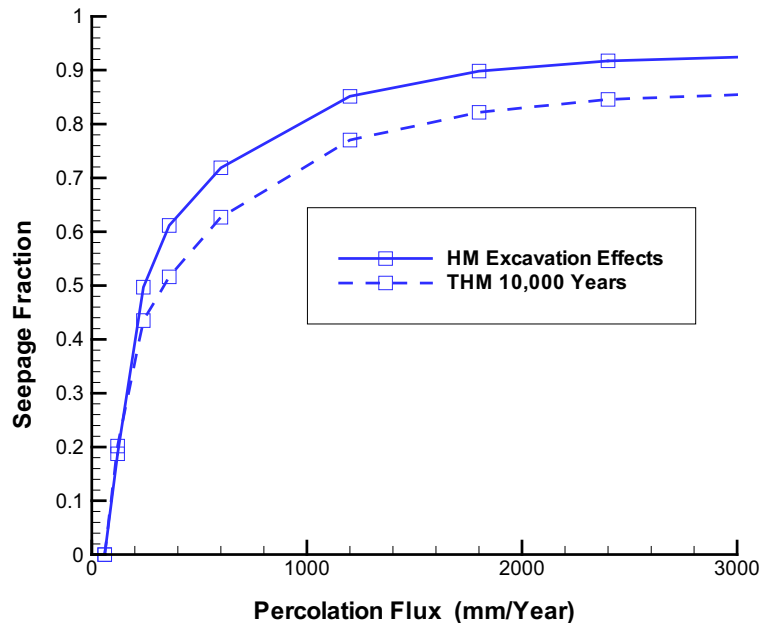
Output DTN: LB0304SMDCREV2.001.

6.7 COMMENT ON LONG-TERM THERMAL-HYDROLOGICAL-CHEMICAL AND THERMAL-HYDROLOGICAL-MECHANICAL EFFECTS ON SEEPAGE

Long-term coupled thermal-hydrological-chemical (THC) processes have been modeled (BSC 2004 [DIRS 169856]). Results from this modeling indicate a zone of permeability reduction corresponding to the boundary between the dryout zone near the drift and the condensation region farther away. Their calculations (BSC 2004 [DIRS 169856], Section 6.8, Figures 6.8-40 and 6.8-41) show that the reduction is in the form of a circular shell between 5 and 7 m, or farther, from the drift ceiling. Thus, it acts as a shield to divert water around the drift, so that the drift sees relatively less percolation flux. As explained in Section 6.2.1, the drift, acting as a capillary barrier, diverts water around it and, where it is unable to do so fast enough, water accumulates, saturation increases, and seepage into drift occurs. However, all these processes act well within 1 m from the drift ceiling and drift wall (Philip et al. 1989 [DIRS 105743]), and are not affected by these THC changes. Consequently, an alternative model with THC at long term is not considered.

The impact of long-term coupled THM processes has also been investigated (BSC 2004 [DIRS 169864]). The results (BSC 2004 [DIRS 169864], Section 6.5.4) show a thermally induced increase (by approximately a factor of 10) in horizontal permeability at 10,000 years, with a decrease in vertical permeability (also by approximately a factor of 10), in the immediate neighborhood (within 1 m) of the drift ceiling. This actually increases the likelihood of flow being diverted around the drift, and the changes are within the parameter ranges used in this report. To confirm this point, calculations for Tptpmn were conducted within the THM modeling (BSC 2004 [DIRS 169864]) using the permeability field after excavation with only mechanical effects (BSC 2004 [DIRS 169864], Figure 6.5.1-1) and the permeability field at 10,000 year with THM effects (BSC 2004 [DIRS 169864], Figures 6.5.4-3(d), and 6.5.4-4 (d)).

Percolation flux was imposed above the drift with a series of values. The $1/\alpha$ value just above the drift crown after excavation was set to be 604.3 Pa (DTN: LB0302SCMREV02.002). Seepage percentages were calculated (Wang 2003 [DIRS 162319], SN-LBNL-SCI-204-V2, p. 162) and shown in Figure 6-22. The reduced seepage for the THM case at 10,000 years is apparent. Thus, an alternative model capturing THM long-term effects is not considered.



Output DTN: LB0304SMDCREV2.004 (Appendix A, Table A-1).

Figure 6-22. Seepage Percentage (Expressed in Fraction) Is Shown as a Function of Percolation Flux for Permeability Fields around the Drift after Excavation and Also at 10,000 Years, Accounting for THM Effects

6.8 FLOW FOCUSING

As discussed in the previous sections, the local percolation flux arriving at individual drift locations is one of the key factors affecting seepage. The spatial and temporal distribution of percolation fluxes in the UZ is provided by the site-scale UZ Model (BSC 2004 [DIRS 169861]). This model derives relevant information on the overall flow and transport fields at the Yucca Mountain, accounting for climate changes and related uncertainties, variability in net infiltration, and the effects of different stratigraphic units and faults. However, because of the large model area, the spatial resolution of the model is much larger than the extent of drift-scale seepage models, and layer-averaged properties are used within stratigraphic units. Thus, intermediate-scale heterogeneity is not represented in the UZ Model. This heterogeneity may lead to focusing of flow on a scale smaller than the resolution of the site-scale model; i.e., it may increase the fluxes in some areas, while reducing them in other areas. The additional variability and uncertainty of percolation flux stemming from this effect is accounted for in the seepage abstraction by appropriate FFFs, to be multiplied with the percolation flux distribution from the site-scale model. The resulting flux distribution is expected to represent the local percolation flux distribution needed as input to the predictive drift-scale seepage models. Specifically, it refers to the range of fluxes Q_p studied in the SMPA (see Section 6.3.6).

The objective of this section is to investigate flow focusing and discrete paths that may occur through unsaturated fractures within the TSw unit. Honoring fracture permeability data, a high-resolution model is developed using a stochastic representation of fracture permeabilities. Frequency and flux distributions at the repository horizon are examined, resulting in a probability or frequency distribution function of FFFs. The FFF is defined as the ratio of the local percolation flux divided by average percolation flux. During TSPA-LA calculations, the local percolation flux used as input parameter to the seepage look-up tables is the product of the percolation flux obtained at the given location, multiplied by a number sampled from the distribution of FFFs. The use of FFFs in TSPA-LA thus fulfills the two purposes of (1) bridging the gap between the site-scale model of unsaturated flow and the drift-scale seepage models, and (2) accounting for variability induced by stochastic heterogeneity. The following subsections describe the development of FFF distribution function.

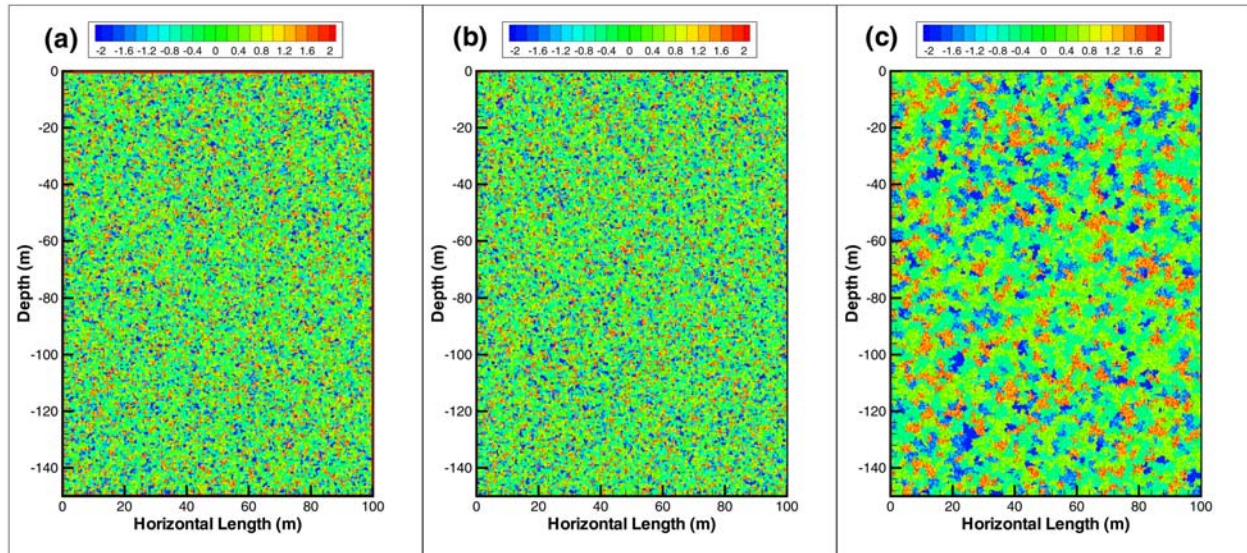
6.8.1 Model Development for Calculating Flow Focusing Factors

The modeling study for flow focusing was conducted on a two-dimensional, vertical cross-sectional model domain in the TSw unit, which has the upper boundary at the bottom of the Paintbrush nonwelded unit (PTn) and the lower boundary at the repository horizon. This cross section has a width of 100 m and a height of 150 m (Figure 6-23), which corresponds to the average distance from the contact interface between the PTn and TSw units to the repository horizon over the repository area. The bottom of the PTn was chosen as the upper boundary because this unit is believed to behave as a porous medium with limited fracture flow. Both uniform and nonuniform percolation flux boundary conditions were prescribed at this upper boundary to study the impact of uncertainty in the boundary flux distribution at this interface. The two side boundaries were treated as no-flow boundaries, and the bottom boundary allowed for gravitational drainage. The model domain was discretized into 400×300 gridblocks, each of which was of 0.25 m and 0.5 m in the horizontal and vertical directions, respectively. This numerical grid is fine enough to capture the effects of heterogeneity in fracture permeability inducing flow focusing, because the gridblock size is smaller than the correlation length (1 m and 3 m, see below).

Only the fracture continuum was modeled in this study because the matrix system is believed to play a limited role in carrying water. Moreover, the matrix with its low permeability is not expected to have a major impact on the development of flow focusing within the model domain. The model domain consists of five different hydrogeologic layers (TSw31 to TSw35). The fracture properties of these five layers are reproduced in Table 4-5.

The impact of heterogeneity in fracture permeability (k_f) on flow focusing is studied by generating spatially correlated, random permeability fields using the sequential-indicator simulator incorporated in iTOUGH2 V5.0 (LBNL 2002 [DIRS 160106]). Three $\log k_n$ fields were generated: two realizations (Fields 1 and 2) with a spherical semivariogram model and a correlation length of 1 m, and one realization (Field 3) with correlation length of 3 m. All fields have a standard deviation of the log-permeability of $\sigma=1.0$ (see Table 6-3). Figure 6-23 shows the three random fields of permeability modifiers ($\log k_n$, where $k_n = k_f/k_0$ with k_0 the mean fracture permeability listed in Table 4-5). Given the large model domain (in comparison to the correlation length), Fields 1 and 2 are statistically very similar, with variations in the detailed

permeability pattern a result of randomness. Field 3 is different from Fields 1 and 2, exhibiting a longer correlation length. Note that the cutoff for the generated $\log k_n$ fields is ± 2.0 , i.e., the fracture-permeability modifier varies over four orders of magnitude.



Output DTN: LB0406U0075FCS.001.

Figure 6-23. Generated Random Fields of Log Fracture-Permeability Modifier in Three Cases: (a) 1 m Correlation Length, Realization 1 (Field 1); (b) 1 m Correlation Length, Realization 2 (Field 2); and (c) 3 m Correlation Length (Field 3)

6.8.2 Results and Sensitivity Analyses

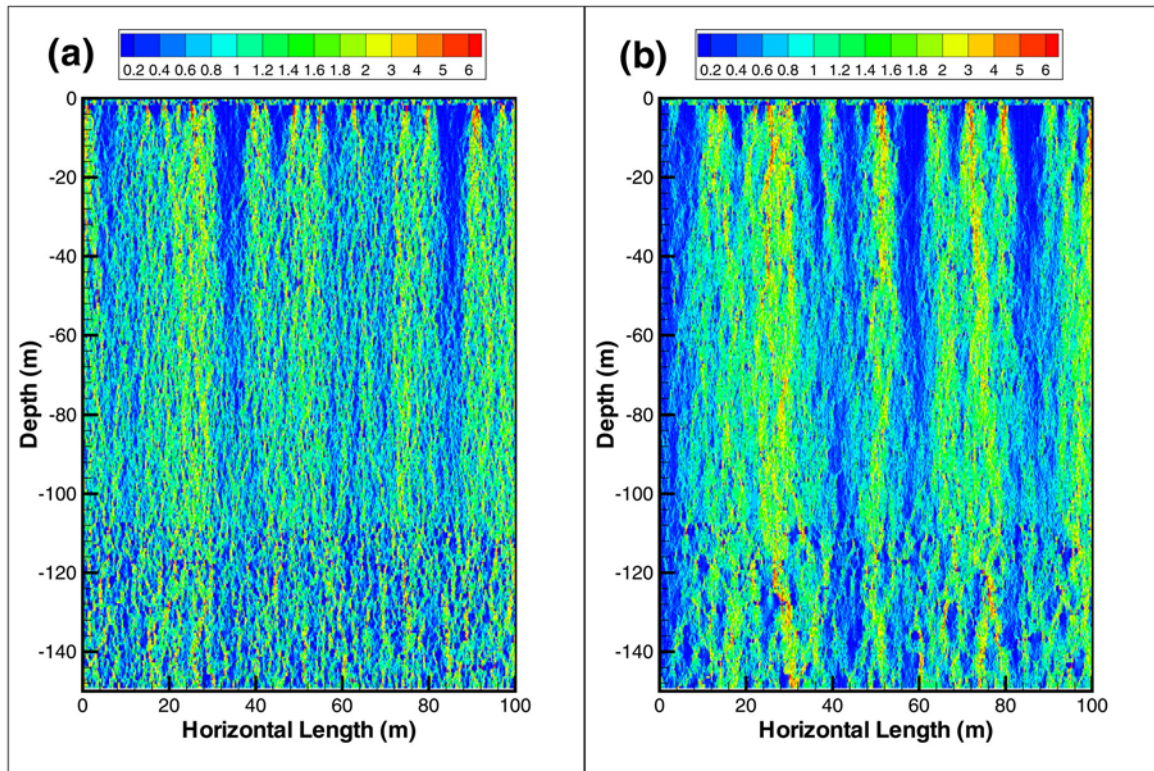
The main objective of this study is to provide a generalized cumulative frequency curve (CFC) of FFF. The FFF is defined by dividing the simulated vertical flux at a gridblock by the mean infiltration rate specified on the top boundary. This generalized CFC is indicative of the overall effects of fracture-permeability heterogeneity on liquid flux distribution.

First, the steady-state flow for a base case scenario (based on fracture permeability Field 1) was simulated, in which a uniform infiltration rate of 5 mm/year was specified on the top boundary (a sensitivity analysis with respect to infiltration is discussed below, see Figure 6-27a). The base case was used to investigate the flow focusing phenomena and the FFF statistical similarity within the model domain. Then a generalized CFC was obtained to account for the uncertainties in mean infiltration rate and its spatial distribution on the top boundary, and those in the fracture permeability field caused by different realizations and correlation lengths.

For each sensitivity case, FFFs were analyzed from the respective steady-state flow field.

Base Case Scenario: Figure 6-24a shows the distribution of FFFs within the two-dimensional model domain using the base-case settings for fracture properties and boundary conditions. The figure shows a number of vertically high-flux, discrete flow paths. These flow paths are initialized within the TSw31 layer, where a uniform flux specified on the top boundary is changed to a nonuniform flux distribution by the heterogeneity in fracture permeability,

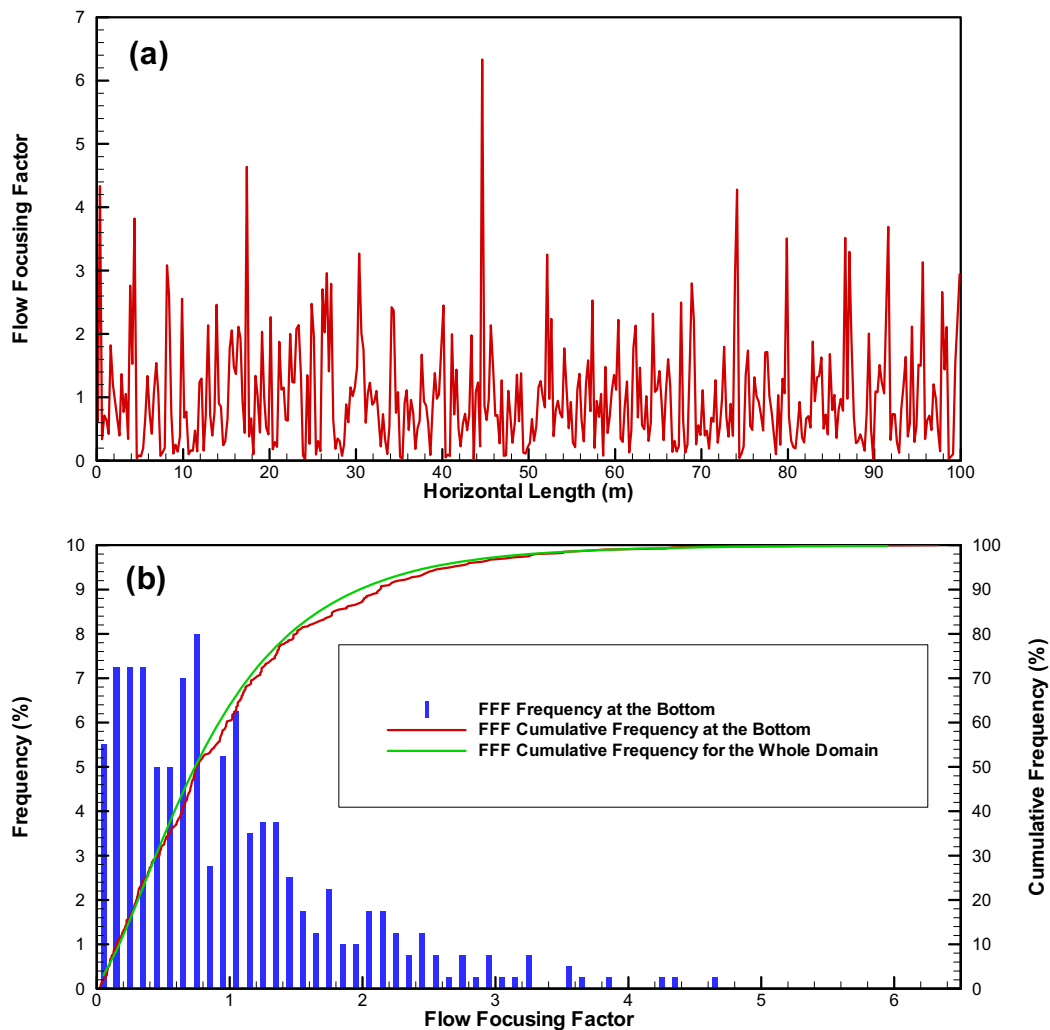
which leads to capillary-pressure gradients that locally redistribute flow. With increase in depth (until -110 m), these flow paths are somewhat smeared by the weaker capillarity within the TSw32 and TSw33 layers. The smeared flow paths above the TSw34 layer change again by the relatively strong capillarity encountered in TSw34 and TSw35, producing more flow paths and higher FFF contrasts.



Output DTN: LB0406U0075FCS.001.

Figure 6-24. Distributions of Flow Focusing Factor within the Two-Dimensional Model Domain, Simulated Using (a) Field 1 and (b) Field 3 of Fracture-Permeability, with 5 mm/year Uniform Infiltration on the Top Boundary

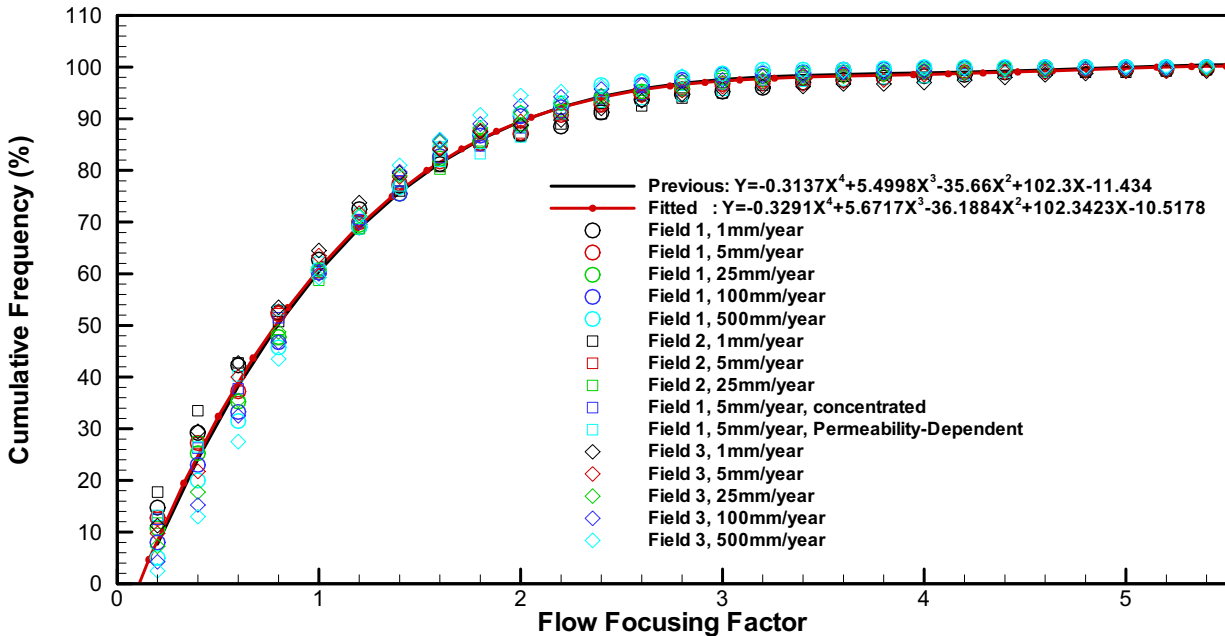
Figure 6-25a shows the spatial variability of FFFs at the bottom boundary. A significant variability in flow focusing is observed, with values ranging from 0.024 to 6.33. As shown in Figure 6-25b, a FFF of 1 has a cumulative frequency of approximately 60 percent, indicating that about 40 percent of the locations experience percolation fluxes that are higher than the average flux applied at the top of the model. However, only about 3 percent of the locations have local fluxes higher than three times the average percolation flux. The CFC of FFF obtained at the bottom boundary is statistically similar to that for the whole model domain, as shown in Figure 6-25b. This statistical similarity indicates that the CFC at the bottom boundary can be used in the TSPA-LA.



Output DTN: LB0406U0075FCS.001.

Figure 6-25. (a) Spatial Variability (0.25 m Horizontal Resolution) and (b) Frequency and Cumulative Frequency of Flow Focusing Factor at the Bottom Boundary for the Base-Case Scenario, as well as Cumulative Frequency Curve for the Entire Model Domain

Generalized CFC: To study the uncertainties in factors affecting flow focusing, sensitivity analyses were conducted with respect to (a) the mean infiltration rates on the top boundary (1, 5, 25, 100, and 500 mm/year), (b) the spatial distribution of the released water at top boundary (uniform, concentrated, and permeability-dependent), and (c) different realizations (three random fields) and different correlation lengths (1 m and 3 m; see Figure 6-23). Based on the CFC calculated for each case, a generalized CFC was created and described using a polynomial regression function. This curve and the data points for the 15 different cases are shown in Figure 6-26, with the generalized CFC obtained by Bodvarsson et al. (2003 [DIRS 163443], Figure 13).

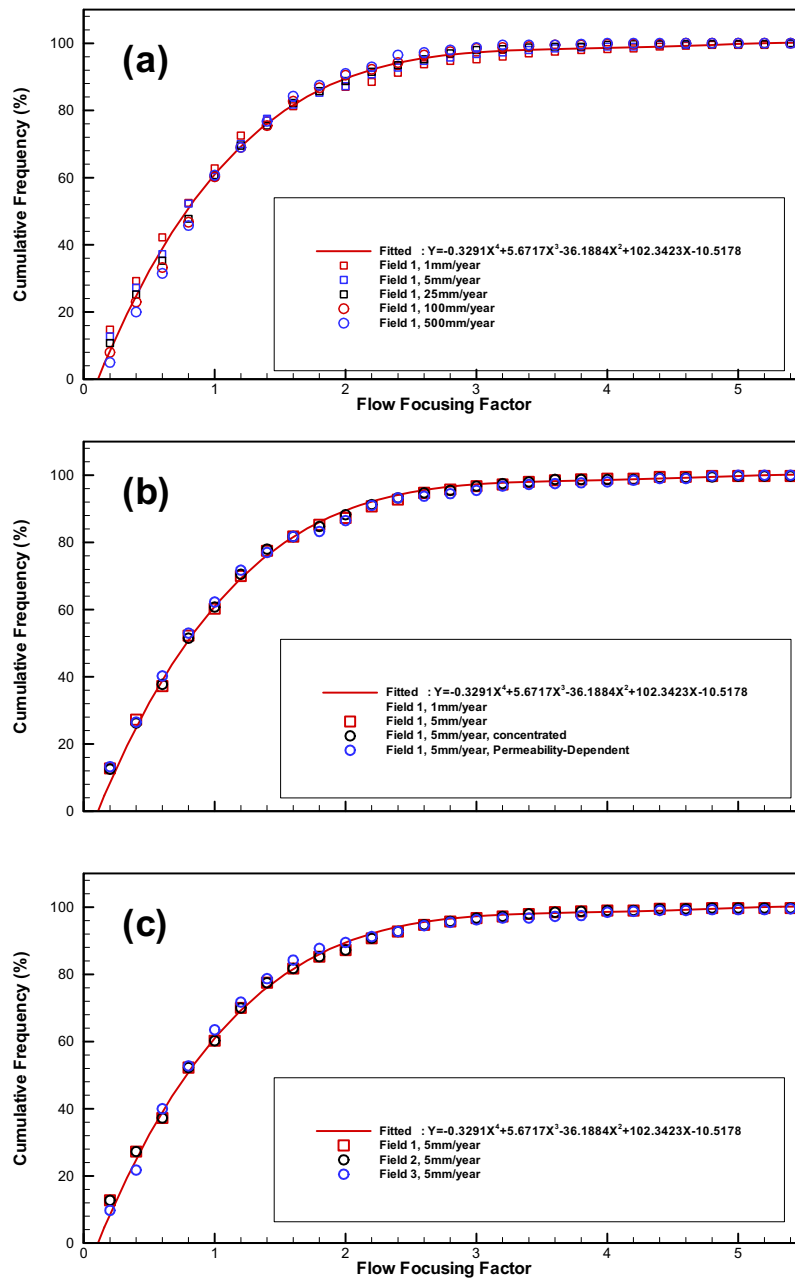


Output DTN: LB0406U0075FCS.002.

Figure 6-26. Generalized Cumulative Frequency Curve of Flow Focusing Factor at the Bottom Boundary (“Fitted”), Data Points from 15 Different Study Cases (Symbols), and the Generalized CFC Obtained by Bodvarsson et al. (2003 [DIRS 163443], Figure 13) (“Previous”)

The results from the various sensitivity analyses are summarized in Figure 6-27. As shown in Figure 6-27a, the mean infiltration rate has a small, albeit noticeable, effect on the CFC. With increase in the mean infiltration rate, the mean steady-state liquid saturation increases, leading to reduced capillary-pressure gradients, which results in less flow focusing. The less flow focusing for a higher mean infiltration rate is indicated by a lower cumulative frequency for an FFF value smaller than 1 and a higher cumulative frequency for an FFF value in the range of [1, 3]. However, the variations in the CFCs caused by different mean infiltration rates is relatively small, indicating that the CFC is not very sensitive to varying infiltration rate. Therefore, the FFF for the four cases are statistically similar to the base case, and are included in the determination of the generalized CFC.

The sensitivity of infiltration distribution on the top boundary was analyzed using three different types of distribution: (1) uniform infiltration rate into each top gridblock, (2) concentrated infiltration rate (increased by a factor of 20) into only one top gridblock for every 5 m (20 gridblock) width, and (3) spatially varying infiltration rate distributed automatically based on the spatially varying fracture permeability along the top boundary. For each of the three infiltration distribution cases, the average percolation flux was identical at 5 mm/year. As shown in Figure 6-27b, the infiltration distribution on the top boundary has little effect on the CFC because the capillary-pressure gradients are sufficient to redistribute the water over a relatively short flow distance (see Figure 6-24).



Output DTN: LB0406U0075FCS.001.

Figure 6-27. Sensitivity Analysis of Cumulative Frequency Curve of Flow Focusing Factor on the Bottom Boundary with Respect to (a) Mean Infiltration Rate, (b) Infiltration Distribution Along the Top Boundary, and (c) Different Fracture-Permeability Fields

The third sensitivity analysis was conducted for different fracture-permeability fields caused by different realizations and different correlation lengths. The three different permeability modifier fields shown in Figure 6-23 were used. Different mean infiltration rates were used for the three permeability fields, and the resulting CFCs were included in the determination of the generalized

CFC. As shown in Figure 6-27c, the two realizations with 1 m correlation length (with 5 mm/year mean infiltration rate and uniform distribution) produce very similar CFCs, indicating that one realization for the same correlation length is sufficient for deriving the statistics of the vertical flux (or the FFF). This is a result of the fact that the model domain covers 100 and 150 times the correlation length in the horizontal and vertical direction, respectively. As shown in Figures 6-23 and 6-24, the third permeability field with 3 m correlation length is different than the first one. As expected, fewer but wider discrete, high-flux flow paths are obtained with Field 3. However, in terms of statistic probability, these cases produce similar CFCs, with a small variability around the generalized CFC. In summary, the CFC of FFF is not sensitive to different fracture permeability fields generated with different realizations and the correlation lengths considered here.

6.9 ALTERNATIVE CONCEPTUAL MODELS AND SENSITIVITY ANALYSIS

6.9.1 Alternative Seepage Prediction Models

The main alternative conceptual model, consistent with available data, is the discrete fracture-network model (DFNM). This has been discussed in BSC (2004 [DIRS 170034], Section 6.4.1) and will not be repeated here (see also Section 6.3 of this report). The results of the discussions in BSC (2004 [DIRS 170034], Section 6.4.1) may be summarized as follows. The development of a defensible DFNM requires collecting a very large amount of geometric and hydrological data from the fracture network, which are mostly unavailable. Moreover, unsaturated hydrological parameters on the scale of individual fractures are required, along with conceptual models and simplifying assumptions regarding unsaturated flow within fractures and across fracture intersections. Thus, the parsimony of the continuum model is considered a key advantage over the complexity of the DFNM, which is difficult to support or justify in spite of its visual appeal. Moreover, a two-dimensional DFNM is not capable of capturing flow diversion within the fracture plane, a mechanism appropriately represented by a two-dimensional (or three-dimensional) continuum model. Hence, the full development of a DFNM as a potential alternative to the base-case continuum model is considered unwarranted.

Another alternative conceptual model is that of a drift in a homogeneous constant-property medium (Philip et al. 1989 [DIRS 105743], pp. 17 to 21). Seepage into drift under conditions discussed in this report is controlled by heterogeneity-induced channeling and local ponding (Birkholzer et al. 1999 [DIRS 105170], pp. 358 to 384), which occurs much earlier than if the medium is homogeneous. In other words, the homogenous, constant-property model would predict seepage to occur at a threshold that is orders of magnitude larger. In this sense, Philip's boundary-layer-flow regime near the drift crown (Philip et al. 1989 [DIRS 105743], p. 21, Figure 1) should not be used to define the required grid size. Note that in this report, the same conceptual approach and the same level of grid refinement as in the SCM are used. The calibration procedure accounts for the selected grid size by matching results with field data.

Another possible alternative could be a two-dimensional conceptual model. However, the drift seepage problem involves the accumulation of unsaturated flow at the location near the drift wall. This accumulation continues until the local saturation is large and capillary suction is small. Then seepage into drift occurs. This problem is intrinsically a three-dimensional problem

because flow accumulation at a two-dimensional location could easily disappear if it is allowed to flow away in the third dimension. Two-dimensional models would consequently overestimate seepage.

The present report considers spatial correlation lengths using a spherical correlation structure and a Gaussian field. There have been suggestions to use alternative geostatistical methods, such as nonparametric representations of the heterogeneity field and multiple-scale correlation structures. However, for a specific problem with a particular scale of a drift, such complications are not needed so long as the parameters used are appropriate to this scale.

The above discussions cover uncertainty related to the conceptual model. The continuum model is considered the best model for the SMPA not only because of these discussions, but also because it makes the SMPA consistent with the SCM (BSC 2004 [DIRS 170034]), which has gone through calibration and validation against field data and observation. This adds confidence to the SMPA.

Concerning parameter uncertainty, the report has made a comprehensive study by conducting Monte Carlo simulations on seepage into drift over wide ranges of parameters covering uncertainties in flow fields and rock properties. The sensitivity of different parameters is an integral part of the results and analysis presented in Section 6.6. It is recognized that parameter uncertainty is different from parameter variability. The latter is represented by the σ and λ parameters discussed in Sections 6.3.3 and 6.3.5; the sensitivity of seepage on those parameters is discussed in Section 6.6.2.

Uncertainty associated with geostatistics (i.e., different realizations corresponding to the same input parameters of k_{FC} , σ , and λ) is evaluated through calculations of 20 realizations for each case (10 for sensitivity studies). In general, establishing geostatistical probability can require more realizations than 20, but the great number of three-dimensional simulations in this report make it impractical to do more realizations. Nevertheless, the spread of results from the 20 realizations does give an indication of geostatistical variation.

6.9.2 Alternative Flow Focusing Model

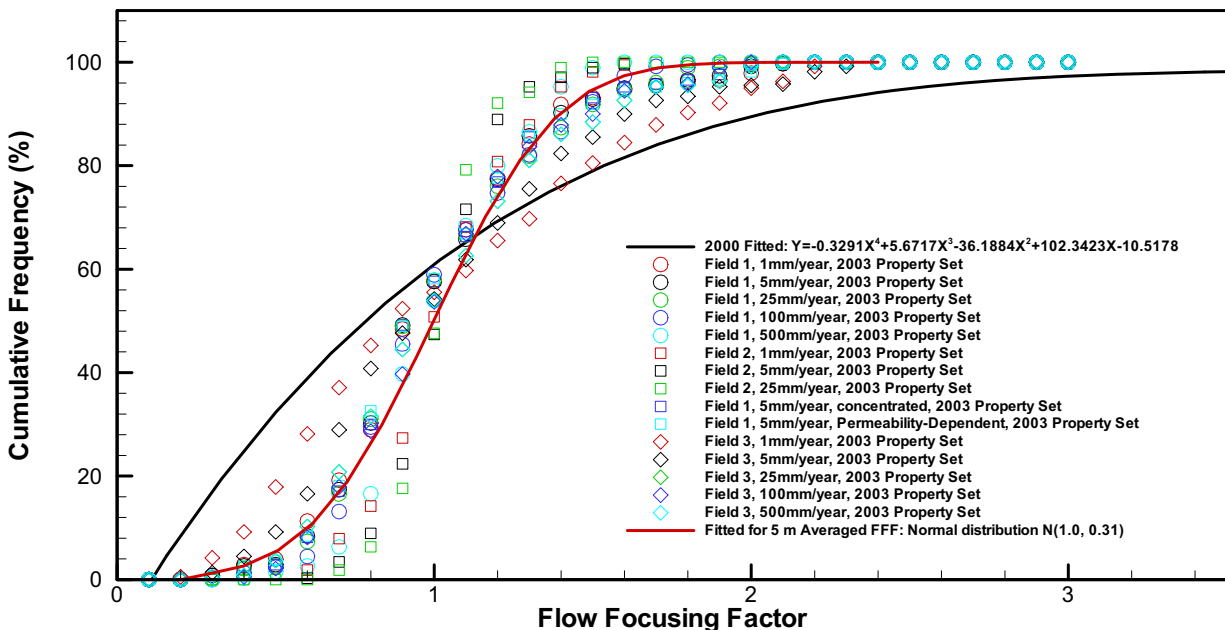
As discussed in Section 6.8.1, the FFF was determined for a gridblock width of 0.25 m. Considering the drift diameter, the horizontal dimension for the seepage models is approximately 5 m. Therefore, the averaged FFF over the sum width should be used. Fifteen flow fields were created analogous to those discussed in Section 6.8.2 (which are based on the property set developed in the year 2000, see Table 4-5), and the resulting FFFs were averaged over 5-m long sections along the bottom boundary. In addition, a different drift-scale fracture property set (referred to as 2003 set) was used (see Table 6-5 below). Comparison of the two property sets (see Tables 4-5 and 6-5) shows two major differences: first, fracture permeability in the 2003 set is two orders of magnitude lower than the 2000 set, because the 2003 set is for smaller-scale models (which excludes large-scale features); second, the capillarity (capillary strength α_F^{-1}) of the fracture system in the 2003 set is higher than that in the 2000 set. A higher capillarity causes more lateral diversion of liquid flow and results in more flow focusing. All other parameters are identical to those used for the model described in Section 6.8.

Table 6-5. The 2003 Set of Fracture Properties Used in Alternative Flow Focusing Modeling Study

| Model Layer | Permeability | van Genuchten Parameters | | Porosity | Residual Saturation |
|-------------|--------------------|--------------------------|--------------|-----------------|---------------------|
| | k_F (m^2) | α_F (1/Pa) | m_F (-) | ϕ_F (-) | S_{rf} (-) |
| TSw31 | 8.13E-13 | 1.60E-5 | 0.633 | 5.0E-3 | 0.01 |
| TSw32 | 7.08E-13 | 1.00E-4 | 0.633 | 8.3E-3 | 0.01 |
| TSw33 | 7.76E-13 | 1.59E-3 | 0.633 | 5.8E-3 | 0.01 |
| TSw34 | 3.31E-13 | 1.04E-4 | 0.633 | 8.5E-3 | 0.01 |
| TSw35 | 9.12E-13 | 1.02E-4 | 0.633 | 9.6E-3 | 0.01 |

DTNs: LB0208UZDSCPMI.002 [DIRS 161243] and
LB0205REVUZPRP.001 [DIRS 159525].

Figure 6-28 shows the CFCs of FFF averaged over 5 m width at the bottom boundary, based on 15 study cases using the 2003 property set. The 5-m averaged FFFs range from 0.2 to 2.4 for all the 15 study cases, indicating that it is less focused than the flow focusing obtained with a grid width of 0.25 m, as expected. The cumulative frequency of FFFs is well represented by a normal distribution with a mean of 1.0 and a standard deviation of 0.31, with cut-off values at 0.2 and 2.4.



Output DTN: LB0406U0075FCS.002.

Figure 6-28. Cumulative Frequency Curves of Flow Focusing Factor, Averaged over 5 m Horizontal Width, on the Bottom Boundary for the 15 Different Study Cases, Obtained for the 2003 Calibrated Fracture Property Set, as well as the Generalized CFCs for a Gridblock Width of 0.25 m

INTENTIONALLY LEFT BLANK

7. VALIDATION

The model validation activities and acceptance criteria presented in the remainder of this section follow those of the TWP's for this report (BSC 2002 [DIRS 160819], Attachment I, Section I-4-2-1; BSC 2004 [DIRS 169654], Section 2.2.1.4) for the SMPA including drift collapse and flow-focusing models, respectively and they exceed the Level I validation activities. Confidence in the adequacy of the SMPA including drift collapse and the flow-focusing model for their intended uses has been gained during the model development process as well as through post development validation activities. The validation approach, based on the intended use for the SMPA including drift collapse and flow-focusing model, has previously been planned and includes confidence building during model development and postdevelopment model activities. Data used to develop the model are not used in postdevelopment model validation activities.

Confidence building during development of the SMPA has included ensuring consistency with the SCM (BSC 2004 [DIRS 170034]) and using wide ranges of values for key parameters affecting seepage, namely fracture continuum permeability, capillary strength, and percolation flux. The sensitivity of seepage results to these and other parameters has been evaluated. It was determined from these evaluations that expected changes in permeability as a result of potential irreversible THM and THC processes (BSC 2004 [DIRS 169864]; BSC 2004 [DIRS 169856]) are within the range of fracture-continuum permeability investigated in this report.

Confidence building during development of the flow-focusing model has included ensuring consistency with the UZ model (BSC 2004 [DIRS 169861]) and conducting sensitivity studies. Thus flow focusing sensitivity analyses were conducted with respect to (a) the mean infiltration rates on the top boundary (1, 5, 25, 100, and 500 mm/year), (b) the spatial distribution of the released water at top boundary (uniform, concentrated, and permeability-dependent), and (c) different realizations (three random fields) and different correlation lengths. Results of these sensitivity calculations have contributed to confidence in the results.

7.1 CONFIDENCE BUILDING DURING MODEL DEVELOPMENT TO ESTABLISH SCIENTIFIC BASIS AND ACCURACY FOR INTENDED USE

For Level I validation, Section 2.2.1.4 of TWP-MGR-HS-000001 REV 00 (BSC 2004 [DIRS 169654]) provides guidelines for Confidence Building During Model Development: The development of the flow-focusing model will be documented in accordance with the requirements of Section 5.3.2(b) of AP-SIII.10Q. The development of the seepage model for PA including drift collapse has been conducted according to these criteria, as follows:

1. *Selection of input parameters and/or input data, and a discussion of how the selection process builds confidence in the model [AP-SIII.10Q 5.3.2(b) (1) and AP-2.27Q Attachment 3 Level I (a)]*

The types and quality of the data selected as input builds confidence in the model. The inputs to the thermal-hydrological seepage model have all been obtained from controlled sources. Section 4.1, Tables 4-1 through 4-5, identify the data and design parameters used. Discussions of parameter ranges and uncertainties

are covered in Section 6.3 and model assumptions have been described in Section 5. Thus, this requirement can be considered satisfied.

2. *Description of calibration activities, and/or initial boundary condition runs, and/or run convergences, and/or simulation conditions set up to span the range of intended use and avoid inconsistent outputs, and a discussion of how the activity or activities build confidence in the model. Inclusion of a discussion of impacts of any non-convergence runs [AP-SIII.10Q 5.3.2(b)(2) and AP-2.27Q Attachment 3 Level I (e)]*

As noted in Section 6.1, calibration activities are performed in the upstream SCM, which provides the underlying conceptual framework for the SMPA including drift collapse. Detailed discussion of the model domain and boundary conditions for the SMPA including drift collapse can be found in Sections 6.1, 6.2, and 6.3.1. Conditions analyzed included evaluation of the impact of drift degradation in Section 6.4, the effects of rockbolts in Section 6.5 and consideration of the long term THC and THM effects on seepage in Section 6.7. These conditions build confidence in the model's ability to appropriately span the range of its intended use. Section 6.6 provides a detailed discussion of various model results (i.e., those of convergence runs). Discussion about non-convergence runs is not relevant for this model report.

The model domain and boundary conditions for flow focusing are discussed in Section 6.8.1. Section 6.8.2 provides a discussion of the results of the flow focusing simulations. Thus, this requirement can also be considered satisfied.

3. *Discussion of the impacts of uncertainties to the model results, including how the model results represent the range of possible outcomes consistent with important uncertainties [AP-SIII.10Q 5.3.2(b)(3) and AP-2.27Q Attachment 3 Level 1 (d) and (f)]*

Uncertainties in the characteristics of the natural system are explicitly considered in the seepage calculations as ranges of the parameters described in Section 6.3. The parameter ranges are technically defensible and reasonably account for system uncertainties and variabilities. The results and sensitivities are discussed in Sections 6.6 and 6.8.

7.2 CONFIDENCE BUILDING AFTER MODEL DEVELOPMENT TO SUPPORT THE SCIENTIFIC BASIS OF THE MODEL

Postdevelopment model validation activities were performed. Postdevelopment-validation of the SMPA is discussed in Section 7.3; postdevelopment validation of the flow focusing model is discussed in Section 7.4.

7.3 VALIDATION OF SEEPAGE MODEL FOR PERFORMANCE ASSESSMENT

The purpose of the SMPA is to provide results of drift-scale seepage rates under a series of parameters and scenarios in support of the TSPA-LA. The intended use of the SMPA is to

evaluate drift-scale seepage rates under the full range of parameter values for three parameters found to be key (fracture permeability, the van Genuchten $1/\alpha$ parameter, and percolation flux) and drift degradation shape scenarios in support of the TSPA-LA during the period of compliance for postclosure performance.

A comparison is made of the SMPA results with an alternative mathematical model, the SCM (BSC 2004 [DIRS 170034]), which has gone through calibration and validation against field data and observations. The basic idea is that, since the SCM has been validated against field data and observations, by demonstrating the consistency between the SMPA and the SCM, the SMPA can be considered to be consistent with these available field data and observations. The rationale for their use for the SCM and indirectly for the SMPA is as follows:

- (a) Short-term seepage test data contain transient behavior in addition to long term behavior relevant to PA. The physics of both behaviors are governed by the same equations, with long term part representing steady-state limit of the transient part. In this sense, the transient behavior is also a good test of the physics of the seepage process modeled by the SCM and SMPA.
- (b) In SCM studies of field data, time-dependent liquid release, as well as transient flow, storage and seepage processes are taken into account. In other words, short-term transient effects have been accounted for in SCM modeling, and will not be confused with the long-term seepage behavior. In this way the underlying long-term part of the data is used for validating our models.
- (c) An attempt has been made in the field tests modeled by the SCM for the tests to be close to steady state condition, so that data would better represent the long-term behavior.

According to TWP (BSC 2004 [DIRS 169654]), results from the SMPA are to be compared with those of the SCM (BSC 2004 [DIRS 170034]) for a particular case. Agreement of the results within 20 percent will be the criterion for accepting the SMPA as having been validated sufficiently for the purpose of LA. This acceptance criterion is adequate given that the sensitivity analyses performed to evaluate the relative importance of seepage to the performance of the repository system indicate that even much larger changes in seepage rates do not significantly affect the mean annual dose estimate for the nominal scenario (BSC 2003 [DIRS 168796], Section 3.3.2). The SCM calculations were carried out using a range of permeability, capillary, and percolation flux values on ten realizations of the heterogeneous field generated for the SCM (Wang 2003 [DIRS 162319], SN-LBNL-SCI-228-V1, pp. 38 to 41). The results are presented in Table 7-1. In this table, the first three columns indicate the many cases with different parameter values of $(\log k, 1/\alpha, Q_p)$, for which the simulations were performed. The fourth column gives the mean over 10 realizations of the seepage percentage, calculated by the SCM using the definition of seepage percentage in this report (Section 6.6). In the SCM, the drift diameter is 5 m, slightly different from the drift diameter of 5.5 m used in the SMPA, and $\lambda = 0.2$ m as compared with $\lambda = 0.3$ m in the SMPA. The SCM results are compared with those of the SMPA (the fifth column in Table 7-1), taken from Section 6.6.1, which are the mean seepage percentages calculated from results using 20 realizations of the heterogeneous permeability field generated for the SMPA. Differences are

on the order of 2 percent or less, and this meets the criterion for accepting the SMPA as having been validated sufficiently for the purpose of LA.

Table 7-1. Comparison Between Mean Seepage Percentages of the SMPA (20 Realizations) and the SCM (10 Realizations)

| log(k) | 1/α | Q _p | Seepage % SCM (mean over 10 realizations) | Seepage % SMPA (mean over 20 realizations) | SMPA % – SCM % |
|--------|--------|----------------|---|--|----------------|
| -13.00 | 200.00 | 200.00 | 99.28 | 98.64 | -0.64 |
| -12.00 | 200.00 | 200.00 | 96.43 | 95.43 | -1.00 |
| -11.00 | 200.00 | 200.00 | 85.49 | 83.86 | -1.63 |
| -13.00 | 400.00 | 200.00 | 92.15 | 90.79 | -1.36 |
| -12.00 | 400.00 | 200.00 | 70.17 | 68.65 | -1.52 |
| -11.00 | 400.00 | 200.00 | 14.01 | 14.55 | 0.54 |
| -13.00 | 600.00 | 200.00 | 79.73 | 77.87 | -1.86 |
| -12.00 | 600.00 | 200.00 | 31.70 | 30.97 | -0.73 |
| -11.00 | 600.00 | 200.00 | 0.01 | 0.00 | -0.01 |
| -13.00 | 200.00 | 500.00 | 99.67 | 99.16 | -0.51 |
| -12.00 | 200.00 | 500.00 | 98.06 | 97.26 | -0.80 |
| -11.00 | 200.00 | 500.00 | 91.43 | 89.98 | -1.45 |
| -13.00 | 400.00 | 500.00 | 95.68 | 94.88 | -0.80 |
| -12.00 | 400.00 | 500.00 | 82.37 | 80.63 | -1.74 |
| -11.00 | 400.00 | 500.00 | 39.36 | 38.09 | -1.27 |
| -13.00 | 600.00 | 500.00 | 88.12 | 86.62 | -1.50 |
| -12.00 | 600.00 | 500.00 | 56.28 | 54.40 | -1.88 |
| -11.00 | 600.00 | 500.00 | 2.94 | 3.14 | 0.20 |
| -13.00 | 200.00 | 800.00 | 99.92 | 99.47 | -0.45 |
| -12.00 | 200.00 | 800.00 | 98.60 | 97.88 | -0.72 |
| -11.00 | 200.00 | 800.00 | 93.58 | 92.26 | -1.32 |
| -13.00 | 400.00 | 800.00 | 96.92 | 96.41 | -0.51 |
| -12.00 | 400.00 | 800.00 | 86.45 | 84.84 | -1.61 |
| -11.00 | 400.00 | 800.00 | 52.06 | 50.11 | -1.95 |
| -13.00 | 600.00 | 800.00 | 91.15 | 90.02 | -1.13 |
| -12.00 | 600.00 | 800.00 | 65.74 | 64.33 | -1.41 |
| -11.00 | 600.00 | 800.00 | 8.61 | 9.15 | 0.54 |

Output DTN: LB0304SMDCREV2.002.

SCM=seepage calibration model; SMPA= seepage model for performance assessment

7.4 VALIDATION OF FLOW FOCUSING MODEL

The intended use of the model for flow focusing in the TSw unit is to provide an estimate of FFFs that (1) bridge the gap between the mountain-scale and drift-scale models, and (2) account for variability in local percolation flux due to stochastic hydrologic properties and flow processes. While no direct observation of flow focusing is available, the concept of local flow redistribution can be corroborated by qualitative evidence of preferential flow paths occurring at Yucca Mountain. For example, secondary minerals form coatings on fracture foot walls and

cavity floors as calcite or silica deposits precipitate by percolating water. Whelan et al. (2002 [DIRS 160442], p. 738) report heterogeneous distribution of these minerals within the UZ, with fewer than 6 percent of fractures (longer than 1 m) mineralized. This indicates that not all fractures contribute to downward flow, qualitatively supporting the concept of flow focusing. A quantitative comparison between the fraction of fractures with mineral coatings and FFFs is difficult because (1) the percentage of coated fractures is an areal measure that cannot be directly related to the amount of water flowing along these fractures; (2) mineralization is affected by many factors and processes, i.e., not all flow channels induce mineral precipitation; and (3) fracture coating data reflect small-scale flow channeling effects that are not (and do not need to be) included in the FFFs to be used for the estimation of local percolation flux on the drift scale. Also note that calcite deposits in lithophysal cavities are affected by the capillary barrier effect; furthermore, they may not reflect fracture flow but capillary wicking through the matrix. Nevertheless, the observed heterogeneity in mineral deposits on fracture walls as reported in Whelan et al. (2002 [DIRS 160442]) qualitatively supports the concept of flow focusing. Deriving an approximate FFF of 17 from the areal fracture coating data of 6 percent represents an upper bound that is not inconsistent with the FFF distribution derived from the high-resolution model discussed in Section 6.8. The modeling results, which predict relatively mild flow focusing, is further supported by the observed distribution of water potentials in the TSw, which is nearly uniform, indicating that there are many small flow paths instead of a few large flow channels.

An alternative conceptual model for estimating bounds on FFFs was presented in CRWMS M&O (2001 [DIRS 154291], Section 6.4.3.2). This model derives FFFs using estimates of the spacing of actively flowing fractures based on the active fracture model (Liu et al. 1998 [DIRS 105729]) and a simple weeps model, resulting in maximum FFFs between 9.7 and 47, depending on which climate scenario was applied. These factors are considered to represent upper bounds because (1) the evaluation of active fracture spacing addresses small-scale heterogeneity, and (2) the weeps model assumes that water is focused into fully saturated flow channels with completely dry fractures in between.

7.5 PUBLICATION IN PEER REVIEWED JOURNALS

For corroboration, the SMPA has also been published in the open scientific literature (Birkholzer et al. 1999 [DIRS 105170], pp. 349 to 384; Li and Tsang 2003 [DIRS 163714]), having gone through anonymous technical review and public scientific scrutiny. Furthermore, the basic formulations of physical processes implemented in the SMPA, as represented by Richards' equation (Richards 1931 [DIRS 104252], pp. 318 to 333), the van Genuchten-Mualem model (Luckner et al. 1989 [DIRS 100590], pp. 2191 to 2192), Philip's studies (Philip et al. 1989 [DIRS 105743], pp. 16 to 28), effects of flow channeling resulting from heterogeneity and ponding (Birkholzer and Tsang 1997 [DIRS 119397], pp. 2221 to 2224; Birkholzer et al. 1999 [DIRS 105170], pp. 370 to 379), and the flow focusing study (Bodvarsson et al. 2003 [DIRS 163443], pp. 23 to 42) are all in the open literature, have gone through proper technical review, and have withstood scrutiny of the scientific community since their dates of publication.

7.6 SUMMARY

The seepage model for PA requires Level 1 validation, and is considered validated for its intended purpose by meeting the acceptance criterion of successful comparison to an alternative model that is calibrated and validated against field data. The flow focusing model is considered validated for its intended purpose by meeting the acceptance criteria of being qualitatively supported by observational data of flow channeling effects, and by being consistent with upper bound estimates provided by an alternative conceptual model. Both models have been published in peer-reviewed journals. No further validation activities are needed.

Criteria for confidence building during model development have also been satisfied. The model development activities and postdevelopment validation activities described establish the scientific bases for the seepage model for PA including drift collapse. Based on this, the seepage models and flow focusing representations used in this report are considered to be sufficiently accurate and adequate for the intended purpose and to the level of confidence required by the model's relative importance to the potential performance of the repository system.

8. CONCLUSIONS

8.1 SUMMARY

The present report is based on the SCM (BSC 2004 [DIRS 170034]) and a review of available in situ field data appropriate to the Tptpmn and the Tptpll. The model has been previously described in Birkholzer et al. (1999 [DIRS 105170]). The FEPs in Table 6-2 are addressed in this model. In reviewing available information (Sections 6.3 to 6.5), ranges of parameters were selected, over which seepage calculations were conducted. All eight items in the work scope in Section 1 have been accomplished: the SMPA has been developed, parameter ranges selected, simulations designed and performed, drift-collapse results reviewed, degradation profiles constructed (and simulations performed accordingly), and impact of rock bolts evaluated. Finally, these results are in partial support of FEP evaluation, as discussed in Section 6.2.2.

The results (Figures 6-4 to 6-21) show the impact of various factors on seepage, and calculated data are provided to TDMS for PA to develop probability distributions. Generally, seepage is found to be larger for smaller fracture continuum permeability (k_{FC}), smaller van Genuchten parameter ($1/\alpha$) and larger percolation flux (Q_p) values. This is very reasonable, since a small k_{FC} reduces flow diversion around the drift, and a small $1/\alpha$ parameter represents a small capillary strength and, thus, a small capillary barrier effect. In addition, a larger Q_p provides more water into the system to induce higher seepage. These results form a useful data set for model abstraction for TSPA.

A series of numerical studies have been conducted to evaluate flow focusing through fractures from the bottom of the PTn to the repository horizon (see Section 6.8). The studies were carried out using a 100 m wide and 150 m deep two-dimensional flow domain and covered the upper five hydrogeologic units of the TSw at Yucca Mountain. Three heterogeneous fracture-permeability fields were generated using a stochastic approach, representing different realizations and different correlation lengths. Sensitivity analyses were conducted regarding mean infiltration rates, realizations and correlation lengths, and uniform/nonuniform infiltration distribution on the top boundary. These sensitivity analyses indicate that statistically similar CFCs of FFF are obtained, allowing the development of a generalized distribution function of FFFs that can be applied to all conditions. Different distribution functions are obtained for different fracture reference scales.

Below is a description of how the acceptance criteria defined in Section 4.2 are satisfied in this report.

8.2 LIMITATIONS

The results in this report are based on available site data and on the SCM (BSC 2004 [DIRS 170034]), and are dependent on the continuum conceptual model. Further, this report is on ambient conditions. Transient short-term THC and THM effects (BSC 2004 [DIRS 169856]; BSC 2004 [DIRS 169864]) are not considered. Application of results should be within these limits.

This report demonstrates that the impact of mechanical effects such as rockfalls and fracture dilation can be evaluated (Sections 6.4 and 6.5). This work builds on BSC (2004 [DIRS 166107]), which includes fracture-dilation scoping analyses. These reports also considered thermal and seismic effects on drift degradation. The impact of mechanical effects on seepage is, thus, limited to the scenarios evaluated by the upstream models (BSC 2004 [DIRS 169864]).

Reasonable changes in the input data used to establish ranges of parameter values used in this report would not affect the choice of these ranges. For example, the permeability data are used to establish a range of values for the simulations. These permeability data could change by an order of magnitude, yet still be within the selected range and not affect the sets of results.

The FFFs derived in Section 6.8 are limited in that they can only be used to estimate local percolation fluxes for a drift-scale model.

8.3 RECOMMENDATIONS

No recommendation.

8.4 HOW THE ACCEPTANCE CRITERIA ARE ADDRESSED

The following information describes how this analysis addresses the acceptance criteria in the Yucca Mountain Review Plan (NRC 2003 [DIRS 163274], Sections 2.2.1.3.3.3 and 2.2.1.3.6.3). In most cases, the applicable acceptance criteria are not addressed solely by this report; rather, the acceptance criteria are fully addressed when this report is considered in conjunction with other analysis and reports that describe drift seepage and flow paths in the UZ. Only those acceptance criteria that are applicable to this report (see Section 4.2) are discussed.

Acceptance Criteria from Section 2.2.1.3.3.3, Quantity and Chemistry of Water Contacting Engineered Barriers and Waste Forms

- **Acceptance Criterion 1: *System Description and Model Integration Are Adequate.***
 - (1) Elements of this report that feed into the TSPA and related abstractions adequately incorporate drift geometry (Section 6.3.1), fracture permeability (Section 6.3.2), van Genuchten capillary-strength parameters (Section 6.3.4), percolation flux (Section 6.3.6), drift degradation impact (Section 6.4), effects of rock bolts (Section 6.5), and other parameters, couplings, and features that affect drift seepage and flow paths in the UZ (as shown in other Section 6 sections) related to this analysis.
 - (2) The model developed in this report is consistent with the models and analyses developed for the abstractions of “Climate and Infiltration” and “Flow Paths in the Unsaturated Zone.” This consistency is shown by analyses of climate changes (Sections 6.6 and 6.8) and incorporation in the seepage abstraction of appropriate flow focusing factors multiplied with the percolation flux distribution from the site-scale model (Section 6.8). The descriptions and technical bases provided in this report for the development of flow focusing factors and consideration of

climate changes are presented by the detailed references to cited material and data in Section 6.8.

- (4) Modeling and analysis of long term coupled thermal-hydrological mechanical processes are presented in Sections 6.7. The potential for flow focusing is analyzed in Section 6.8.
- (5) Sufficient technical bases and justification are provided for total system performance assessment assumptions and approximations for modeling coupled thermal-hydrologic-mechanical-chemical effects on seepage and flow through long term analysis in Section 6.7 and through the flow-focusing analysis presented in Section 6.8.
- (8) Adequate technical bases are provided through use of field data (Section 4.1) and sensitivity studies investigating the effect of varying the van Genuchten parameter $1/\alpha$, fracture permeability, and percolation flux described in Section 6.1.1.

Acceptance Criterion 2: *Data are Sufficient for Model Justification.*

- (1) Data employed in developing this model are justified in the references cited in Section 4.1 and in the development of the model in Section 6.3, which discusses selection of parameter ranges. Section 6.3 provides an adequate description of how the data were used, interpreted, and appropriately synthesized into the parameters.
- (2) Initial conditions and boundary conditions reflecting expected and future climate conditions (Section 6.3.6) and the expected influence of stratigraphic layers (Sections 4.1, 6.2, and 6.3.2 through 6.3.4) at Yucca Mountain (from interpretation of borehole samples and tests) are incorporated in the model.

• **Acceptance Criterion 3: *Data Uncertainty is Characterized and Propagated Through the Model Abstraction.***

- (1) Seepage calculations (via the SMPA) use parameter values and ranges that are technically defensible, reasonably account for uncertainties and variabilities, and do not result in an under-representation of risk (Section 6.3). The technical bases for the parameter values used in calculations are provided in Section 6.3 and were conservatively chosen. For example, the limits of the range of k_{FC} are moved toward lower values that result in more seepage, which results in a conservative approach toward seepage. Accordingly, the model is conservative and does not result in an under-representation of the risk estimate.
- (4) Uncertainties in the characteristics of the natural system are explicitly considered in the seepage calculations as ranges of parameters (see Sections 6.3.7 and 6.9.1) through Monte Carlo analyses.

- **Acceptance Criterion 4: *Model Uncertainty is Characterized and Propagated Through the Model Abstraction.***

- (1) Alternative modeling approaches have been investigated in the upstream SCM that feeds into this model report (Section 6.3). Section 6.9 cites available data and current scientific understanding in analyzing alternative conceptual models that were considered. These models were investigated, their results and limitations were appropriately considered, and they were determined not to enhance the analysis of the Yucca Mountain drift seepage over that of the chosen model, the SMPA.
- (2) Alternative modeling approaches have been investigated in the upstream SCM that feeds into this model report (Section 6.3). Section 6.9 analyzes alternative conceptual models that were considered, including a discrete fracture-network model, a model with the drift in a homogeneous constant-property medium, a 2-D conceptual model, and an alternative flow-focusing model. These models were investigated, their results and limitations appropriately considered, and they were determined not to enhance the analysis of the Yucca Mountain drift seepage over that of the chosen model, the SMPA.
- (3) The SMPA was calibrated against the SCM, which was calibrated against Yucca Mountain seepage characterization data (see Sections 6.3 and 7.1). Model uncertainty is mitigated by the choice of conservative parameters (Section 6.3) and the calibration of the model to the SCM, both of which result in model uncertainty that does not result in under-representation of risk.
- (4) Adequate consideration is given to effects of thermal-hydrologic-mechanical-chemical coupled processes in Section 6.7. Section 6.7 concludes that thermal effects (elevated temperature in and around the drift) increase the likelihood of flow being diverted around the drift. The effects of change of drift size and geometry due to drift collapse from thermal or other influences are analyzed in Section 6.4.

Acceptance Criteria from Section 2.2.1.3.6.3, *Flow Paths in the Unsaturated Zone*

- **Acceptance Criterion 1: *System Description and Model Integration Are Adequate.***

- (1) Elements of this report that feed into the TSPA and abstractions adequately incorporate drift geometry (Section 6.3.1), fracture permeability (Section 6.3.2), van Genuchten capillary-strength parameters (Section 6.3.4), percolation flux (Section 6.3.6), drift degradation impact (Section 6.4), effects of rock bolts (Section 6.5), and other parameters, couplings, and features that affect drift seepage (as shown in other Section 6 sections) related to this analysis.

- (2) All aspects of geology and hydrology affecting flow paths in the UZ are adequately considered in the seepage calculation through use of input flux on model domain and heterogeneous flow domain containing the drift (see Sections 6.3.2, 6.3.3, 6.3.5, and 6.3.6).
- (6) Adequate spatial variability of model parameters is used to construct the flow domain for calculating flow paths in the unsaturated zone and seepage flux (see Sections 6.3.2, 6.3.3, and 6.3.5). Spatial variability of boundary conditions is incorporated through consideration of infiltration distribution for the top boundary and its effect on flow focusing (Section 6.8.2).
- (7) The derivation, data, and rationale used in determining average parameters incorporated in this model are discussed in detail in Sections 6.3.2 through 6.3.7. The selection of these parameters reflects temporal and spatial discretizations considered in the model by consideration of long-term coupled thermal-hydrological-chemical processes (Section 6.7), changes in drift geometry over time (Section 6.6.3), spatial and temporal distribution of percolation fluxes (Section 6.8), and other parametric effects (Sections 6.2 through 6.5).

Acceptance Criterion 2: *Data Are Sufficient for Model Justification.*

- (1) The values and sources of the hydrologic parameters used as direct input to the model are listed in Section 4.1 (Table 4-1). The derivations, interpretations, and justifications for use of data incorporated in this model are discussed in detail in Sections 6.3.2 through 6.3.7 and 6.5. The data is incorporated into average parameters, as noted in Acceptance Criteria 1 (7), and includes adequate consideration of both hydrological processes (Sections 6.2 through 6.6) and long-term coupled thermal-hydrological-chemical processes (Section 6.7).
- (2) The values and sources of the hydrologic parameters used as direct input to the model are listed in Section 4.1 (Table 4-1). These data were collected using acceptable techniques that are described and justified in the input source documents listed in Table 4-1.
- (5) Parameter uncertainty was studied by use of Monte Carlo simulations on seepage into drift over wide ranges of parameters covering uncertainties in flow fields and rock properties (Section 6.9.1). Sensitivity analyses were also conducted for flow focusing factors, including mean infiltration rates, realizations and correlation lengths, and uniform/nonuniform infiltration distribution on the top boundary (Section 6.8.2).
- (6) Approved QA procedures identified in the TWP (BSC 2004 [DIRS 169654], Section 4) have been used to conduct and document the activities described in this model report. The calibration of the SMPA model was accomplished via predictive simulations against high-rate liquid-release tests performed with the SCM, which was calibrated against actual seepage data (see Sections 6.3 and 7.1).

- (7) The SMPA is a reasonably complete (process-level), fracture continuum conceptual model as explained in Section 6.2.1. The SMPA uses the same conceptual framework as in the SCM, with the same level of grid-design refinement. The choice of a continuum model is justified in Section 6.2.1. As noted in Acceptance Criterion 2 (6), above, the SMPA was calibrated against the SCM, which was calibrated against Yucca Mountain seepage data. Extrapolated seepage predictions performed with the SMPA were also found to be consistent with the synthetically generated data from the discrete fracture model under low percolation conditions (Section 6.3).

Acceptance Criterion 3: *Data Uncertainty Is Characterized and Propagated through the Model Abstraction.*

- (1) Seepage calculations (via the SMPA) use parameter values and ranges that are technically defensible, reasonably account for uncertainties and variabilities, and do not result in an under-representation of risk (Section 6.3). The technical bases for the parameter values used in calculations are provided in Section 6.3 and were conservatively chosen. For example, the limits of the range of k_{FC} are moved toward lower values that result in more seepage, which results in a conservative approach toward seepage.
- (4) The initial conditions and boundary conditions used in drift wall (Section 6.3.1) and percolation flux upper boundary (in flow focusing studies, Section 6.8.2) are consistent with the range of possibilities and available data used in sensitivity analyses. The computational domain (the SMPA model and codes) parameters are consistent with available data and boundary conditions as described in Sections 6.3.1 through 6.3.7.
- (5) The impact of coupled processes is adequately discussed in the seepage results (Section 6.7).
- (6) Uncertainties in the characteristics of the natural system are explicitly considered in the seepage calculations as ranges of parameters (see Sections 6.3.7 and 6.9.1) through Monte Carlo analyses.

8.5 OUTPUT DTNS

Table 8-1 summarizes the DTNs containing the data developed in the current or previous revisions of this report. They have been submitted to the TDMS. Descriptions of the files found in these DTNs are given in Appendix A. No confirmatory actions were taken as they are not in the TWP.

Table 8-1. Output DTNs

| Data Tracking Number | Description |
|-----------------------------|--|
| LB0304SMDCREV2.001 | Input and output files supporting analyses of drift seepage |
| LB0304SMDCREV2.002 | Summary figures and tables of drift seepage analyses, presented in Section 6.6 |
| LB0304SMDCREV2.003 | Input and output files supporting analyses of THM effects, discussed in Section 6.7 |
| LB0304SMDCREV2.004 | Summary figure of drift THM effects on drift seepage, presented as Figure 6-22. |
| LB0307SEEPDRCL.001 | Input and output files supporting analyses of seepage into collapsed drift |
| LB0307SEEPDRCL.002 | Look-up table for seepage into collapsed drifts |
| LB0406U0075FCS.001 | Simulation files for flow focusing factors discussed in Sections 6.8 and 6.9.2 |
| LB0406U0075FCS.002 | Summary files for flow focusing factor distributions discussed in Sections 6.8 and 6.9.2 |

INTENTIONALLY LEFT BLANK

9. INPUTS AND REFERENCES

9.1 DOCUMENTS CITED

- Birkholzer, J. and Tsang, C.F. 1997. "Solute Channeling in Unsaturated Heterogeneous Porous Media." *Water Resources Research*, 33, (10), 2221-2238. Washington, D.C.: American Geophysical Union. TIC: 235675. 119397
- Birkholzer, J.; Li, G.; Tsang, C-F.; and Tsang, Y. 1999. "Modeling Studies and Analysis of Seepage into Drifts at Yucca Mountain." *Journal of Contaminant Hydrology*, 38, (1-3), 349-384. New York, New York: Elsevier. TIC: 244160. 105170
- Bodvarsson, G.S.; Wu, Y-S.; and Zhang, K. 2003. "Development of Discrete Flow Paths in Unsaturated Fractures at Yucca Mountain." *Journal of Contaminant Hydrology*, 62-63, 23-42. New York, New York: Elsevier. TIC: 254205. 163443
- Brekke, T.L.; Cording, E.J.; Daemen, J.; Hart, R.D.; Hudson, J.A.; Kaiser, P.K.; and Pelizza, S. 1999. *Panel Report on the Drift Stability Workshop, Las Vegas, Nevada, December 9-11, 1998*. Las Vegas, Nevada: Management and Technical Support Services. ACC: MOL.19990331.0102. 119404
- BSC (Bechtel SAIC Company) 2001. *Drift Degradation Analysis*. ANL-EBS-MD-000027 REV 01 ICN 01. Las Vegas, Nevada: Bechtel SAIC Company. ACC: MOL.20011029.0311. 156304
- BSC 2001. *Ground Control for Emplacement Drifts for SR*. ANL-EBS-GE-000002 REV 00 ICN 01. Las Vegas, Nevada: Bechtel SAIC Company. ACC: MOL.20010627.0028. 155187
- BSC 2002. *Requirements Document (RD) for iTOUGH2 V5.0-00*. DI: 10003-RD-5.0-0. Las Vegas, Nevada: Bechtel SAIC Company. ACC: MOL.20020923.0143. 161067
- BSC 2002. *Technical Work Plan for: Performance Assessment Unsaturated Zone*. TWP-NBS-HS-000003 REV 02. Las Vegas, Nevada: Bechtel SAIC Company. ACC: MOL.20030102.0108. 160819
- BSC 2002. *User's Manual (UM) for iTOUGH2 V5.0*. DI: 10003-UM-5.0-00. Las Vegas, Nevada: Bechtel SAIC Company. ACC: MOL.20020923.0147. 161066
- BSC 2003. *Drift Degradation Analysis*. ANL-EBS-MD-000027 REV 02. Las Vegas, Nevada: Bechtel SAIC Company. ACC: DOC.20030709.0003. 162711
- BSC 2003. *Risk Information to Support Prioritization of Performance Assessment Models*. TDR-WIS-PA-000009 REV 01 ICN 01, Errata 001. Las Vegas, Nevada: Bechtel SAIC Company. ACC: MOL.20021017.0045; DOC.20031014.0003. 168796

| | |
|--|--------|
| BSC 2004. <i>Q-List</i> . 000-30R-MGR0-00500-000-000 REV 00. Las Vegas, Nevada: Bechtel SAIC Company. ACC: ENG.20040721.0007. | 168361 |
| BSC 2004. <i>Abstraction of Drift Seepage</i> . MDL-NBS-HS-000019, Rev. 01. Las Vegas, Nevada: Bechtel SAIC Company. | 169131 |
| BSC 2004. <i>Analysis of Hydrologic Properties Data</i> . ANL-NBS-HS-000042, Rev. 00. Las Vegas, Nevada: Bechtel SAIC Company. | 170038 |
| BSC 2004. <i>Calibrated Properties Model</i> . MDL-NBS-HS-000003, Rev. 02. Las Vegas, Nevada: Bechtel SAIC Company. | 169857 |
| BSC 2004. <i>D&E / PA/C IED Emplacement Drift Configuration and Environment</i> . 800-IED-MGR0-00201-000-00B. Las Vegas, Nevada: Bechtel SAIC Company. ACC: ENG.20040326.0001. | 168489 |
| BSC 2004. <i>D&E / PA/C IED Typical Waste Package Components Assembly</i> . 800-IED-WIS0-00205-000-00C. Las Vegas, Nevada: Bechtel SAIC Company. ACC: ENG.20040202.0013. | 167758 |
| BSC 2004. <i>Drift Degradation Analysis</i> . ANL-EBS-MD-000027, Rev. 03. Las Vegas, Nevada: Bechtel SAIC Company. | 166107 |
| BSC 2004. <i>Drift Scale THM Model</i> . MDL-NBS-HS-000017, Rev. 01. Las Vegas, Nevada: Bechtel SAIC Company. | 169864 |
| BSC 2004. <i>Drift-Scale THC Seepage Model</i> . MDL-NBS-HS-000001, Rev. 03. Las Vegas, Nevada: Bechtel SAIC Company. | 169856 |
| BSC 2004. <i>Seepage Calibration Model and Seepage Testing Data</i> . MDL-NBS-HS-000004, Rev. 03. Las Vegas, Nevada: Bechtel SAIC Company | 170034 |
| BSC 2004. <i>Seismic Consequence Abstraction</i> . MDL-WIS-PA-000003, Rev. 01. Las Vegas, Nevada: Bechtel SAIC Company. | 169183 |
| BSC 2004. <i>Technical Work Plan for: Regulatory Integration Evaluation of Analysis and Model Reports Supporting the TSPA-LA</i> . TWP-MGR-PA-000014 REV 00 ICN 01. Las Vegas, Nevada: Bechtel SAIC Company. ACC: DOC.20040603.0001. | 169653 |
| BSC 2004. <i>Technical Work Plan for: Unsaturated Zone Flow Analysis and Model Report Integration</i> . TWP-MGR-HS-000001 REV 00. Las Vegas, Nevada: Bechtel SAIC Company. ACC: DOC.20040701.0005. | 169654 |
| BSC 2004. <i>UZ Flow Models and Submodels</i> . MDL-NBS-HS-000006, Rev. 02. Las Vegas, Nevada: Bechtel SAIC Company. | 169861 |

- Canori, G.F. and Leitner, M.M. 2003. *Project Requirements Document*. 166275
TER-MGR-MD-000001 REV 02. Las Vegas, Nevada: Bechtel SAIC Company.
ACC: DOC.20031222.0006.
- CRWMS (Civilian Radioactive Waste Management System) M&O (Management and Operating Contractor) 2000. *Seepage Model for PA Including Drift Collapse*. 153314
MDL-NBS-HS-000002 REV 01. Las Vegas, Nevada: CRWMS M&O. ACC:
MOL.20010221.0147.
- CRWMS M&O 2000. *UZ Flow Models and Submodels*. MDL-NBS-HS-000006 122797
REV 00. Las Vegas, Nevada: CRWMS M&O. ACC: MOL.19990721.0527.
- CRWMS M&O 2001. *Abstraction of Drift Seepage*. ANL-NBS-MD-000005 154291
REV 01. Las Vegas, Nevada: CRWMS M&O. ACC: MOL.20010309.0019.
- Finsterle, S. 2000. "Using the Continuum Approach to Model Unsaturated Flow in Fractured Rock." *Water Resources Research*, 36, (8), 2055-2066. Washington, D.C.: American Geophysical Union. TIC: 248769. 151875
- Jackson, C.P.; Hoch, A.R.; and Todman, S. 2000. "Self-Consistency of a Heterogeneous Continuum Porous Medium Representation of a Fractured Medium." *Water Resources Research*, 36, (1), 189-202. Washington, D.C.: American Geophysical Union. TIC: 247466. 141523
- Knight, J.H.; Philip, J.R.; and Waechter, R.T. 1989. "The Seepage Exclusion Problem for Spherical Cavities." *Water Resources Research*, 25, (1), 29-37. Washington, D.C.: American Geophysical Union. TIC: 240851. 154293
- Li, G. and Tsang, C-F. 2003. "Seepage into Drifts with Mechanical Degradation." *Journal of Contaminant Hydrology*, 62-63, 157-172. New York, New York: Elsevier. TIC: 254205. 163714
- Liu, H.H.; Doughty, C.; and Bodvarsson, G.S. 1998. "An Active Fracture Model for Unsaturated Flow and Transport in Fractured Rocks." *Water Resources Research*, 34, (10), 2633-2646. Washington, D.C.: American Geophysical Union. TIC: 243012. 105729
- Luckner, L.; van Genuchten, M.T.; and Nielsen, D.R. 1989. "A Consistent Set of Parametric Models for the Two-Phase Flow of Immiscible Fluids in the Subsurface." *Water Resources Research*, 25, (10), 2187-2193. Washington, D.C.: American Geophysical Union. TIC: 224845. 100590
- NRC (U.S. Nuclear Regulatory Commission) 2003. *Yucca Mountain Review Plan, Final Report*. NUREG-1804, Rev. 2. Washington, D.C.: U.S. Nuclear Regulatory Commission, Office of Nuclear Material Safety and Safeguards. TIC: 254568. 163274

- Philip, J.R. 1989. "The Seepage Exclusion Problem for Sloping Cylindrical Cavities." *Water Resources Research*, 25, (6), 1447-1448. Washington, D.C.: American Geophysical Union. TIC: 239729. 152651
- Philip, J.R.; Knight, J.H.; and Waechter, R.T. 1989. "Unsaturated Seepage and Subterranean Holes: Conspectus, and Exclusion Problem for Circular Cylindrical Cavities." *Water Resources Research*, 25, (1), 16-28. Washington, D.C.: American Geophysical Union. TIC: 239117. 105743
- Richards, L.A. 1931. "Capillary Conduction of Liquids Through Porous Mediums." *Physics*, 1, 318-333. New York, New York: American Physical Society. TIC: 225383. 104252
- Ritcey, A.C. and Wu, Y.S. 1999. "Evaluation of the Effect of Future Climate Change on the Distribution and Movement of Moisture in the Unsaturated Zone at Yucca Mountain, NV." *Journal of Contaminant Hydrology*, 38, (1-3), 257-279. New York, New York: Elsevier. TIC: 244160. 139174
- van Genuchten, M.T. 1980. "A Closed-Form Equation for Predicting the Hydraulic Conductivity of Unsaturated Soils." *Soil Science Society of America Journal*, 44, (5), 892-898. Madison, Wisconsin: Soil Science Society of America. TIC: 217327. 100610
- Wang, J. 2004. Scientific Notebooks Referenced in Model Report U0075 Seepage Model for PA Including Drift Collapse MDL-NBS-HS-000002 REV 03 "Memorandum from J.S. Wang (BSC) to File, July 14, 2004, with attachment. ACC: MOL.20040727.0453. 170511
- Wang, J.S. 2003. "Scientific Notebooks Referenced in Model Report U0075, Seepage Model for PA Including Drift Collapse, MDL-NBS-HS-000002 REV 02." Memorandum from J.S. Wang (BSC) to File, May 5, 2003, with attachments. ACC: MOL.20030506.0299. 162319
- Wang, J.S.Y.; Trautz, R.C.; Cook, P.J.; Finsterle, S.; James, A.L.; and Birkholzer, J. 1999. "Field Tests and Model Analyses of Seepage into Drift." *Journal of Contaminant Hydrology*, 38, (1-3), 323-347. New York, New York: Elsevier. TIC: 244160. 106146
- Whelan, J.F.; Paces, J.B.; and Peterman, Z.E. 2002. "Physical and Stable-Isotope Evidence for Formation of Secondary Calcite and Silica in the Unsaturated Zone, Yucca Mountain, Nevada." *Applied Geochemistry*, 17, ([6]), 735-750. New York, New York: Elsevier. TIC: 253462. 160442
- Wu, Y.S.; Haukwa, C.; and Bodvarsson, G.S. 1999. "A Site-Scale Model for Fluid and Heat Flow in the Unsaturated Zone of Yucca Mountain, Nevada." *Journal of Contaminant Hydrology*, 38, (1-3), 185-215. New York, New York: Elsevier. TIC: 244160. 117161

9.2 CODES, STANDARDS, REGULATIONS, AND PROCEDURES

10 CFR 63. Energy: Disposal of High-Level Radioactive Wastes in a Geologic Repository at Yucca Mountain, Nevada. Readily available. 156605

AP-2.22Q, Rev. 1, ICN 0. *Classification Analyses and Maintenance of the Q-List*. Washington, D.C.: U.S. Department of Energy, Office of Civilian Radioactive Waste Management. ACC: DOC.20030807.0002.

AP-SIII.10Q, Rev. 2, ICN 7. *Models*. Washington, D.C.: U.S. Department of Energy, Office of Civilian Radioactive Waste Management. ACC: DOC.20040920.0002.

9.3 SOURCE DATA, LISTED BY DATA TRACKING NUMBER

LB0011AIRKTEST.001. Air Permeability Testing in Niches 3566 and 3650. Submittal date: 11/08/2000. 153155

LB0012AIRKTEST.001. Niche 5 Air K Testing 3/23/00-4/3/00. Submittal date: 12/21/2000. 154586

LB0205REVUZPRP.001. Fracture Properties for UZ Model Layers Developed from Field Data. Submittal date: 05/14/2002. 159525

LB0208UZDSCPMI.002. Drift-Scale Calibrated Property Sets: Mean Infiltration Data Summary. Submittal date: 08/26/2002. 161243

LB0302PTNTSW9I.001. PTN/TSW Interface Percolation Flux Maps for 9 Infiltration Scenarios. Submittal date: 02/28/2003. 162277

LB0302SCMREV02.002. Seepage-Related Model Parameters K and 1/A: Data Summary. Submittal date: 02/28/2003. 162273

LB0306DRSCLTHM.001. Drift Scale THM Model Predictions: Simulations. Submittal date: 06/26/2003. 169733

LB980901233124.101. Pneumatic Pressure and Air Permeability Data from Niche 3107 and Niche 4788 in the ESF from Chapter 2 of Report SP33PBM4: Fracture Flow and Seepage Testing in the ESF, FY98. Submittal date: 11/23/1999. 136593

LB991121233129.001. Calibrated Parameters for the Present-Day, Mean Infiltration Scenario, Used for Simulations With Perched Water Conceptual Model #1 (Flow Through) for the Mean Infiltration Scenarios of the Present-Day, Monsoon and Glacial Transition Climates. Submittal date: 03/11/2000. 147328

MO0306MWDDPPDR.000. Drift Profile Prediction and Degraded Rock Mass Characteristics. Submittal date: 06/18/2003. 164736

MO0407SEPFEPPLA.000. LA FEP List. Submittal date: 07/20/2004. 170760

9.4 OUTPUT DATA, LISTED BY DATA TRACKING NUMBER

LB0304SMDCREV2.001. Seepage Modeling for Performance Assessment, Including Drift Collapse: Input/Output Files. Submittal date: 04/11/2003.

LB0304SMDCREV2.002. Seepage Modeling for Performance Assessment, Including Drift Collapse: Summary Plot Files and Tables. Submittal date: 04/11/2003.

LB0304SMDCREV2.003. Impact of Thermal-Hydrologic-Mechanical Effects on Seepage: Simulations. Submittal date: 04/23/2003.

LB0304SMDCREV2.004. Impact of Thermal-Hydrologic-Mechanical Effects on Seepage: Summary Plot Files and Tables. Submittal date: 04/23/2003.

LB0307SEEPDRCL.001. Seepage Into Collapsed Drift: Simulations. Submittal date: 07/21/2003.

LB0307SEEPDRCL.002. Seepage Into Collapsed Drift: Data Summary. Submittal date: 07/21/2003.

LB0406U0075FCS.001. Flow Focusing In Heterogeneous Fractured Rock: Simulations. Submittal date: 06/30/2004.

LB0406U0075FCS.002. Flow Focusing In Heterogeneous Fractured Rock: Summaries. Submittal date: 06/30/2004.

9.5 SOFTWARE CODES

LBNL (Lawrence Berkeley National Laboratory) 1999. *Software Code: EXT*. V1.0. Sun. 10047-1.0-00. 134141

LBNL 2000. *Software Routine: AddBound*. V1.0. SUN w/Unix OS. 10357-1.0-00. 152823

LBNL 2000. *Software Routine: CutDrift*. V1.0. SUN w/Unix OS. 10375-1.0-00. 152816

LBNL 2000. *Software Routine: CutNiche*. V1.3. SUN w/Solaris OS. 10402-1.3-00. 152828

LBNL 2000. *Software Code: GSLIB*. V1.0SISIMV1.204. SUN w/Unix OS. 10397-1.0SISIMV1.204-00. 153100

| | |
|---|--------|
| LBNL 2000. <i>Software Routine: MoveMesh</i> . V1.0. SUN w/Unix OS. 10358-1.0-00. | 152824 |
| LBNL 2000. <i>Software Routine: Perm2Mesh</i> . V1.0. SUN w/Unix OS. 10359-1.0-00. | 152826 |
| LBNL 2000. <i>Software Code: TOUGH2</i> . V1.4. Sun Workstation and DEC/ALPHA. 10007-1.4-01. | 146496 |
| LBNL 2002. <i>Software Code: iTOUGH2</i> . V5.0. SUN UltraSparc., DEC ALPHA, LINUX. 10003-5.0-00. | 160106 |
| LBNL 2003. <i>Software Code: TOUGH2</i> . V1.6. PC/MS-DOS Windows 98, Sun UltraSparc/Sun OS 5.5.1, DEC-Alpha OSF1 V4.0. 10007-1.6-01. | 161491 |

INTENTIONALLY LEFT BLANK

APPENDIX A

**LIST OF COMPUTER FILES SUBMITTED WITH THIS MODEL REPORT UNDER
OUTPUT DTNS: LB0304SMDCREV2.001; LB0304SMDCREV2.002;
LB0304SMDCREV2.003; LB0304SMDCREV2.004; LB0307SEEPDRCL.001;
LB0307SEEPDRCL.002; LB0406U0075FCS.001; AND LB0406U0075FCS.002**

Computer files used in this model report are listed below and are submitted to the Technical Data Management System under DTNs: LB0304SMDCREV2.001; LB0304SMDCREV2.002; LB0304SMDCREV2.003; LB0304SMDCREV2.004; LB0307SEEPDRCL.001; LB0307SEEPDRCL.002; LB0406U0075FCS.001; and LB0406U0075FCS.002. Each file name is complemented with a short description of its contents and/or purpose. The detail could be found on the scientific notebook pages listed in Table 6-1.

Table A-1 lists the files of numerical simulations with the seepage model for performance assessment for three seepage-relevant parameters: fracture k, the capillary-strength, and percolation flux. Multiple realizations of the underlying stochastic permeability field are performed. Selected sensitivity analyses are performed on the effects of variable stages of drift collapse. Different design scenarios are modeled for rockfall and rock bolt installations.

Table A-1. File Name and Description for Numerical Simulations DTN: LB0304SMDCREV2.001 (All Occurred During 2003)

| Bytes | Date | | Time | File or Folder Name |
|---|------|----|-------|--|
| 16381467 | Apr | 22 | 18:17 | 20_k-realizations.tar.gz |
| 3673336 | Apr | 22 | 16:08 | Rockbolt_analysis.tar.gz |
| 61555 | Apr | 22 | 16:20 | SMPA-SCMi.tar.gz |
| 67962754 | Apr | 22 | 16:05 | k1-10_realizations_10-scenarios.tar.gz |
| 16076925 | Apr | 22 | 16:07 | k1-r_6-s_moisture-mapping.tar.gz |
| ./20_k-realizations: | | | | |
| Bytes | Date | | Time | File or Folder Name |
| 4096 | Apr | 21 | 19:30 | Tough2 mesh |
| 4096 | Apr | 17 | 18:26 | iTOUGH2 mesh |
| ./20_k-realizations/Tough2 mesh generation: | | | | |
| Bytes | Date | | Time | File or Folder Name |
| 4096 | Apr | 17 | 18:22 | Input |
| 4096 | Apr | 17 | 18:22 | Output |
| ./20_k-realizations/Tough2 mesh generation/Input: | | | | |
| Bytes | Date | | Time | File or Folder Name |
| 337 | Dec | 19 | 13:12 | mesh3dblock |
| ./20_k-realizations/Tough2 mesh generation/Output: | | | | |
| Bytes | Date | | Time | File or Folder Name |
| 9131570 | Dec | 19 | 13:12 | mesh3dblock.mes |
| ./20_k-realizations/iTOUGH2 mesh generation: | | | | |
| Bytes | Date | | Time | File or Folder Name |
| 1647 | Apr | 9 | 16:12 | SMPA |
| 4096 | Apr | 17 | 18:20 | iT2 input |
| 4096 | Apr | 17 | 18:19 | iT2 output |
| 4096 | Apr | 17 | 18:25 | pre-processing |
| 444 | Apr | 9 | 16:23 | sh.onestep |

Table A-1. File Name and Description for Numerical Simulations DTN: LB0304SMDCREV2.001
(All Occurred During 2003) (Continued)

| Bytes | Date | | Time | File or Folder Name |
|------------------------------------|-------------|-----------------------|----------------|---------------------|
| ./20_k-realizations/iTOUGH2 | mesh | generation/iT2 | input: | |
| 8529107 | Dec | 19 | 15:00 | SMPA.mes1 |
| 8529107 | Dec | 19 | 17:30 | SMPA.mes10 |
| 8529107 | Dec | 19 | 17:47 | SMPA.mes11 |
| 8529107 | Dec | 19 | 18:04 | SMPA.mes12 |
| 8529107 | Dec | 19 | 18:21 | SMPA.mes13 |
| 8529107 | Dec | 19 | 18:38 | SMPA.mes14 |
| 8529107 | Dec | 19 | 18:54 | SMPA.mes15 |
| 8529107 | Dec | 19 | 19:11 | SMPA.mes16 |
| 8529107 | Dec | 19 | 19:28 | SMPA.mes17 |
| 8529107 | Dec | 19 | 19:45 | SMPA.mes18 |
| 8529107 | Dec | 19 | 20:01 | SMPA.mes19 |
| 8529107 | Dec | 19 | 15:17 | SMPA.mes2 |
| 8529107 | Dec | 19 | 20:18 | SMPA.mes20 |
| 8529107 | Dec | 19 | 15:33 | SMPA.mes3 |
| 8529107 | Dec | 19 | 15:50 | SMPA.mes4 |
| 8529107 | Dec | 19 | 16:07 | SMPA.mes5 |
| 8529107 | Dec | 19 | 16:23 | SMPA.mes6 |
| 8529107 | Dec | 19 | 16:39 | SMPA.mes7 |
| 8529107 | Dec | 19 | 16:56 | SMPA.mes8 |
| 8529107 | Dec | 19 | 17:13 | SMPA.mes9 |
| 7812 | Apr | 9 | 16:12 | SMPAi |
| 124950 | Apr | 3 | 10:41 | parameterset.dat |
| ./20_k-realizations/iTOUGH2 | mesh | generation/iT2 | output: | |
| Bytes | Date | | Time | File or Folder Name |
| 269134 | Apr | 9 | 16:12 | SMPAi.out1 |
| 269142 | Apr | 9 | 16:12 | SMPAi.out10 |
| 269141 | Apr | 9 | 16:12 | SMPAi.out11 |
| 269142 | Apr | 9 | 16:12 | SMPAi.out12 |
| 269139 | Apr | 9 | 16:12 | SMPAi.out13 |
| 269141 | Apr | 9 | 16:12 | SMPAi.out14 |
| 269142 | Apr | 9 | 16:12 | SMPAi.out15 |
| 269142 | Apr | 9 | 16:12 | SMPAi.out16 |
| 269142 | Apr | 9 | 16:12 | SMPAi.out17 |
| 269140 | Apr | 9 | 16:12 | SMPAi.out18 |
| 269142 | Apr | 9 | 16:12 | SMPAi.out19 |
| 269142 | Apr | 9 | 16:12 | SMPAi.out2 |
| 269141 | Apr | 9 | 16:12 | SMPAi.out20 |
| 269141 | Apr | 9 | 16:12 | SMPAi.out3 |
| 269142 | Apr | 9 | 16:12 | SMPAi.out4 |

Table A-1. File Name and Description for Numerical Simulations DTN: LB0304SMDCREV2.001
(All Occurred During 2003) (Continued)

| ./20_k-realizations/iTOUGH2 | mesh | generation/iT2 | output: | (Continued) |
|--|-------------|-----------------------------------|----------------|------------------------------------|
| Bytes | Date | | Time | File or Folder Name |
| 269141 | Apr | 9 | 16:12 | SMPAi.out5 |
| 269141 | Apr | 9 | 16:12 | SMPAi.out6 |
| 269143 | Apr | 9 | 16:12 | SMPAi.out7 |
| 269142 | Apr | 9 | 16:12 | SMPAi.out8 |
| 269137 | Apr | 9 | 16:12 | SMPAi.out9 |
| ./20_k-realizations/iTOUGH2 | mesh | generation/pre-processing: | | |
| Bytes | Date | | Time | File or Folder Name |
| 1605 | Dec | 18 | 15:33 | onestep |
| 3562 | Dec | 19 | 13:11 | perm.par |
| 9131613 | Dec | 19 | 13:13 | primary.mes |
| 3793 | Dec | 19 | 14:39 | sh.mesh |
| ./Rockbolt_analysis: | | | | |
| Bytes | Date | | Time | File or Folder Name |
| 4096 | Apr | 21 | 13:19 | 10cm_discrete_fracture_simulations |
| 4096 | Apr | 21 | 13:20 | 50cm_discrete_fracture_simulations |
| 23040 | Apr | 21 | 12:22 | Rockboltsreadme.doc |
| 4096 | Apr | 21 | 13:18 | SCM_simulations |
| ./Rockbolt_analysis/10cm_discrete_fracture_simulations: | | | | |
| Bytes | Date | | Time | File or Folder Name |
| 4096 | Apr | 10 | 13:38 | t21.5df1 |
| 4096 | Apr | 10 | 13:38 | t21.5df1_23 |
| 4096 | Apr | 10 | 13:38 | t21.5df1_24 |
| ./Rockbolt_analysis/10cm_discrete_fracture_simulations/t21.5df1: | | | | |
| Bytes | Date | | Time | File or Folder Name |
| 26576 | Apr | 21 | 12:37 | sh.22v1.4 |
| 2769 | Mar | 3 | 20:58 | vh_aX22 |
| 4140845 | Mar | 3 | 21:09 | vh_aX22.out |
| 428051 | Mar | 3 | 21:09 | vh_aX22.seep |
| ./Rockbolt_analysis/10cm_discrete_fracture_simulations/t21.5df1_23: | | | | |
| Bytes | Date | | Time | File or Folder Name |
| 39531 | Apr | 21 | 12:39 | sh.23v1.4 |
| 2769 | Mar | 1 | 21:25 | vh_aX23 |
| 4153033 | Mar | 1 | 21:36 | vh_aX23.out |
| 642063 | Mar | 1 | 21:36 | vh_aX23.seep |
| ./Rockbolt_analysis/10cm_discrete_fracture_simulations/t21.5df1_24: | | | | |
| Bytes | Date | | Time | File or Folder Name |
| 65540 | Apr | 21 | 12:40 | sh.24v1.4 |
| 2769 | Mar | 3 | 15:55 | vh_aX24 |
| 4149020 | Mar | 3 | 16:06 | vh_aX24.out |
| 1070073 | Mar | 3 | 16:06 | vh_aX24.seep |

Table A-1. File Name and Description for Numerical Simulations DTN: LB0304SMDCREV2.001
(All Occurred During 2003) (Continued)

| ./Rockbolt_analysis/50cm_discrete_fracture_simulations: | | | | |
|--|-------------|----|-------------|----------------------------|
| Bytes | Date | | Time | File or Folder Name |
| 4096 | Apr | 10 | 13:38 | t21.5df5 |
| 4096 | Apr | 10 | 13:38 | t21.5df5_23 |
| 4096 | Apr | 10 | 13:38 | t21.5df5_24 |
| ./Rockbolt_analysis/50cm_discrete_fracture_simulations/t21.5df5: | | | | |
| Bytes | Date | | Time | File or Folder Name |
| 26576 | Apr | 21 | 12:40 | sh.22v1.4 |
| 2769 | Mar | 2 | 23:42 | vh_aX22 |
| 4444483 | Mar | 3 | 0:08 | vh_aX22.out |
| 428051 | Mar | 3 | 0:08 | vh_aX22.seep |
| ./Rockbolt_analysis/50cm_discrete_fracture_simulations/t21.5df5_23: | | | | |
| Bytes | Date | | Time | File or Folder Name |
| 39536 | Apr | 21 | 12:40 | sh.23v1.4 |
| 2769 | Mar | 2 | 0:57 | vh_aX23 |
| 4402838 | Mar | 2 | 1:21 | vh_aX23.out |
| 642063 | Mar | 2 | 1:21 | vh_aX23.seep |
| ./Rockbolt_analysis/50cm_discrete_fracture_simulations/t21.5df5_24: | | | | |
| Bytes | Date | | Time | File or Folder Name |
| 65540 | Apr | 21 | 12:40 | sh.24v1.4 |
| 2769 | Mar | 3 | 17:42 | vh_aX24 |
| 4367274 | Mar | 3 | 18:04 | vh_aX24.out |
| 1070073 | Mar | 3 | 18:04 | vh_aX24.seep |
| ./Rockbolt_analysis/SCM_simulations: | | | | |
| Bytes | Date | | Time | File or Folder Name |
| 1393453 | Apr | 21 | 13:09 | MESH |
| 4096 | Apr | 10 | 13:38 | t21.5 |
| 4096 | Apr | 10 | 13:38 | t21.5_23 |
| 4096 | Apr | 10 | 13:38 | t21.5_24 |
| ./Rockbolt_analysis/SCM_simulations/t21.5: | | | | |
| Bytes | Date | | Time | File or Folder Name |
| 26576 | Apr | 21 | 13:15 | sh.22v1.4 |
| 2769 | Mar | 1 | 18:46 | vh_aX22 |
| 4103009 | Mar | 1 | 18:55 | vh_aX22.out |
| 428051 | Mar | 1 | 18:55 | vh_aX22.seep |
| ./Rockbolt_analysis/SCM_simulations/t21.5_23: | | | | |
| Bytes | Date | | Time | File or Folder Name |
| 39536 | Apr | 21 | 12:38 | sh.23v1.4 |
| 2769 | Mar | 1 | 19:11 | vh_aX23 |
| 4127888 | Mar | 1 | 19:21 | vh_aX23.out |
| 642063 | Mar | 1 | 19:21 | vh_aX23.seep |

Table A-1. File Name and Description for Numerical Simulations DTN: LB0304SMDCREV2.001
(All Occurred During 2003) (Continued)

| ./Rockbolt_analysis/SCM_simulations/t21.5_24: | | | | |
|--|-------------|----|-------------|----------------------------------|
| Bytes | Date | | Time | File or Folder Name |
| 65540 | Apr | 21 | 12:38 | sh.24v1.4 |
| 2769 | Mar | 3 | 19:38 | vh_aX24 |
| 4139791 | Mar | 3 | 19:48 | vh_aX24.out |
| 1070073 | Mar | 3 | 19:48 | vh_aX24.seep |
| ./SMPA-SCMi: | | | | |
| Bytes | Date | | Time | File or Folder Name |
| 4096 | Apr | 21 | 2003 | T2_input |
| 4096 | Apr | 21 | 2003 | T2_output-iT2_input |
| 4096 | Apr | 21 | 2003 | iT2_Output |
| ./SMPA-SCMi/T2_input: | | | | |
| Bytes | Date | | Time | File or Folder Name |
| 1927 | Mar | 12 | 16:35 | SMPA-SCM |
| ./SMPA-SCMi/T2_output-iT2_input: | | | | |
| Bytes | Date | | Time | File or Folder Name |
| 22790 | Mar | 20 | 11:27 | SMPA-SCMi |
| 1012 | Mar | 20 | 11:28 | run_SMPA-SCM |
| ./SMPA-SCMi/iT2_Output: | | | | |
| Bytes | Date | | Time | File or Folder Name |
| 38275 | Mar | 21 | 1:37 | SMPA-SCMi.out1 |
| 38106 | Mar | 21 | 0:34 | SMPA-SCMi.out10 |
| 38645 | Mar | 21 | 1:24 | SMPA-SCMi.out2 |
| 38460 | Mar | 21 | 1:34 | SMPA-SCMi.out3 |
| 37937 | Mar | 21 | 1:07 | SMPA-SCMi.out4 |
| 38581 | Mar | 21 | 1:33 | SMPA-SCMi.out5 |
| 38967 | Mar | 21 | 0:39 | SMPA-SCMi.out6 |
| 38460 | Mar | 20 | 23:24 | SMPA-SCMi.out7 |
| 38460 | Mar | 21 | 0:09 | SMPA-SCMi.out8 |
| 38798 | Mar | 21 | 1:01 | SMPA-SCMi.out9 |
| ./k1-10_realizations_10-scenarios: | | | | |
| Bytes | Date | | Time | File or Folder Name |
| 4096 | Apr | 21 | 15:52 | Sensitivity_analysis_4-scenarios |
| 4096 | Apr | 21 | 16:29 | k1-10_realizations_6-scenarios |
| 1605 | Jan | 27 | 16:55 | onestep |
| 444 | Jan | 27 | 16:55 | sh.onestep |
| ./k1-10_realizations_10-scenarios/Sensitivity_analysis_4-scenarios: | | | | |
| Bytes | Date | | Time | File or Folder Name |
| 4096 | Apr | 21 | 15:56 | Common_input |
| 4096 | Apr | 21 | 14:47 | Correlation_length |
| 4096 | Apr | 21 | 14:45 | Logk_Stdev |

Table A-1. File Name and Description for Numerical Simulations DTN: LB0304SMDCREV2.001
(All Occurred During 2003) (Continued)

| ./k1-10_realizations_10-scenarios/Sensitivity_analysis_4-scenarios/Common_input: | | | | |
|--|-------------|----|-------------|----------------------------|
| Bytes | Date | | Time | File or Folder Name |
| 8101 | Feb | 18 | 16:57 | SMPAi |
| 59 | Feb | 20 | 14:56 | parameterset1.dat |
| ./k1-10_realizations_10-scenarios/Sensitivity_analysis_4-scenarios/Correlation_length: | | | | |
| Bytes | Date | | Time | File or Folder Name |
| 4096 | Apr | 21 | 14:48 | lambda=1m |
| 4096 | Apr | 21 | 14:48 | lambda=2m |
| ./k1-10_realizations_10-scenarios/Sensitivity_analysis_4-scenarios/Correlation_length/lambda=1m: | | | | |
| Bytes | Date | | Time | File or Folder Name |
| 4096 | Apr | 21 | 16:59 | Input |
| 4096 | Apr | 21 | 14:52 | Output |
| ./k1-10_realizations_10-scenarios/Sensitivity_analysis_4-scenarios/Correlation_length/lambda=1m/Input: | | | | |
| Bytes | Date | | Time | File or Folder Name |
| 8529107 | Feb | 20 | 16:23 | SMPAa1.mes1 |
| 8529107 | Feb | 20 | 18:59 | SMPAa1.mes10 |
| 8529107 | Feb | 20 | 16:40 | SMPAa1.mes2 |
| 8529107 | Feb | 20 | 16:57 | SMPAa1.mes3 |
| 8529107 | Feb | 20 | 17:14 | SMPAa1.mes4 |
| 8529107 | Feb | 20 | 17:32 | SMPAa1.mes5 |
| 8529107 | Feb | 20 | 17:49 | SMPAa1.mes6 |
| 8529107 | Feb | 20 | 18:07 | SMPAa1.mes7 |
| 8529107 | Feb | 20 | 18:24 | SMPAa1.mes8 |
| 8529107 | Feb | 20 | 18:42 | SMPAa1.mes9 |
| 3562 | Feb | 20 | 14:19 | perma1.par |
| 3805 | Feb | 20 | 14:14 | sh.mesha1 |
| ./k1-10_realizations_10-scenarios/Sensitivity_analysis_4-scenarios/Correlation_length/lambda=1m/Output: | | | | |
| Bytes | Date | | Time | File or Folder Name |
| 19473 | Feb | 21 | 2:21 | SMPAi.outa11 |
| 19473 | Feb | 21 | 7:03 | SMPAi.outa110 |
| 19473 | Feb | 21 | 2:49 | SMPAi.outa12 |
| 19473 | Feb | 21 | 3:21 | SMPAi.outa13 |
| 19473 | Feb | 21 | 3:49 | SMPAi.outa14 |
| 19473 | Feb | 21 | 4:23 | SMPAi.outa15 |
| 19473 | Feb | 21 | 4:53 | SMPAi.outa16 |
| 19473 | Feb | 21 | 5:22 | SMPAi.outa17 |
| 19473 | Feb | 21 | 5:56 | SMPAi.outa18 |
| 19473 | Feb | 21 | 6:31 | SMPAi.outa19 |
| ./k1-10_realizations_10-scenarios/Sensitivity_analysis_4-scenarios/Correlation_length/lambda=2m: | | | | |
| Bytes | Date | | Time | File or Folder Name |
| 4096 | Apr | 21 | 16:59 | Input |
| 4096 | Apr | 21 | 14:53 | Output |

Table A-1. File Name and Description for Numerical Simulations DTN: LB0304SMDCREV2.001
(All Occurred During 2003) (Continued)

| ./k1-10_realizations_10-scenarios/Sensitivity_analysis_4-scenarios/Correlation_length/lambda=2m/Input: | | | | |
|--|-------------|----|-------------|----------------------------|
| Bytes | Date | | Time | File or Folder Name |
| 8529107 | Feb | 20 | 16:35 | SMPAa2.mes1 |
| 8529107 | Feb | 20 | 19:12 | SMPAa2.mes10 |
| 8529107 | Feb | 20 | 16:52 | SMPAa2.mes2 |
| 8529107 | Feb | 20 | 17:09 | SMPAa2.mes3 |
| 8529107 | Feb | 20 | 17:27 | SMPAa2.mes4 |
| 8529107 | Feb | 20 | 17:44 | SMPAa2.mes5 |
| 8529107 | Feb | 20 | 18:01 | SMPAa2.mes6 |
| 8529107 | Feb | 20 | 18:20 | SMPAa2.mes7 |
| 8529107 | Feb | 20 | 18:37 | SMPAa2.mes8 |
| Bytes | Date | | Time | File or Folder Name |
| 8529107 | Feb | 20 | 18:54 | SMPAa2.mes9 |
| 7713 | Jan | 28 | 14:08 | SMPAia2 |
| 3562 | Feb | 20 | 14:19 | perma2.par |
| 3833 | Feb | 20 | 16:17 | sh.mesha2 |
| ./k1-10_realizations_10-scenarios/Sensitivity_analysis_4-scenarios/Correlation_length/lambda=2m/Output: | | | | |
| Bytes | Date | | Time | File or Folder Name |
| 19473 | Feb | 21 | 7:35 | SMPAi.outa21 |
| 19473 | Feb | 21 | 12:16 | SMPAi.outa210 |
| 19473 | Feb | 21 | 8:06 | SMPAi.outa22 |
| 19473 | Feb | 21 | 8:41 | SMPAi.outa23 |
| 19473 | Feb | 21 | 9:08 | SMPAi.outa24 |
| 19473 | Feb | 21 | 9:44 | SMPAi.outa25 |
| 19473 | Feb | 21 | 10:11 | SMPAi.outa26 |
| 19473 | Feb | 21 | 10:45 | SMPAi.outa27 |
| 19473 | Feb | 21 | 11:17 | SMPAi.outa28 |
| 19473 | Feb | 21 | 11:46 | SMPAi.outa29 |
| ./k1-10_realizations_10-scenarios/Sensitivity_analysis_4-scenarios/Logk_Stdev: | | | | |
| Bytes | Date | | Time | File or Folder Name |
| 4096 | Apr | 21 | 14:45 | stdev=0.5 |
| 4096 | Apr | 21 | 14:45 | stdev=2.0 |
| ./k1-10_realizations_10-scenarios/Sensitivity_analysis_4-scenarios/Logk_Stdev/stdev=0.5: | | | | |
| Bytes | Date | | Time | File or Folder Name |
| 4096 | Apr | 21 | 17:00 | Input |
| 4096 | Apr | 21 | 14:58 | Output |

Table A-1. File Name and Description for Numerical Simulations DTN: LB0304SMDCREV2.001
(All Occurred During 2003) (Continued)

| ./k1-10_realizations_10-scenarios/Sensitivity_analysis_4-scenarios/Logk_Stdev/stdev=0.5/Input: | | | | |
|--|-------------|----|-------------|----------------------------|
| Bytes | Date | | Time | File or Folder Name |
| 8529107 | Feb | 20 | 16:43 | SMPAsd5.mes1 |
| 8529107 | Feb | 20 | 19:19 | SMPAsd5.mes10 |
| 8529107 | Feb | 20 | 17:00 | SMPAsd5.mes2 |
| 8529107 | Feb | 20 | 17:17 | SMPAsd5.mes3 |
| 8529107 | Feb | 20 | 17:35 | SMPAsd5.mes4 |
| 8529107 | Feb | 20 | 17:51 | SMPAsd5.mes5 |
| 8529107 | Feb | 20 | 18:09 | SMPAsd5.mes6 |
| 8529107 | Feb | 20 | 18:27 | SMPAsd5.mes7 |
| 8529107 | Feb | 20 | 18:44 | SMPAsd5.mes8 |
| 8529107 | Feb | 20 | 19:02 | SMPAsd5.mes9 |
| 3562 | Feb | 20 | 14:33 | permsd5.par |
| 3839 | Feb | 20 | 16:24 | sh.meshsd5 |
| ./k1-10_realizations_10-scenarios/Sensitivity_analysis_4-scenarios/Logk_Stdev/stdev=0.5/Output: | | | | |
| Bytes | Date | | Time | File or Folder Name |
| 19474 | Feb | 20 | 17:16 | SMPAi.outsd51 |
| 19474 | Feb | 20 | 21:04 | SMPAi.outsd510 |
| 19474 | Feb | 20 | 17:42 | SMPAi.outsd52 |
| 19474 | Feb | 20 | 18:09 | SMPAi.outsd53 |
| 19474 | Feb | 20 | 18:36 | SMPAi.outsd54 |
| 19474 | Feb | 20 | 19:03 | SMPAi.outsd55 |
| 19474 | Feb | 20 | 19:24 | SMPAi.outsd56 |
| 19474 | Feb | 20 | 19:50 | SMPAi.outsd57 |
| 19474 | Feb | 20 | 20:14 | SMPAi.outsd58 |
| 19474 | Feb | 20 | 20:39 | SMPAi.outsd59 |
| ./k1-10_realizations_10-scenarios/Sensitivity_analysis_4-scenarios/Logk_Stdev/stdev=2.0: | | | | |
| Bytes | Date | | Time | File or Folder Name |
| 4096 | Apr | 21 | 16:59 | Input |
| 4096 | Apr | 21 | 14:57 | Output |
| ./k1-10_realizations_10-scenarios/Sensitivity_analysis_4-scenarios/Logk_Stdev/stdev=2.0/Input: | | | | |
| Bytes | Date | | Time | File or Folder Name |
| 8529107 | Feb | 20 | 16:37 | SMPAs2.mes1 |
| 8529107 | Feb | 20 | 19:14 | SMPAs2.mes10 |
| 8529107 | Feb | 20 | 16:54 | SMPAs2.mes2 |
| 8529107 | Feb | 20 | 17:11 | SMPAs2.mes3 |
| 8529107 | Feb | 20 | 17:29 | SMPAs2.mes4 |
| 8529107 | Feb | 20 | 17:46 | SMPAs2.mes5 |
| 8529107 | Feb | 20 | 18:03 | SMPAs2.mes6 |
| 8529107 | Feb | 20 | 18:21 | SMPAs2.mes7 |
| 8529107 | Feb | 20 | 18:39 | SMPAs2.mes8 |
| 8529107 | Feb | 20 | 18:57 | SMPAs2.mes9 |
| 3562 | Feb | 20 | 14:32 | perms2.par |
| 3833 | Feb | 20 | 16:20 | sh.meshs2 |

Table A-1. File Name and Description for Numerical Simulations DTN: LB0304SMDCREV2.001
(All Occurred During 2003) (Continued)

| ./k1-10_realizations_10-scenarios/Sensitivity_analysis_4-scenarios/Logk_Stdev/stdev=2.0/Output: | | | | |
|--|-------------|----|-------------|----------------------------|
| Bytes | Date | | Time | File or Folder Name |
| 19474 | Feb | 20 | 21:30 | SMPAi.outs21 |
| 19474 | Feb | 21 | 1:52 | SMPAi.outs210 |
| 19474 | Feb | 20 | 22:01 | SMPAi.outs22 |
| 19474 | Feb | 20 | 22:32 | SMPAi.outs23 |
| 19474 | Feb | 20 | 22:59 | SMPAi.outs24 |
| 19474 | Feb | 20 | 23:28 | SMPAi.outs25 |
| 19474 | Feb | 20 | 23:58 | SMPAi.outs26 |
| 19474 | Feb | 21 | 0:25 | SMPAi.outs27 |
| 19474 | Feb | 21 | 0:54 | SMPAi.outs28 |
| 19474 | Feb | 21 | 1:22 | SMPAi.outs29 |
| ./k1-10_realizations_10-scenarios/k1-10_realizations_6-scenarios: | | | | |
| Bytes | Date | | Time | File or Folder Name |
| 4096 | Apr | 21 | 2003 | Common_input |
| 4096 | Apr | 21 | 14:39 | Tptpll_75percentile_case |
| 4096 | Apr | 21 | 14:39 | Tptpll_base_case |
| 4096 | Apr | 21 | 14:39 | Tptpll_worst_case |
| 4096 | Apr | 21 | 14:39 | Tptpmn_75percentile_case |
| 4096 | Apr | 21 | 14:39 | Tptpmn_base_case |
| 4096 | Apr | 21 | 14:38 | Tptpmn_worst_case |
| ./k1-10_realizations_10-scenarios/k1-10_realizations_6-scenarios/Common_input: | | | | |
| Bytes | Date | | Time | File or Folder Name |
| 4096 | Apr | 21 | 2003 | 75+wst_inputs |
| 1728 | Feb | 13 | 16:31 | SMPA |
| 4096 | Apr | 21 | 2003 | Tptpll_inputs |
| 4096 | Apr | 21 | 2003 | Tptpmn_inputs |
| 4096 | Apr | 21 | 16:45 | base_case_inputs |
| ./k1-10_realizations_10-scenarios/k1-10_realizations_6-scenarios/Common_input/75+wst_inputs: | | | | |
| Bytes | Date | | Time | File or Folder Name |
| 3562 | Feb | 20 | 14:34 | perm.par |
| ./k1-10_realizations_10-scenarios/k1-10_realizations_6-scenarios/Common_input/Tptpll_inputs: | | | | |
| Bytes | Date | | Time | File or Folder Name |
| 1232 | Feb | 20 | 14:51 | parametersetfrll.dat |
| ./k1-10_realizations_10-scenarios/k1-10_realizations_6-scenarios/Common_input/Tptpmn_inputs: | | | | |
| Bytes | Date | | Time | File or Folder Name |
| 1232 | Feb | 19 | 15:01 | parametersetfrmn.dat |

Table A-1. File Name and Description for Numerical Simulations DTN: LB0304SMDCREV2.001
(All Occurred During 2003) (Continued)

| ./k1-10_realizations_10-scenarios/k1-10_realizations_6-scenarios/Common_input/base_case_inputs: | | | | |
|--|-------------|----|-------------|----------------------------|
| Bytes | Date | | Time | File or Folder Name |
| 8529107 | Jan | 28 | 13:58 | SMPA.mes1 |
| 8529107 | Jan | 27 | 16:54 | SMPA.mes10 |
| 8529107 | Jan | 27 | 16:55 | SMPA.mes2 |
| 8529107 | Jan | 27 | 16:55 | SMPA.mes3 |
| 8529107 | Jan | 27 | 16:55 | SMPA.mes4 |
| 8529107 | Jan | 27 | 16:55 | SMPA.mes5 |
| 8529107 | Jan | 27 | 16:55 | SMPA.mes6 |
| 8529107 | Jan | 27 | 16:55 | SMPA.mes7 |
| 8529107 | Jan | 27 | 16:55 | SMPA.mes8 |
| 8529107 | Jan | 27 | 16:55 | SMPA.mes9 |
| ./k1-10_realizations_10-scenarios/k1-10_realizations_6-scenarios/Tptpll_75percentile_case: | | | | |
| Bytes | Date | | Time | File or Folder Name |
| 4096 | Apr | 21 | 16:55 | Input |
| 4096 | Apr | 21 | 15:48 | Output |
| ./k1-10_realizations_10-scenarios/k1-10_realizations_6-scenarios/Tptpll_75percentile_case/Input: | | | | |
| Bytes | Date | | Time | File or Folder Name |
| 8499 | Feb | 20 | 14:53 | SMPAII75 |
| 8516282 | Feb | 20 | 11:05 | SMPAII75.mes1 |
| 8516282 | Feb | 20 | 12:10 | SMPAII75.mes10 |
| 8516282 | Feb | 20 | 11:12 | SMPAII75.mes2 |
| 8516282 | Feb | 20 | 11:20 | SMPAII75.mes3 |
| 8516282 | Feb | 20 | 11:27 | SMPAII75.mes4 |
| 8516282 | Feb | 20 | 11:34 | SMPAII75.mes5 |
| 8516282 | Feb | 20 | 11:41 | SMPAII75.mes6 |
| 8516282 | Feb | 20 | 11:48 | SMPAII75.mes7 |
| 8516282 | Feb | 20 | 11:56 | SMPAII75.mes8 |
| 8516282 | Feb | 20 | 12:03 | SMPAII75.mes9 |
| 7321109 | Feb | 20 | 10:52 | SMPAII75cut.mes |
| 1724 | Feb | 20 | 10:50 | sh.meshII75 |
| ./k1-10_realizations_10-scenarios/k1-10_realizations_6-scenarios/Tptpll_75percentile_case/Output: | | | | |
| Bytes | Date | | Time | File or Folder Name |
| 25280 | Feb | 21 | 0:34 | SMPAi.outII751 |
| 25279 | Feb | 21 | 8:03 | SMPAi.outII7510 |
| 25280 | Feb | 21 | 1:31 | SMPAi.outII752 |
| 25280 | Feb | 21 | 2:29 | SMPAi.outII753 |
| 25279 | Feb | 21 | 3:12 | SMPAi.outII754 |
| 25279 | Feb | 21 | 3:54 | SMPAi.outII755 |
| 25279 | Feb | 21 | 4:44 | SMPAi.outII756 |
| 25279 | Feb | 21 | 5:35 | SMPAi.outII757 |
| 25279 | Feb | 21 | 6:15 | SMPAi.outII758 |
| 25279 | Feb | 21 | 7:05 | SMPAi.outII759 |
| 9771 | Feb | 21 | 12:56 | SMPAioutII75.dat |

Table A-1. File Name and Description for Numerical Simulations DTN: LB0304SMDCREV2.001
(All Occurred During 2003) (Continued)

| ./k1-10_realizations_10-scenarios/k1-10_realizations_6-scenarios/Tptpl_base_case: | | | | |
|---|-------------|----|-------------|----------------------------|
| Bytes | Date | | Time | File or Folder Name |
| 4096 | Apr | 21 | 16:53 | Input |
| 4096 | Apr | 21 | 15:48 | Output |
| ./k1-10_realizations_10-scenarios/k1-10_realizations_6-scenarios/Tptpl_base_case/Input: | | | | |
| Bytes | Date | | Time | File or Folder Name |
| 8105 | Feb | 21 | 13:14 | SMPAill |
| ./k1-10_realizations_10-scenarios/k1-10_realizations_6-scenarios/Tptpl_base_case/Output: | | | | |
| Bytes | Date | | Time | File or Folder Name |
| 24657 | Feb | 21 | 21:02 | SMPAi.outllb1 |
| 24657 | Feb | 22 | 3:47 | SMPAi.outllb10 |
| 24657 | Feb | 21 | 21:50 | SMPAi.outllb2 |
| 24657 | Feb | 21 | 22:30 | SMPAi.outllb3 |
| 24657 | Feb | 21 | 23:17 | SMPAi.outllb4 |
| 24657 | Feb | 22 | 0:02 | SMPAi.outllb5 |
| 24657 | Feb | 22 | 0:44 | SMPAi.outllb6 |
| 24657 | Feb | 22 | 1:26 | SMPAi.outllb7 |
| 24657 | Feb | 22 | 2:10 | SMPAi.outllb8 |
| 24657 | Feb | 22 | 2:57 | SMPAi.outllb9 |
| 9770 | Feb | 24 | 12:25 | SMPAioutllb.dat |
| ./k1-10_realizations_10-scenarios/k1-10_realizations_6-scenarios/Tptpl_worst_case: | | | | |
| Bytes | Date | | Time | File or Folder Name |
| 4096 | Apr | 21 | 16:55 | Input |
| 4096 | Apr | 21 | 15:49 | Output |
| ./k1-10_realizations_10-scenarios/k1-10_realizations_6-scenarios/Tptpl_worst_case/Input: | | | | |
| Bytes | Date | | Time | File or Folder Name |
| 12309 | Feb | 20 | 14:54 | SMPAllw |
| 8442005 | Feb | 20 | 12:32 | SMPAllw.mes1 |
| 8442005 | Feb | 20 | 13:37 | SMPAllw.mes10 |
| 8442005 | Feb | 20 | 12:39 | SMPAllw.mes2 |
| 8442005 | Feb | 20 | 12:46 | SMPAllw.mes3 |
| 8442005 | Feb | 20 | 12:54 | SMPAllw.mes4 |
| 8442005 | Feb | 20 | 13:01 | SMPAllw.mes5 |
| 8442005 | Feb | 20 | 13:08 | SMPAllw.mes6 |
| 8442005 | Feb | 20 | 13:15 | SMPAllw.mes7 |
| 8442005 | Feb | 20 | 13:23 | SMPAllw.mes8 |
| 8442005 | Feb | 20 | 13:30 | SMPAllw.mes9 |
| 7256781 | Feb | 20 | 12:24 | SMPAllwcut.mes |
| 1718 | Feb | 20 | 12:25 | sh.meshllws |

Table A-1. File Name and Description for Numerical Simulations DTN: LB0304SMDCREV2.001
(All Occurred During 2003) (Continued)

| ./k1-10_realizations_10-scenarios/k1-10_realizations_6-scenarios/Tptpl Worst Case/Output: | | | | |
|--|-------------|----|-------------|----------------------------|
| Bytes | Date | | Time | File or Folder Name |
| 31554 | Feb | 21 | 8:44 | SMPAi.outllw1 |
| 31554 | Feb | 21 | 13:51 | SMPAi.outllw10 |
| 31554 | Feb | 21 | 9:43 | SMPAi.outllw2 |
| 31554 | Feb | 21 | 10:42 | SMPAi.outllw3 |
| 31554 | Feb | 21 | 11:18 | SMPAi.outllw4 |
| 31554 | Feb | 21 | 12:01 | SMPAi.outllw5 |
| 31554 | Feb | 21 | 16:41 | SMPAi.outllw6 |
| 31554 | Feb | 21 | 17:31 | SMPAi.outllw7 |
| 31554 | Feb | 21 | 18:15 | SMPAi.outllw8 |
| 31554 | Feb | 21 | 12:50 | SMPAi.outllw9 |
| 9770 | Apr | 8 | 16:26 | SMPAioutllw.dat |
| ./k1-10_realizations_10-scenarios/k1-10_realizations_6-scenarios/Tptpmn_75percentile Case: | | | | |
| Bytes | Date | | Time | File or Folder Name |
| 4096 | Apr | 21 | 16:55 | Input |
| 4096 | Apr | 21 | 15:49 | Output |
| ./k1-10_realizations_10-scenarios/k1-10_realizations_6-scenarios/Tptpmn_75percentile Case/Input: | | | | |
| Bytes | Date | | Time | File or Folder Name |
| 9343 | Feb | 20 | 11:25 | SMPAimn75 |
| 8430768 | Feb | 20 | 13:48 | SMPAmn75.mes1 |
| 8430768 | Feb | 20 | 14:53 | SMPAmn75.mes10 |
| 8430768 | Feb | 20 | 13:55 | SMPAmn75.mes2 |
| 8430768 | Feb | 20 | 14:02 | SMPAmn75.mes3 |
| 8430768 | Feb | 20 | 14:09 | SMPAmn75.mes4 |
| 8430768 | Feb | 20 | 14:16 | SMPAmn75.mes5 |
| 8430768 | Feb | 20 | 14:24 | SMPAmn75.mes6 |
| 8430768 | Feb | 20 | 14:31 | SMPAmn75.mes7 |
| 8430768 | Feb | 20 | 14:38 | SMPAmn75.mes8 |
| 8430768 | Feb | 20 | 14:45 | SMPAmn75.mes9 |
| 7247604 | Feb | 20 | 11:16 | SMPAmn75cut.mes |
| 1723 | Feb | 20 | 11:14 | sh.meshmn75 |
| ./k1-10_realizations_10-scenarios/k1-10_realizations_6-scenarios/Tptpmn_75percentile Case/Output: | | | | |
| Bytes | Date | | Time | File or Folder Name |
| 26683 | Feb | 21 | 14:47 | SMPAi.outmn751 |
| 26684 | Feb | 20 | 23:51 | SMPAi.outmn7510 |
| 26683 | Feb | 21 | 15:53 | SMPAi.outmn752 |
| 26684 | Feb | 20 | 17:04 | SMPAi.outmn753 |
| 26684 | Feb | 20 | 17:53 | SMPAi.outmn754 |
| 26684 | Feb | 20 | 18:51 | SMPAi.outmn755 |
| 26684 | Feb | 20 | 20:00 | SMPAi.outmn756 |
| 26684 | Feb | 20 | 21:05 | SMPAi.outmn757 |
| 26684 | Feb | 20 | 21:54 | SMPAi.outmn758 |
| 26684 | Feb | 20 | 22:54 | SMPAi.outmn759 |

Table A-1. File Name and Description for Numerical Simulations DTN: LB0304SMDCREV2.001
(All Occurred During 2003) (Continued)

| ./k1-10_realizations_10-scenarios/k1-10_realizations_6-scenarios/Tptpmn_base_case: | | | | |
|--|-------------|----|-------------|----------------------------|
| Bytes | Date | | Time | File or Folder Name |
| 15697 | Mar | 13 | 18:43 | SMPAioutmn75.dat |
| 4096 | Apr | 21 | 15:46 | Input |
| 4096 | Apr | 21 | 15:49 | Output |
| ./k1-10_realizations_10-scenarios/k1-10_realizations_6-scenarios/Tptpmn_base_case/Input: | | | | |
| Bytes | Date | | Time | File or Folder Name |
| 8103 | Feb | 21 | 13:15 | SMPAimn |
| ./k1-10_realizations_10-scenarios/k1-10_realizations_6-scenarios/Tptpmn_base_case/Output: | | | | |
| Bytes | Date | | Time | File or Folder Name |
| 24657 | Feb | 22 | 5:51 | SMPAi.outmnb1 |
| 24657 | Feb | 22 | 14:01 | SMPAi.outmnb10 |
| 24657 | Feb | 22 | 6:48 | SMPAi.outmnb2 |
| 24657 | Feb | 22 | 7:40 | SMPAi.outmnb3 |
| 24657 | Feb | 22 | 8:35 | SMPAi.outmnb4 |
| 24657 | Feb | 22 | 9:26 | SMPAi.outmnb5 |
| 24657 | Feb | 22 | 10:18 | SMPAi.outmnb6 |
| 24657 | Feb | 22 | 11:11 | SMPAi.outmnb7 |
| 24657 | Feb | 22 | 12:07 | SMPAi.outmnb8 |
| 24657 | Feb | 22 | 13:07 | SMPAi.outmnb9 |
| 9770 | Feb | 24 | 12:30 | SMPAioutmnb.dat |
| ./k1-10_realizations_10-scenarios/k1-10_realizations_6-scenarios/Tptpmn_worst_case: | | | | |
| Bytes | Date | | Time | File or Folder Name |
| 4096 | Apr | 21 | 17:02 | Input |
| 4096 | Apr | 21 | 15:49 | Output |
| ./k1-10_realizations_10-scenarios/k1-10_realizations_6-scenarios/Tptpmn_worst_case/Input: | | | | |
| Bytes | Date | | Time | File or Folder Name |
| 12975 | Mar | 12 | 15:52 | SMPAimnw |
| 8123989 | Mar | 12 | 15:44 | SMPAmnw.mes1 |
| 8123989 | Mar | 12 | 16:47 | SMPAmnw.mes10 |
| 8123989 | Mar | 12 | 15:51 | SMPAmnw.mes2 |
| 8123989 | Mar | 12 | 15:57 | SMPAmnw.mes3 |
| 8123989 | Mar | 12 | 16:05 | SMPAmnw.mes4 |
| 8123989 | Mar | 12 | 16:12 | SMPAmnw.mes5 |
| 8123989 | Mar | 12 | 16:20 | SMPAmnw.mes6 |
| 8123989 | Mar | 12 | 16:27 | SMPAmnw.mes7 |
| 8123989 | Mar | 12 | 16:33 | SMPAmnw.mes8 |
| 8123989 | Mar | 12 | 16:40 | SMPAmnw.mes9 |
| 6983023 | Mar | 12 | 15:36 | SMPAmnwcut.mes |
| 1718 | Feb | 20 | 10:41 | sh.meshmwns |

Table A-1. File Name and Description for Numerical Simulations DTN: LB0304SMDCREV2.001
(All Occurred During 2003) (Continued)

| ./k1-10_realizations_10-scenarios/k1-10_realizations_6-scenarios/Tptpmn_worst_case/Output: | | | | |
|---|-------------|----|-------------|----------------------------|
| Bytes | Date | | Time | File or Folder Name |
| 32653 | Mar | 12 | 16:39 | SMPAi.outmnw1 |
| 32653 | Mar | 13 | 0:42 | SMPAi.outmnw10 |
| 32653 | Mar | 12 | 17:36 | SMPAi.outmnw2 |
| 32653 | Mar | 12 | 18:27 | SMPAi.outmnw3 |
| 32653 | Mar | 12 | 19:23 | SMPAi.outmnw4 |
| 32653 | Mar | 12 | 20:15 | SMPAi.outmnw5 |
| 32653 | Mar | 12 | 21:05 | SMPAi.outmnw6 |
| 32653 | Mar | 12 | 21:57 | SMPAi.outmnw7 |
| 32653 | Mar | 12 | 22:51 | SMPAi.outmnw8 |
| 32653 | Mar | 12 | 23:48 | SMPAi.outmnw9 |
| 14711 | Mar | 13 | 11:54 | SMPAioutmnws.dat |
| ./k1-r_6-s_moisture-mapping: | | | | |
| Bytes | Date | | Time | File or Folder Name |
| 4096 | Apr | 21 | 2003 | T2_input |
| 4096 | Apr | 21 | 2003 | T2_output |
| 4096 | Apr | 21 | 2003 | iT2_input |
| 4096 | Apr | 21 | 2003 | iT2_output |
| ./k1-r_6-s_moisture-mapping/T2_input: | | | | |
| Bytes | Date | | Time | File or Folder Name |
| 1728 | Apr | 10 | 8:18 | SMPA |
| 8529107 | Apr | 10 | 8:19 | SMPA.mes1 |
| 8516282 | Apr | 10 | 8:19 | SMPAII75.mes1 |
| 8442005 | Apr | 10 | 8:19 | SMPAllw.mes1 |
| 8430768 | Apr | 10 | 8:19 | SMPAmn75.mes1 |
| 8123989 | Apr | 10 | 8:20 | SMPAmnw.mes1 |
| 56 | Apr | 10 | 8:20 | parametersetrfll.dat |
| 56 | Apr | 10 | 8:20 | parametersetrfmn.dat |
| ./k1-r_6-s_moisture-mapping/T2_output: | | | | |
| Bytes | Date | | Time | File or Folder Name |
| 9102877 | Apr | 10 | 8:18 | SMPA.II1s |
| 9072799 | Apr | 10 | 8:18 | SMPA.II751s |
| 8989847 | Apr | 10 | 8:18 | SMPA.llw1s |
| 9113025 | Apr | 10 | 8:19 | SMPA.mn1s |
| 9005619 | Apr | 10 | 8:19 | SMPA.mn751s |
| 8664537 | Apr | 10 | 8:19 | SMPA.mnw1s |
| ./k1-r_6-s_moisture-mapping/iT2_input: | | | | |
| Bytes | Date | | Time | File or Folder Name |
| 7764 | Apr | 10 | 8:19 | SMPAill |
| 8158 | Apr | 10 | 8:19 | SMPAill75 |
| 11968 | Apr | 10 | 8:19 | SMPAillw |
| 7762 | Apr | 10 | 8:19 | SMPAimn |
| 9002 | Apr | 10 | 8:19 | SMPAimn75 |

Table A-1. File Name and Description for Numerical Simulations DTN: LB0304SMDCREV2.001
(All Occurred During 2003) (Continued)

| ./k1-r_6-s_moisture-mapping/iT2_output: | | | | |
|--|-------------|----|-------------|----------------------------|
| Bytes | Date | | Time | File or Folder Name |
| 12634 | Apr | 10 | 8:19 | SMPAimnw |
| 19474 | Apr | 10 | 8:19 | SMPAi.outll1s |
| 20097 | Apr | 10 | 8:19 | SMPAi.outll751s |
| 26372 | Apr | 10 | 8:19 | SMPAi.outllw1s |
| 19474 | Apr | 10 | 8:19 | SMPAi.outmn1s |
| 21501 | Apr | 10 | 8:19 | SMPAi.outmn751s |
| 27477 | Apr | 10 | 8:19 | SMPAi.outmnw1s |

Table A-2 lists the plot files and tables in this model report. The .wmf files produced by TecPlot can be viewed by opening MS Word 97 (or newer), going to the pull-down menu for Insert → Picture, and then choosing the desired figure file.

Table A-2. File for Figures and Tables in This Model Report DTN: LB0304SMDCREV2.002

| File name | Folder | Bytes | Date | Time |
|------------------|------------------------|--------------|-------------|-------------|
| fig6-1.wmf | \Completed image files | 560614 | 4/8/2003 | 6:36:40 PM |
| fig6-10.wmf | \Completed image files | 48972 | 4/8/2003 | 7:43:56 PM |
| fig6-11.wmf | \Completed image files | 61876 | 4/8/2003 | 7:54:37 PM |
| fig6-12.wmf | \Completed image files | 42522 | 4/8/2003 | 8:04:50 PM |
| fig6-13.wmf | \Completed image files | 42724 | 4/8/2003 | 8:11:29 PM |
| fig6-14a.wmf | \Completed image files | 401190 | 4/8/2003 | 6:22:11 PM |
| fig6-14b.wmf | \Completed image files | 416932 | 4/8/2003 | 6:30:24 PM |
| fig6-15.wmf | \Completed image files | 50168 | 4/8/2003 | 8:55:53 PM |

Table A-2. File for Figures and Tables in This Model Report
DTN: LB0304SMDCREV2.002 (Continued)

| File name | Folder | Bytes | Date | Time |
|-----------------|------------------------------------|---------|-----------|------------|
| fig6-16a.wmf | \Completed image files | 411286 | 4/8/2003 | 6:16:26 PM |
| fig6-16b.wmf | \Completed image files | 416932 | 4/8/2003 | 6:30:13 PM |
| fig6-17.wmf | \Completed image files | 50816 | 4/8/2003 | 8:42:59 PM |
| fig6-18a.wmf | \Completed image files | 372440 | 4/8/2003 | 6:31:31 PM |
| fig6-18b.wmf | \Completed image files | 360542 | 4/8/2003 | 6:33:21 PM |
| fig6-19.wmf | \Completed image files | 50168 | 4/8/2003 | 8:51:07 PM |
| fig6-20a.wmf | \Completed image files | 362244 | 4/8/2003 | 6:31:03 PM |
| fig6-20b.wmf | \Completed image files | 360542 | 4/8/2003 | 6:33:32 PM |
| fig6-21.wmf | \Completed image files | 50304 | 4/8/2003 | 9:00:44 PM |
| fig6-3.wmf | \Completed image files | 6514 | 4/8/2003 | 7:13:51 PM |
| fig6-4a.wmf | \Completed image files | 588962 | 4/8/2003 | 7:22:27 PM |
| fig6-4b.wmf | \Completed image files | 221700 | 4/11/2003 | 4:22:00 PM |
| fig6-5.wmf | \Completed image files | 1087160 | 4/8/2003 | 7:19:29 PM |
| fig6-6.wmf | \Completed image files | 167524 | 4/8/2003 | 7:21:29 PM |
| fig6-7.wmf | \Completed image files | 116500 | 4/8/2003 | 7:20:21 PM |
| fig6-8.wmf | \Completed image files | 224222 | 4/8/2003 | 7:21:06 PM |
| fig6-9.wmf | \Completed image files | 45804 | 4/8/2003 | 7:38:55 PM |
| fig_llbmean.xls | \Supporting data for tecplot input | 20992 | 4/8/2003 | 2:18:24 PM |
| fig_mnbmean.xls | \Supporting data for tecplot input | 20992 | 4/8/2003 | 2:26:02 PM |
| fig6-10.txt | \Supporting data for tecplot input | 3251 | 4/8/2003 | 7:38:25 PM |
| fig6-10_1.xls | \Supporting data for tecplot input | 37376 | 4/7/2003 | 5:12:51 PM |
| fig6-10_2.xls | \Supporting data for tecplot input | 18432 | 4/7/2003 | 5:22:11 PM |
| fig6-11.txt | \Supporting data for tecplot input | 4305 | 4/8/2003 | 7:53:07 PM |
| fig6-11_1.xls | \Supporting data for tecplot input | 41472 | 4/7/2003 | 4:51:33 PM |
| fig6-11_2.xls | \Supporting data for tecplot input | 32256 | 4/7/2003 | 5:03:43 PM |
| fig6-12.txt | \Supporting data for tecplot input | 634 | 4/8/2003 | 7:57:45 PM |
| fig6-12.xls | \Supporting data for tecplot input | 15360 | 4/8/2003 | 1:59:01 PM |
| fig6-13.txt | \Supporting data for tecplot input | 638 | 4/8/2003 | 8:08:55 PM |
| fig6-13.xls | \Supporting data for tecplot input | 15360 | 4/8/2003 | 2:08:53 PM |
| fig6-15.txt | \Supporting data for tecplot input | 3242 | 4/8/2003 | 8:33:12 PM |
| fig6-15.xls | \Supporting data for tecplot input | 34816 | 4/8/2003 | 3:59:49 PM |
| fig6-15_1.xls | \Supporting data for tecplot input | 25088 | 4/8/2003 | 3:20:00 PM |
| fig6-15_2.xls | \Supporting data for tecplot input | 20480 | 4/8/2003 | 2:34:04 PM |
| fig6-17.txt | \Supporting data for tecplot input | 3003 | 4/8/2003 | 8:35:54 PM |
| fig6-17.xls | \Supporting data for tecplot input | 28672 | 4/8/2003 | 4:01:20 PM |
| fig6-17_1.xls | \Supporting data for tecplot input | 25088 | 4/8/2003 | 3:39:25 PM |
| fig6-17_2.xls | \Supporting data for tecplot input | 15872 | 4/8/2003 | 2:40:37 PM |
| fig6-19.txt | \Supporting data for tecplot input | 2913 | 4/8/2003 | 8:44:29 PM |
| fig6-19.xls | \Supporting data for tecplot input | 34304 | 4/8/2003 | 4:10:46 PM |
| fig6-19_1.xls | \Supporting data for tecplot input | 25088 | 4/8/2003 | 3:42:57 PM |
| fig6-19_2.xls | \Supporting data for tecplot input | 15872 | 4/8/2003 | 2:47:32 PM |
| fig6-2.doc | \Supporting data for tecplot input | 76288 | 4/8/2003 | 6:49:19 PM |

Table A-2. File for Figures and Tables in This Model Report
DTN: LB0304SMDCREV2.002 (Continued)

| File name | Folder | Bytes | Date | Time |
|-----------------|------------------------------------|---------|-----------|-------------|
| fig6-21.txt | \Supporting data for tecplot input | 2919 | 4/8/2003 | 8:57:00 PM |
| fig6-21.xls | \Supporting data for tecplot input | 34304 | 4/8/2003 | 4:14:18 PM |
| fig6-21_1.xls | \Supporting data for tecplot input | 25088 | 4/8/2003 | 3:45:34 PM |
| fig6-21_2.xls | \Supporting data for tecplot input | 15872 | 4/8/2003 | 3:01:19 PM |
| fig6-3.txt | \Supporting data for tecplot input | 334 | 4/8/2003 | 7:07:07 PM |
| Fig6-3to6-8.xls | \Supporting data for tecplot input | 1372160 | 4/11/2003 | 3:39:20 PM |
| fig6-9.txt | \Supporting data for tecplot input | 2326 | 4/8/2003 | 7:36:18 PM |
| fig6-9_1.xls | \Supporting data for tecplot input | 29184 | 4/7/2003 | 3:55:50 PM |
| fig6-9_2.xls | \Supporting data for tecplot input | 16896 | 4/7/2003 | 3:46:01 PM |
| readme-fig3to8 | | 1927 | 4/3/2003 | 10:41:00 AM |
| Table7-1.xls | | 22528 | 4/14/2003 | 10:22:00 AM |

Table A-3 lists computer files to simulate the impact of thermal-hydrological-mechanical effects on seepage (Section 6.7). The simulation result is used to compare seepage rates immediately after excavation and 10,000 years after spent nuclear fuel emplacement.

Table A-3. Files for the Impact of Thermal-Hydrologic-Mechanical Effects on Seepage
DTN: LB0304SMDCREV2.003

| File name | Folder | Bytes | Date | Time |
|-----------------------------|--------|---------|-----------|-------------|
| incon | | 292058 | 4/14/2003 | 9:37:14 AM |
| SVPARAM.DAT | | 265914 | 1/29/2003 | 5:17:00 PM |
| Hmdelb_10ky | \10ky | 53766 | 4/8/2003 | 11:14:20 PM |
| Tmn1_mh_1200mm_10ky_5cm.dat | \10ky | 723057 | 4/14/2003 | 12:19:56 PM |
| Tmn1_mh_1200mm_10ky_5cm.out | \10ky | 2815421 | 4/14/2003 | 1:53:30 PM |
| Tmn1_mh_120mm_10ky_5cm.dat | \10ky | 723056 | 4/14/2003 | 1:32:30 PM |
| Tmn1_mh_120mm_10ky_5cm.out | \10ky | 2814877 | 4/14/2003 | 2:03:54 PM |
| Tmn1_mh_1800mm_10ky.dat | \10ky | 724483 | 4/14/2003 | 12:24:46 PM |
| Tmn1_mh_1800mm_10ky.out | \10ky | 2818233 | 4/14/2003 | 2:50:26 PM |
| Tmn1_mh_2400mm_10ky_5cm.dat | \10ky | 725909 | 4/14/2003 | 12:29:18 PM |
| Tmn1_mh_2400mm_10ky_5cm.out | \10ky | 2825522 | 4/14/2003 | 3:00:18 PM |
| Tmn1_mh_240mm_10ky_5cm.dat | \10ky | 725908 | 4/14/2003 | 12:01:36 PM |
| Tmn1_mh_240mm_10ky_5cm.out | \10ky | 2825050 | 4/14/2003 | 2:09:14 PM |
| Tmn1_mh_360mm_10ky_5cm.dat | \10ky | 728760 | 4/14/2003 | 12:09:12 PM |
| Tmn1_mh_360mm_10ky_5cm.out | \10ky | 2835223 | 4/14/2003 | 2:16:02 PM |

Table A-3. Files for the Impact of Thermal-Hydrologic-Mechanical Effects on Seepage DTN: LB0304SMDCREV2.003 (Continued)

| File name | Folder | Bytes | Date | Time |
|----------------------------|------------------|---------|-----------|-------------|
| Tmn1_mh_6000mm_10ky.dat | \10ky | 721631 | 4/14/2003 | 1:24:34 PM |
| Tmn1_mh_6000mm_10ky.out | \10ky | 2813940 | 4/14/2003 | 3:06:08 PM |
| Tmn1_mh_600mm_10ky_5cm.dat | \10ky | 721630 | 4/14/2003 | 12:14:30 PM |
| Tmn1_mh_600mm_10ky_5cm.out | \10ky | 2807709 | 4/14/2003 | 2:30:46 PM |
| Tmn1_mh_60mm_10ky_5cm.dat | \10ky | 721629 | 4/14/2003 | 11:55:28 AM |
| Tmn1_mh_60mm_10ky_5cm.out | \10ky | 2810382 | 4/14/2003 | 1:49:32 PM |
| Hmdelb_001y_excavation | \post-excavation | 53766 | 4/10/2003 | 5:22:04 PM |
| Tmn1_mh_1200mm_exc_5cm.dat | \post-excavation | 723057 | 4/14/2003 | 12:19:56 PM |
| Tmn1_mh_1200mm_exc_5cm.out | \post-excavation | 2810872 | 4/14/2003 | 12:22:12 PM |
| Tmn1_mh_120mm_exc_5cm.dat | \post-excavation | 723056 | 4/14/2003 | 1:32:30 PM |
| Tmn1_mh_120mm_exc_5cm.out | \post-excavation | 2811477 | 4/14/2003 | 1:34:44 PM |
| Tmn1_mh_1800mm_exc_5cm.dat | \post-excavation | 724483 | 4/14/2003 | 12:24:46 PM |
| Tmn1_mh_1800mm_exc_5cm.out | \post-excavation | 2817386 | 4/14/2003 | 12:27:00 PM |
| Tmn1_mh_2400mm_exc_5cm.dat | \post-excavation | 725909 | 4/14/2003 | 12:29:18 PM |
| Tmn1_mh_2400mm_exc_5cm.out | \post-excavation | 2824433 | 4/14/2003 | 12:31:38 PM |
| Tmn1_mh_240mm_exc_5cm.dat | \post-excavation | 725908 | 4/14/2003 | 12:01:36 PM |
| Tmn1_mh_240mm_exc_5cm.out | \post-excavation | 2821771 | 4/14/2003 | 12:03:42 PM |
| Tmn1_mh_360mm_exc_5cm.dat | \post-excavation | 728760 | 4/14/2003 | 12:09:12 PM |
| Tmn1_mh_360mm_exc_5cm.out | \post-excavation | 2831823 | 4/14/2003 | 12:11:12 PM |
| Tmn1_mh_6000mm_exc_5cm.dat | \post-excavation | 721631 | 4/14/2003 | 1:24:34 PM |
| Tmn1_mh_6000mm_exc_5cm.out | \post-excavation | 2812004 | 4/14/2003 | 1:27:18 PM |
| Tmn1_mh_600mm_exc_5cm.dat | \post-excavation | 721630 | 4/14/2003 | 12:14:30 PM |
| Tmn1_mh_600mm_exc_5cm.out | \post-excavation | 2801526 | 4/14/2003 | 12:16:10 PM |
| Tmn1_mh_60mm_exc_5cm.dat | \post-excavation | 721629 | 4/14/2003 | 11:55:28 AM |
| Tmn1_mh_60mm_exc_5cm.out | \post-excavation | 2807334 | 4/14/2003 | 11:57:56 AM |

Table A-4 gives the plot file in this model report and support data files for the impact of thermal-hydrologic-mechanical effects on seepage. The .wmf files produced by TecPlot can be viewed by opening MS Word 97 (or newer), going to the pull-down menu for Insert → Picture, and then choosing the desired figure file.

Table A-4. Files for Plotting Results of the Impact of Thermal-Hydrologic-Mechanical Effects on Seepage; DTN: LB0304SMDCREV2.004



Table A-5 lists the supporting files for mesh generation and simulations of seepage into a collapsed drift of radius 5.5 m. Starting with a block mesh, a primary mesh with a circular drift of 5.5 m radius is generated. Multiple realizations of a three-dimensional permeability field are generated and mapped onto the mesh. Steady-state seepage rates are calculated for each realization and for many a combination of three seepage-relevant parameters (percolation flux, permeability, and capillary). The results are compiled, and a look-up table is created for use within the Total System Performance Assessment for License Application (Table A-6).

Table A-5. File Listing for DTN: LB0307SEEPDRCL.001

| File Name | Bytes | Date | Time |
|-------------------------|----------|-----------|-------|
| ResponseSurfaceSMPA.xls | 1371136 | 7/15/2003 | 8:27 |
| SMPAC | 2042 | 7/18/2003 | 18:51 |
| SMPAC.mes10 | 13691290 | 7/18/2003 | 18:50 |
| SMPAC.mes11 | 13691290 | 7/18/2003 | 18:46 |
| SMPAC.mes2 | 13691290 | 7/18/2003 | 18:48 |
| SMPAC.mes3 | 13691290 | 7/18/2003 | 18:48 |
| SMPAC.mes4 | 13691290 | 7/18/2003 | 18:48 |
| SMPAC.mes5 | 13691290 | 7/18/2003 | 18:49 |
| SMPAC.mes6 | 13691290 | 7/18/2003 | 18:49 |
| SMPAC.mes7 | 13691290 | 7/18/2003 | 18:49 |
| SMPAC.mes8 | 13691290 | 7/18/2003 | 18:50 |
| SMPAC.mes9 | 13691290 | 7/18/2003 | 18:50 |
| SMPAC.results | 627300 | 7/18/2003 | 18:56 |
| SMPAC.xls | 839680 | 7/18/2003 | 18:58 |
| SMPACi | 14338 | 7/18/2003 | 18:52 |
| SMPACi.out10 | 741081 | 7/18/2003 | 18:54 |
| SMPACi.out11 | 738779 | 7/18/2003 | 18:54 |
| SMPACi.out2 | 739866 | 7/18/2003 | 18:52 |
| SMPACi.out3 | 739220 | 7/18/2003 | 18:52 |
| SMPACi.out4 | 736623 | 7/18/2003 | 18:53 |

Table A-5. File Listing for DTN: LB0307SEEPDRCL.001 (Continued)

| File Name | Bytes | Date | Time |
|------------------|----------|-----------|-------|
| SMPACi.out5 | 742167 | 7/18/2003 | 18:53 |
| SMPACi.out6 | 737453 | 7/18/2003 | 18:53 |
| SMPACi.out7 | 738458 | 7/18/2003 | 18:53 |
| SMPACi.out8 | 739537 | 7/18/2003 | 18:53 |
| SMPACi.out9 | 735840 | 7/18/2003 | 18:53 |
| driftC.con | 23232 | 7/18/2003 | 18:51 |
| mesh3dblock | 337 | 7/18/2003 | 18:45 |
| mesh3dblock.mes | 18088930 | 7/18/2003 | 18:45 |
| parameterset.dat | 130050 | 7/18/2003 | 18:52 |
| perm.par | 3562 | 7/18/2003 | 18:46 |
| primary.mes | 18088973 | 7/18/2003 | 18:46 |
| read_me.txt | 32407 | 7/18/2003 | 19:24 |
| sh.meshC | 3809 | 7/18/2003 | 18:46 |
| sh.runC10 | 120 | 7/18/2003 | 18:55 |
| sh.runC11 | 119 | 7/18/2003 | 18:55 |
| sh.runC2 | 117 | 7/18/2003 | 18:55 |
| sh.runC3 | 117 | 7/18/2003 | 18:55 |
| sh.runC4 | 117 | 7/18/2003 | 18:55 |
| sh.runC5 | 117 | 7/18/2003 | 18:55 |
| sh.runC6 | 117 | 7/18/2003 | 18:55 |
| sh.runC7 | 117 | 7/18/2003 | 18:55 |
| sh.runC8 | 117 | 7/18/2003 | 18:55 |
| sh.runC9 | 117 | 7/18/2003 | 18:55 |

Table A-6. File Listing for DTN: LB0307SEEPDRCL.002

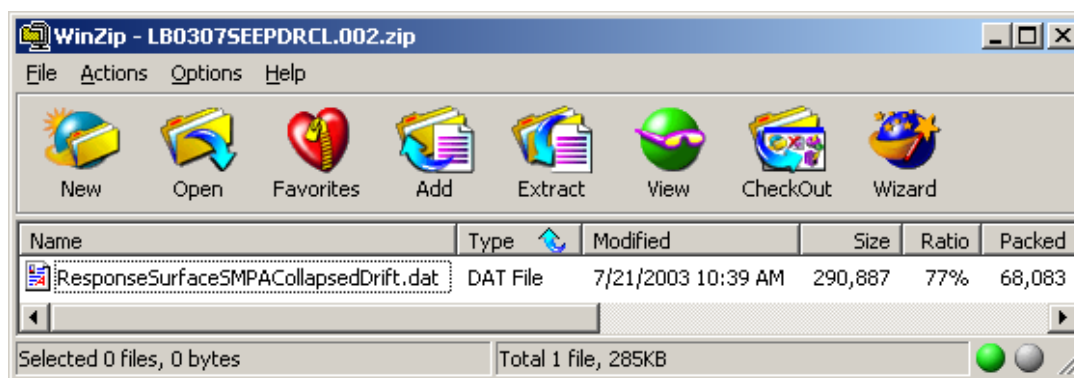


Table A-7 lists the files of numerical simulations of the flow focusing factor using two different sets of rock properties: the 2000 set (DTN: LB991121233129.001 [DIRS 147328]) and the 2003 set (DTNS: LB0208UZDSCPMI.002 [DIRS 161243] and LB0205REVUZPRP.001 [DIRS 159525]). Fifteen study cases are created for each rock set using (1) different fracture permeability fields by varying realizations and correlation lengths (1 m and 3 m), (2) different mean infiltration rates (1, 5, 25, 100, 500 mm/year), and (3) different infiltration distributions

(uniform, concentrated, and permeability-dependent). For the 2000 rock set, a generalized cumulative frequency curve (CFC) of the flow focusing factor (FFF) values over the 0.25-m horizontal width is obtained by fitting the 15 CFCs for the 15 study cases. For the 2003 rock set, a generalized CFC is obtained for the FFF values averaged over 5-m horizontal width.

Table A-7. File Listing for DTN: LB0406U0075FCS.001

| Volume Serial Number is E48E-4EB9 | | |
|---|------------|--|
| Directory of D:\YuccaMountain\FlowFocusing\QAruns\Figures | | |
| 07/12/2004 | 09:33a | <DIR> |
| 07/12/2004 | 09:33a | <DIR> |
| 06/25/2004 | 02:15p | 1,955,752 Figure1_3logKFields.jpg |
| 06/25/2004 | 09:41a | 2,446,904 Figure1_3logKFields.lpk |
| 06/24/2004 | 04:16p | 8,338,501 Figure1_3logKFields.tec |
| 06/25/2004 | 02:23p | 1,263,078 Figure2_FFFcontours.jpg |
| 06/25/2004 | 09:24a | 1,968,481 Figure2_FFFcontours.lpk |
| 07/12/2004 | 09:33a | 5,262,561 Figure2_FFFcontours.tec |
| 06/18/2004 | 04:32p | 21,517 Figure3_bottomflux.lpk |
| 06/16/2004 | 03:53p | 29,609 Figure3_bottomflux.tec |
| 06/28/2004 | 04:55p | 19,686 Figure4_CumulativeFrequency_Rocks2000.lpk |
| 06/28/2004 | 04:55p | 15,126 Figure4_CumulativeFrequency_Rocks2000.tec |
| 06/28/2004 | 04:17p | 33,217 Figure5_Sensitivity.lpk |
| 06/28/2004 | 04:17p | 14,118 Figure5_sensitivity.tec |
| 07/12/2004 | 09:23a | 21,590 Figure6_5mCumulativeFrequency_Rocks2003.lpk |
| 07/12/2004 | 09:21a | 12,678 Figure6_5mCumulativeFrequency_Rocks2003.tec |
| Directory of D:\YuccaMountain\FlowFocusing\QAruns\Figures (Continued) | | |
| 07/12/2004 | 09:30a | 43,550 Figure6_5mCumulativeFrequency_Rocks2003.wmf |
| 06/25/2004 | 11:47a | 176,700 Figure7_5mAveragedFFF_Fitting.dat |
| 07/12/2004 | 09:28a | 166,658 Figure7_5mAveragedFFF_Fitting.opj |
| | 17 File(s) | 21,789,726 bytes |
| | 2 Dir(s) | 13,326,614,528 bytes free |
| (1) Directory of D:\YuccaMountain\FlowFocusing\QAruns\2000Rocks\Case1mR1 | | |
| 06/25/2004 | 01:57p | <DIR> |
| 06/25/2004 | 01:57p | <DIR> |
| 06/08/2004 | 02:59p | 20,980 1mR1_100mm_bottomflux.dat |
| 06/07/2004 | 04:18p | 25,876,622 1mR1_100mm_flow9.dat |
| 06/08/2004 | 08:37a | 20,980 1mR1_1mm_bottomflux.dat |
| 06/07/2004 | 04:58p | 25,876,622 1mR1_1mm_flow9.dat |
| 06/08/2004 | 08:43a | 20,980 1mR1_25mm_bottomflux.dat |
| 06/07/2004 | 05:24p | 25,876,622 1mR1_25mm_flow9.dat |
| 06/08/2004 | 08:50a | 20,980 1mR1_500mm_bottomflux.dat |
| 06/07/2004 | 05:49p | 25,876,622 1mR1_500mm_flow9.dat |
| 06/08/2004 | 10:16a | 20,980 1mR1_5mmpulse_bottomflux.dat |
| 06/08/2004 | 09:35a | 25,876,622 1mR1_5mmpulse_flow9.dat |

Table A-7. File Listing for DTN: LB0406U0075FCS.001 (Continued)

| Volume Serial Number is E48E-4EB9 | | |
|---|------------|--------------------------------------|
| (1) Directory of D:\YuccaMountain\FlowFocusing\QAruns\2000Rocks\Case1mR1 (Continued) | | |
| 06/08/2004 | 09:26a | 20,980 1mR1_5mm_fbottomflux.dat |
| 06/16/2004 | 10:58a | 4,066,525 1mR1_5mm_FFF.tec |
| 06/08/2004 | 08:50a | 25,876,622 1mR1_5mm_flow9.dat |
| 06/17/2004 | 04:55p | 57,180 1mR1_5mm_NewBC_bottomflux.dat |
| 06/17/2004 | 01:44p | 25,901,514 1mR1_5mm_NewBC_flow9.dat |
| | 15 File(s) | 185,410,831 bytes |
| | 2 Dir(s) | 13,360,402,432 bytes free |
| (2) Directory of D:\YuccaMountain\FlowFocusing\QAruns\2000Rocks\Case1mR2 | | |
| 06/25/2004 | 01:57p | <DIR> |
| 06/25/2004 | 01:57p | <DIR> |
| 06/08/2004 | 12:28p | 20,980 1mR2_1mm_bottomflux.dat |
| 06/08/2004 | 11:46a | 25,876,622 1mR2_1mm_flow9.dat |
| 06/08/2004 | 12:50p | 20,980 1mR2_25mm_bottomflux.dat |
| 06/08/2004 | 11:44a | 25,876,622 1mR2_25mm_flow9.dat |
| 06/08/2004 | 12:26p | 20,980 1mR2_5mm_bottomflux.dat |
| 06/08/2004 | 11:40a | 25,876,622 1mR2_5mm_flow9.dat |
| | 6 File(s) | 77,692,806 bytes |
| | 2 Dir(s) | 13,360,427,008 bytes free |
| (3) Directory of D:\YuccaMountain\FlowFocusing\QAruns\2000Rocks\Case3mR1 | | |
| 06/25/2004 | 01:58p | <DIR> |
| 06/25/2004 | 01:58p | <DIR> |
| 06/09/2004 | 11:32a | 20,980 3mR1_100mm_bottomflux.dat |
| 06/09/2004 | 09:42a | 25,876,622 3mR1_100mm_flow9.dat |
| 06/09/2004 | 11:34a | 20,980 3mR1_1mm_bottomflux.dat |
| 06/09/2004 | 09:58a | 25,876,622 3mR1_1mm_flow9.dat |
| 06/09/2004 | 11:35a | 20,980 3mR1_25mm_bottomflux.dat |
| 06/09/2004 | 09:50a | 25,876,622 3mR1_25mm_flow9.dat |
| 06/09/2004 | 11:37a | 20,980 3mR1_500mm_bottomflux.dat |
| 06/09/2004 | 09:46a | 25,876,622 3mR1_500mm_flow9.dat |
| 06/09/2004 | 11:49a | 20,980 3mR1_5mm_bottomflux.dat |
| 06/16/2004 | 11:02a | 4,066,400 3mR1_5mm_FFF.dat |
| 06/09/2004 | 11:10a | 25,876,622 3mR1_5mm_flow9.dat |
| | 11 File(s) | 133,554,410 bytes |
| | 2 Dir(s) | 13,360,398,336 bytes free |
| (4) Directory of D:\YuccaMountain\FlowFocusing\QAruns\2000Rocks\InputFiles | | |
| 06/09/2004 | 02:22p | <DIR> |
| 06/09/2004 | 02:22p | <DIR> |

Table A-7. File Listing for DTN: LB0406U0075FCS.001 (Continued)

| Volume Serial Number is E48E-4EB9 | | |
|---|------------|----------------------------------|
| (4) Directory of D:\YuccaMountain\FlowFocusing\QAruns\2000Rocks\InputFiles (Continued) | | |
| 06/09/2004 | 02:22p | 2,283 DriftRocks2003.dat |
| 06/02/2004 | 11:56a | 24,833 GENER_100mm.dat |
| 06/02/2004 | 11:56a | 24,831 GENER_1mm.dat |
| 06/02/2004 | 11:57a | 24,832 GENER_25mm.dat |
| 06/02/2004 | 11:56a | 24,833 GENER_500mm.dat |
| 06/02/2004 | 11:57a | 24,831 GENER_5mm.dat |
| 06/08/2004 | 09:35a | 1,351 GENER_5mm_pulse.dat |
| 06/07/2004 | 02:34p | 30,341,120 gslib_3mR1.tar |
| 06/07/2004 | 10:11a | 28,269,621 Mesh_3mR1.dat |
| 06/09/2004 | 02:18p | 1,978 si_heat |
| 06/07/2004 | 10:26a | 2,218 TopBlocks.dat |
| | 11 File(s) | 58,742,731 bytes |
| | 2 Dir(s) | 13,360,455,680 bytes free |
| (5) Directory of D:\YuccaMountain\FlowFocusing\QAruns\2000Rocks\KFields | | |
| 06/29/2004 | 09:08a | <DIR> |
| 06/29/2004 | 09:08a | <DIR> |
| 06/08/2004 | 11:01a | 5,320 gslib_1mR1.dat |
| 06/08/2004 | 11:02a | 5,320 gslib_1mR2.dat |
| 06/08/2004 | 04:45p | 5,320 gslib_3mR1.dat |
| 06/07/2004 | 03:11p | 3,092 gslib_block.dat |
| 06/07/2004 | 03:31p | 29,462,656 MESH_K_1mR1.dat |
| 06/10/2004 | 11:15a | 28,269,621 MESH_K_1mR1.in |
| 06/07/2004 | 04:04p | 29,112,320 MESH_K_1mR1.tar |
| 06/10/2004 | 03:15p | 28,298,511 MESH_K_1mR1_NewBC.in |
| 06/08/2004 | 10:33a | 29,462,656 MESH_K_1mR2.dat |
| 06/08/2004 | 11:16a | 28,269,622 MESH_K_1mR2.in |
| 06/08/2004 | 11:07a | 29,112,320 MESH_K_1mR2.tar |
| 06/08/2004 | 04:54p | 29,462,656 MESH_K_3mR1.dat |
| 06/09/2004 | 09:22a | 28,269,621 MESH_K_3mR1.in |
| 06/08/2004 | 05:28p | 29,112,320 MESH_K_3mR1.tar |
| | 14 File(s) | 288,851,355 bytes |
| | 2 Dir(s) | 13,360,451,584 bytes free |
| (6) Directory of D:\YuccaMountain\FlowFocusing\QAruns\2003Rocks\Case1mR1 | | |
| 06/29/2004 | 09:05a | <DIR> |
| 06/29/2004 | 09:05a | <DIR> |
| 06/25/2004 | 11:11a | 45,460 1mR1_100mm_bottomflux.dat |
| 06/09/2004 | 05:51p | 25,876,622 1mR1_100mm_flow9.dat |
| 06/25/2004 | 11:12a | 45,460 1mR1_1mm_bottomflux.dat |
| 06/09/2004 | 06:25p | 25,876,622 1mR1_1mm_flow9.dat |

Table A-7. File Listing for DTN: LB0406U0075FCS.001 (Continued)

| Volume Serial Number is E48E-4EB9 | | |
|---|------------|--|
| (6) Directory of D:\YuccaMountain\FlowFocusing\QAruns\2003Rocks\Case1mR1 (Continued) | | |
| 06/25/2004 | 11:14a | 45,460 1mR1_25mm_bottomflux.dat |
| 06/09/2004 | 06:06p | 25,876,622 1mR1_25mm_flow9.dat |
| 06/25/2004 | 11:15a | 45,460 1mR1_500mm_bottomflux.dat |
| 06/09/2004 | 05:37p | 25,876,622 1mR1_500mm_flow9.dat |
| 06/25/2004 | 11:17a | 45,460 1mR1_5mm_bottomflux.dat |
| 06/11/2004 | 01:49p | 4,066,400 1mR1_5mm_FFF.tec |
| 06/10/2004 | 09:51a | 25,876,622 1mR1_5mm_flow9.dat |
| 06/25/2004 | 11:18a | 45,460 1mR1_5mm_NewBC_Rocks2003_bottomflux.dat |
| 06/18/2004 | 09:35a | 25,901,514 1mR1_5mm_NewBC_Rocks2003_flow9.dat |
| 06/25/2004 | 11:19a | 45,460 1mR1_5mm_pulse_Rocks2003_bottomflux.dat |
| 06/18/2004 | 09:53a | 25,876,622 1mR1_5mm_pulse_Rocks2003_flow9.dat |
| | 15 File(s) | 185,545,866 bytes |
| | 2 Dir(s) | 13,360,476,160 bytes free |
| (7) Directory of D:\YuccaMountain\FlowFocusing\QAruns\2003Rocks\Case1mR2 | | |
| 06/29/2004 | 09:05a | <DIR> |
| 06/29/2004 | 09:05a | <DIR> |
| 06/25/2004 | 11:21a | 45,460 1mR2_1mm_Rocks2003_bottomflux.dat |
| 06/08/2004 | 11:46a | 25,876,622 1mR2_1mm_Rocks2003_flow9.dat |
| 06/25/2004 | 11:23a | 45,460 1mR2_25mm_Rocks2003_bottomflux.dat |
| 06/08/2004 | 11:44a | 25,876,622 1mR2_25mm_Rocks2003_flow9.dat |
| 06/25/2004 | 11:24a | 45,460 1mR2_5mm_Rocks2003_bottomflux.dat |
| 06/08/2004 | 11:40a | 25,876,622 1mR2_5mm_Rocks2003_flow9.dat |
| | 6 File(s) | 77,766,246 bytes |
| | 2 Dir(s) | 13,360,472,064 bytes free |
| (8) Directory of D:\YuccaMountain\FlowFocusing\QAruns\2003Rocks\Case3mR1 | | |
| 06/29/2004 | 09:05a | <DIR> |
| 06/29/2004 | 09:05a | <DIR> |
| 06/25/2004 | 11:32a | 45,460 3mR1_100mm_Rocks2003_bottomflux.dat |
| 06/17/2004 | 07:33p | 25,876,622 3mR1_100mm_Rocks2003_flow9.dat |
| 06/25/2004 | 11:33a | 45,460 3mR1_1mm_Rocks2003_bottomflux.dat |
| 06/18/2004 | 07:10a | 25,876,622 3mR1_1mm_Rocks2003_flow9.dat |
| 06/25/2004 | 11:35a | 45,460 3mR1_25mm_Rocks2003_bottomflux.dat |
| 06/18/2004 | 02:39a | 25,876,622 3mR1_25mm_Rocks2003_flow9.dat |
| 06/25/2004 | 11:36a | 45,460 3mR1_500mm_Rocks2003_Bottomflux.dat.dat |
| 06/17/2004 | 05:49p | 25,876,622 3mR1_500mm_Rocks2003_flow9.dat |
| 06/25/2004 | 11:37a | 45,460 3mR1_5mm_Rocks2003_bottomflux.dat |
| 06/18/2004 | 09:17a | 4,066,400 3mR1_5mm_Rocks2003_FFF.tec |
| 06/18/2004 | 06:29a | 25,876,622 3mR1_5mm_Rocks2003_flow9.dat |
| | 11 File(s) | 133,676,810 bytes |
| | 2 Dir(s) | 13,360,467,968 bytes free |

Table A-7. File Listing for DTN: LB0406U0075FCS.001 (Continued)

| Volume Serial Number is E48E-4EB9 | | |
|--|------------|--|
| (9) Directory of D:\YuccaMountain\FlowFocusing\QAruns\Figures | | |
| 07/12/2004 | 09:33a | <DIR> |
| 07/12/2004 | 09:33a | <DIR> |
| 06/25/2004 | 02:15p | 1,955,752 Figure1_3logKFields.jpg |
| 06/25/2004 | 09:41a | 2,446,904 Figure1_3logKFields.lpk |
| 06/24/2004 | 04:16p | 8,338,501 Figure1_3logKFields.tec |
| 06/25/2004 | 02:23p | 1,263,078 Figure2_FFFcontours.jpg |
| 06/25/2004 | 09:24a | 1,968,481 Figure2_FFFcontours.lpk |
| 07/12/2004 | 09:33a | 5,262,561 Figure2_FFFcontours.tec |
| 06/18/2004 | 04:32p | 21,517 Figure3_bottomflux.lpk |
| 06/16/2004 | 03:53p | 29,609 Figure3_bottomflux.tec |
| 06/28/2004 | 04:55p | 19,686 Figure4_CumulativeFrequency_Rocks2000.lpk |
| 06/28/2004 | 04:55p | 15,126 Figure4_CumulativeFrequency_Rocks2000.tec |
| 06/28/2004 | 04:17p | 33,217 Figure5_Sensitivity.lpk |
| 06/28/2004 | 04:17p | 14,118 Figure5_sensitivity.tec |
| 07/12/2004 | 09:23a | 21,590 Figure6_5mCumulativeFrequency_Rocks2003.lpk |
| 07/12/2004 | 09:21a | 12,678 Figure6_5mCumulativeFrequency_Rocks2003.tec |
| 07/12/2004 | 09:30a | 43,550 Figure6_5mCumulativeFrequency_Rocks2003.wmf |
| 06/25/2004 | 11:47a | 176,700 Figure7_5mAveragedFFF_Fitting.dat |
| 07/12/2004 | 09:28a | 166,658 Figure7_5mAveragedFFF_Fitting.opj |
| | 17 File(s) | 21,789,726 bytes |
| | 2 Dir(s) | 13,326,614,528 bytes free |
| (10) Directory of D:\YuccaMountain\FlowFocusing\QAruns\MeshGeneration | | |
| 06/30/2004 | 03:05p | <DIR> |
| 06/30/2004 | 03:05p | <DIR> |
| 06/07/2004 | 02:45p | 974 grid120k.dat |
| 06/30/2004 | 03:05p | 0 j.list |
| 06/07/2004 | 02:11p | 25,872,628 MESH |
| 06/07/2004 | 02:44p | 25,518,080 mesh.tar |
| 06/07/2004 | 03:05p | 25,872,621 MESH_update.dat |
| | 5 File(s) | 77,264,303 bytes |
| | 2 Dir(s) | 13,360,447,488 bytes free |

Table A-8 lists three summary files for the FFF study using the two different sets of rock properties. For the 2000 rock set, the 15 CFCs of the 0.25-m FFF and the generalized CFC are listed. For the 2003 rock set, the 15 CFCs of different study cases and the generalized CFC of the FFF averaged over 5-m width are listed. In addition, a world file with all six figures in Sections 6.8 and 6.9 of this model report is listed.

Table A-8. File Listing for DTN: LB0406U0075FCS.002

| Name | Type | Modified | Size | Ratio | Packed | Path |
|------------------------------|---------------------|--------------------|-----------|-------|-----------|------|
| LB0406U0075FCS.002ReadMe.doc | Microsoft Word ... | 7/12/2004 11:06 AM | 35,328 | 51% | 17,398 | |
| Summary_5mCFC_2003Rocks.xls | Microsoft Excel ... | 7/12/2004 11:48 AM | 22,528 | 79% | 4,819 | |
| Summary_CFC_2000Rocks.xls | Microsoft Excel ... | 7/12/2004 11:51 AM | 20,480 | 79% | 4,321 | |
| Summary_Figures.doc | Microsoft Word ... | 7/12/2004 9:30 AM | 3,314,688 | 4% | 3,179,126 | |

Selected 0 files, 0 bytes Total 4 files, 3,314KB

APPENDIX B

DATA REDUCTION STEPS FOR *RESPONSESURFACESMPA.DOC*

Section 6.6.1 discusses the seepage results. The seepage percentage is defined as the ratio of the seepage rate into a drift section to the percolation rate applied to the top of the model over the projected cross-sectional area of that drift section. The seepage rate for model calculation is transformed to response surface of seepage into drift in kilograms of water per year per waste package (kg/year/wp) of 5.5 m diameter and 5.1 m length (design drawings 800-IED-MGR0-00201-000-00B (BSC 2004 [DIRS 168489]) and 800-IED-WIS0-00205-000-00C (BSC 2004 [DIRS 167758])). An excerpt is shown in Table B-1. The data reductions were performed using standard functions of the exempt software EXCEL (2000 SR-1). Detailed simulation results for all 20 realizations with every combination of k_{FC} , $1/\alpha$, and Q_p values were submitted to the Technical Data Management System (Output-DTN: LB0304SMDCREV2.002). The following steps explain the data reduction to obtain *ResponseSurfaceSMPA.dat*.

Steps:

1. In *SMPAi.out**, delete all lines containing word “MESSAGE” and the empty line that follows it.
2. Copy *SMPAi.out* to *ResponseSurfaceSMPA.dat*.
3. Remove all lines with “MESSAGE” and surrounding empty lines.
4. Remove lines 1-227 and 2778-end of file; remove columns 5 and 6.
5. Copy column 5 between lines 228 and 2777 from files *SMPAi.out2* to *SMPAi.out20* and add as column 5-23 to file *ResponseSurfaceSMPA.dat*.
6. Open file *ResponseSurfaceSMPA.dat* in EXCEL and sort rows according to first three columns.
7. Insert new columns 4-7; column 1 is $\log(k)$, column 2 is $1/\alpha$, column 3 is percolation flux, columns 8-27 are the seep flow rates for 20 realizations. In file *SMPAi*, an adjustment factor of 10 should be imposed as part of unit conversion.
8. Column 4 = (average of columns 8-27)*10; this is the average seepage flux (kg/year/wp); the adjustment factor of 10 is multiplied to results.
9. Column 5 = (std. dev. of columns 8-27)*10; this is the standard deviation of the seepage flux.
10. Column 6 = column 4 / (5.5*5.1*column 3) * 100; this is the average seepage percentage.
11. Column 7 = column 5 / (5.5*5.1*column 3) * 100; this is the seepage percentage standard deviation.
12. Save Columns 1-7 as formatted text file to *ResponseSurfaceSMPA.prn*.

13. Copy *ResponseSurfaceSMPA.prn* to *ResponseSurfaceSMPA.dat*.
14. Replace results from runs with convergence failure with a seepage percentage of 100 percent and std. dev. of 14 percent.
15. Add following header for Tecplot plotting:
 - variables = “log(k [m²])” “1/α [Pa]” “Percolation [mm/year]” “Mean Seepage [kg/year/wp]” “Std. Dev. Seepage [kg/year/wp]” “Mean Seepage [%]” “Std. Dev. Seepage [%].”
 - ZONE i=15 j=10 k=17.

Table B-1. Portion of the EXCEL Spreadsheet *ResponseSurfaceSMPA.dat*

| log(k [m ²]) | 1/α [Pa] | Q [mm/year] | Mean Seepage [kg/year/WP] | Std. Dev. Seepage [kg/year/WP] | Mean Seepage [%] | Std. Dev. Seepage [%] |
|--------------------------|----------|-------------|---------------------------|--------------------------------|------------------|-----------------------|
| -14.00 | 100.00 | 1.00 | 27.73 | 4.09 | 98.86 | 14.59 |
| -14.00 | 100.00 | 5.00 | 138.92 | 20.55 | 99.05 | 14.65 |
| -14.00 | 100.00 | 10.00 | 277.90 | 41.19 | 99.07 | 14.68 |
| -14.00 | 100.00 | 20.00 | 555.87 | 82.54 | 99.09 | 14.71 |
| -14.00 | 100.00 | 50.00 | 1391.67 | 205.57 | 99.23 | 14.66 |
| -14.00 | 100.00 | 100.00 | 2793.55 | 406.70 | 99.59 | 14.50 |
| -14.00 | 100.00 | 200.00 | 5647.67 | 785.46 | 100.67 | 14.00 |
| -14.00 | 100.00 | 300.00 | 8549.04 | 1138.98 | 101.59 | 13.54 |
| -14.00 | 100.00 | 400.00 | 11501.48 | 1444.29 | 102.51 | 12.87 |
| -14.00 | 100.00 | 500.00 | 14438.54 | 1717.99 | 102.95 | 12.25 |
| -14.00 | 100.00 | 600.00 | 17465.25 | 2000.48 | 103.77 | 11.89 |
| -14.00 | 100.00 | 700.00 | 20002.63 | 3090.90 | 101.87 | 15.74 |
| -14.00 | 100.00 | 800.00 | 23071.27 | 2838.05 | 102.81 | 12.65 |
| -14.00 | 100.00 | 900.00 | 25411.46 | 3312.18 | 100.66 | 13.12 |
| -14.00 | 100.00 | 1000.00 | 27391.33 | 4644.34 | 97.65 | 16.56 |
| -14.00 | 200.00 | 1.00 | 26.14 | 4.21 | 93.21 | 15.00 |
| -14.00 | 200.00 | 5.00 | 136.40 | 20.51 | 97.26 | 14.62 |
| -14.00 | 200.00 | 10.00 | 275.20 | 40.73 | 98.11 | 14.52 |
| -14.00 | 200.00 | 20.00 | 553.39 | 81.32 | 98.64 | 14.49 |
| -14.00 | 200.00 | 50.00 | 1390.78 | 201.98 | 99.16 | 14.40 |
| -14.00 | 200.00 | 100.00 | 2791.65 | 395.09 | 99.52 | 14.09 |
| -14.00 | 200.00 | 200.00 | 5640.64 | 772.08 | 100.55 | 13.76 |
| -14.00 | 200.00 | 300.00 | 8535.17 | 1112.75 | 101.43 | 13.22 |
| -14.00 | 200.00 | 400.00 | 11470.97 | 1423.23 | 102.24 | 12.68 |
| -14.00 | 200.00 | 500.00 | 14390.11 | 1766.79 | 102.60 | 12.60 |
| -14.00 | 200.00 | 600.00 | 16614.64 | 3155.42 | 98.72 | 18.75 |

Table B-1. Portion of the EXCEL Spreadsheet *ResponseSurfaceSMPA.dat* (Continued)

| log(k [m²]) | 1/alpha [Pa] | Q [mm/year] | Mean Seepage [kg/year/WP] | Std. Dev. Seepage [kg/year/WP] | Mean Seepage [%] | Std. Dev. Seepage [%] |
|-----------------------------------|---------------------|------------------------|--------------------------------------|---|-----------------------------|----------------------------------|
| -14.00 | 200.00 | 700.00 | 18537.22 | 4460.73 | 94.41 | 22.72 |
| -14.00 | 200.00 | 800.00 | 19405.12 | 5588.98 | 86.48 | 24.91 |
| -14.00 | 200.00 | 900.00 | 20536.87 | 5452.22 | 81.35 | 21.60 |

NOTE: Of the thousands of simulation runs, the few nonconvergent runs were not used in the analysis. The results for these few nonconvergent runs were replaced with a seepage percentage of 100 percent and standard deviation of 14 percent. Validation was not impacted by nonconvergent runs because the results were replaced.

INTENTIONALLY LEFT BLANK

APPENDIX C

DATA REDUCTION STEPS FOR FIGURES 6-9 TO 6-11

Figures 6-9 to 6-11 discuss the seepage results in the form of seepage percentage. The seepage percentage is defined as the ratio of the seepage rate into a drift section to the percolation rate applied to the top of the model over the projected cross-sectional area of that drift section. It corresponds to simulated total seepage rates into a drift of 5.5 m diameter and 5.1 m length (design drawings 800-IED-MGR0-00201-000-00B (BSC 2004 [DIRS 168489]) and 800-IED-WIS0-00205-000-00C (BSC 2004 [DIRS 167758])). The data reductions were performed using standard functions of the exempt software EXCEL (2000 SR-1). Detailed simulation results were submitted to TDMS (Output-DTN: LB0304SMDCREV2.002). The following steps explain the data reduction for seepage results, using worksheets *fig6-10_1.xls* and *fig6-10_2.xls* as examples; excerpts are shown in Tables C-1 and C-2.

Steps:

1. Generate a new file *qq** from *SMPAi.out** by using command “`grep “-0.1200000E+02 0.5000000E+03” SMPAi.out* > qq*.`”
2. Copy *qq** to *qqq.dat*.
3. Open file *qqq.dat* and save as *fig6-10_1* in EXCEL and delete columns A, B, E, and F.
4. Insert new column 2; column 1 is $\log(k)$, column 3 is the seepage flow rate.
5. Insert new row 1 and add header.
6. Column 2 = column 2 * 10 / (5.5*5.1* 200) * 100; this is the seepage percentage; the factor of 10 is an adjustment factor as part of scaling specification required in the ITOUGH code, and 200 is the percolation flux.
7. Save *fig6-10_1* as formatted text file.
8. Open EXCEL file *fig6-10_1* and save as *fig6-10_2* in EXCEL.
9. Copy rows C17 to C31 as D2 to D16; C32 to C46 as E2 to E16; ... C287 to C301 as V2 to V16; columns C to V are 20 realizations.
10. Column 2 = (average of columns C-V)*10 / (5.5*5.1*200) * 100; this is the average seepage percentage.
11. Save *fig6-10_2* as formatted text file.
12. Keep columns 1 and 2 in the text files *fig6-10_1* and *fig6-10_2* and save together as a *fig6-10* for Tecplot plotting.

Table C-1. Portion of the EXCEL Spreadsheet *fig6-10_1*

| Q_p (mm/year) | Seep.(%) | Real. |
|-----------------|----------|----------|
| 1.00E+00 | 0.00 | 1.00E-50 |
| 5.00E+00 | 0.00 | 1.00E-50 |
| 1.00E+01 | 0.16 | 4.60E-02 |
| 2.00E+01 | 5.44 | 3.05E+00 |
| 5.00E+01 | 31.65 | 4.44E+01 |
| 1.00E+02 | 42.98 | 1.21E+02 |
| 2.00E+02 | 50.59 | 2.84E+02 |
| 3.00E+02 | 54.40 | 4.58E+02 |
| 4.00E+02 | 56.90 | 6.38E+02 |
| 5.00E+02 | 58.78 | 8.24E+02 |
| 6.00E+02 | 60.13 | 1.01E+03 |
| 7.00E+02 | 61.25 | 1.20E+03 |
| 8.00E+02 | 62.12 | 1.39E+03 |
| 9.00E+02 | 62.90 | 1.59E+03 |
| 1.00E+03 | 63.59 | 1.78E+03 |
| 1.00E+00 | 0.00 | 1.00E-50 |
| 5.00E+00 | 0.00 | 1.00E-50 |
| 1.00E+01 | 0.01 | 4.08E-03 |
| 2.00E+01 | 19.01 | 1.07E+01 |
| 5.00E+01 | 50.01 | 7.01E+01 |
| 1.00E+02 | 73.56 | 2.06E+02 |
| 2.00E+02 | 87.52 | 4.91E+02 |
| 3.00E+02 | 92.69 | 7.80E+02 |
| 4.00E+02 | 96.09 | 1.08E+03 |

Table C-2. Portion of the EXCEL Spreadsheet *fig6-10_2*

| Q_p (mm/year) | Mean Seep. (%) | Real.1 | Real. 2 | Real. 3 | Real. 4 | Real. 5 | Real. 6 | Real. 7 |
|-----------------|----------------|----------|----------|----------|----------|----------|----------|----------|
| 1.00E+00 | 0.00 | 1.00E-50 |
| 5.00E+00 | 0.22 | 1.00E-50 |
| 1.00E+01 | 3.82 | 4.60E-02 | 4.08E-03 | 9.06E-02 | 7.41E-02 | 6.82E-01 | 1.00E-50 | 3.81E-01 |
| 2.00E+01 | 14.55 | 3.05E+00 | 1.07E+01 | 6.66E+00 | 2.93E+00 | 1.28E+01 | 5.24E+00 | 3.50E+00 |
| 5.00E+01 | 38.09 | 4.44E+01 | 7.01E+01 | 4.99E+01 | 6.60E+01 | 7.29E+01 | 4.56E+01 | 3.31E+01 |
| 1.00E+02 | 55.27 | 1.21E+02 | 2.06E+02 | 1.50E+02 | 2.01E+02 | 1.94E+02 | 1.45E+02 | 1.22E+02 |
| 2.00E+02 | 68.65 | 2.84E+02 | 4.91E+02 | 3.69E+02 | 4.83E+02 | 4.45E+02 | 3.79E+02 | 3.54E+02 |
| 3.00E+02 | 74.55 | 4.58E+02 | 7.80E+02 | 5.97E+02 | 7.68E+02 | 7.00E+02 | 6.20E+02 | 5.95E+02 |
| 4.00E+02 | 78.19 | 6.38E+02 | 1.08E+03 | 8.28E+02 | 1.06E+03 | 9.73E+02 | 8.68E+02 | 8.44E+02 |
| 5.00E+02 | 80.63 | 8.24E+02 | 1.38E+03 | 1.06E+03 | 1.36E+03 | 1.25E+03 | 1.12E+03 | 1.10E+03 |
| 6.00E+02 | 82.39 | 1.01E+03 | 1.68E+03 | 1.30E+03 | 1.66E+03 | 1.53E+03 | 1.37E+03 | 1.36E+03 |
| 7.00E+02 | 83.75 | 1.20E+03 | 1.98E+03 | 1.54E+03 | 1.96E+03 | 1.81E+03 | 1.62E+03 | 1.62E+03 |
| 8.00E+02 | 98.86 | 1.39E+03 | 2.29E+03 | 1.78E+03 | 2.26E+03 | 2.10E+03 | 1.87E+03 | 1.88E+03 |
| 9.00E+02 | 85.74 | 1.59E+03 | 2.59E+03 | 2.02E+03 | 2.57E+03 | 2.38E+03 | 2.13E+03 | 2.14E+03 |
| 1.00E+03 | 86.51 | 1.78E+03 | 2.89E+03 | 2.25E+03 | 2.88E+03 | 2.67E+03 | 2.38E+03 | 2.40E+03 |

APPENDIX D
DATA REDUCTION STEPS FOR FIGURES OF ROCKFALL

Section 6.6.3 discusses the seepage results of rockfall. The seepage percentage is defined as the ratio of the seepage rate into a drift section to the percolation rate applied to the top of the model over the projected cross-sectional area of that drift section. It corresponds to simulated total seepage rates into a drift of 5.5 m diameter and 5.1 m length (design drawings 800-IED-MGR0-00201-000-00B (BSC 2004 [DIRS 168489]) and 800-IED-WIS0-00205-000-00C (BSC 2004 [DIRS 167758])). The data reductions were performed using standard functions of the exempt software EXCEL (2000 SR-1). Detailed simulation results were submitted to TDMS (Output-DTN: LB0304SMDCREV2.002). The following steps explain the data reduction for seepage results, using worksheets *fig6-17_1.xls* and *fig6-17_2.xls* as examples; excerpts are shown in Tables D-1 and D-2.

Steps:

1. In *SMPAi.outmnw**, delete all lines containing word “MESSAGE” and the empty line that follows it and only keep the seepage results.
2. Copy *SMPAi.outmnw** to *SMPAioutmnw.dat*.
3. Open file to *SMPAioutmnw.dat* and save as *fig6-17_1* in EXCEL and delete columns 1, 2, 5, and 6.
4. Insert new column 2; column 1 is log(k), column 3 is the seepage flow rate.
5. Insert row 1 and add header.
6. Column 2 = column 3 *10 / (5.5*5.1* 200) * 100; this is the seepage percentage; the factor of 10 is an adjustment factor as part of scaling specification required in the ITOUGH code, and 200 is the percolation flux.
7. Save *fig6-17_1* as formatted text file.
8. Open EXCEL file *fig6-17_1* and save as *fig6-17_2* in EXCEL.
9. Open EXCEL file *fig6-17_2* and copy rows C17 to C31 as D2 to D16; C32 to C46 as E2 to E16; ... C137 to C151 as L2 to L16; columns C to L are 10 realizations.
10. Column 2 = (average of columns C-L)*10 / (5.5*5.1*200) * 100; this is the average seepage percentage.
11. Save *fig6-17_2* as formatted text file.
12. Use above steps to calculate the average seepage percentage for base case on data *SMPAimnb.dat* and get formatted text file *fig_mnbmean*.
13. Keep columns A and B in the text files *fig6-17_1*, *fig6-17_2*, and *fig_mnbmean* and save together as a *fig6-17* for Tecplot plotting.

Table D-1. Portion of the EXCEL Spreadsheet *fig6-17_1*

| Q_p(mm/year) | Seep. (%) | Seep. |
|-------------------------------|------------------|--------------|
| 1.00E+00 | 0.00 | 1.00E-50 |
| 5.00E+00 | 0.00 | 1.00E-50 |
| 1.00E+01 | 0.00 | 1.00E-50 |
| 2.00E+01 | 0.00 | 1.00E-50 |
| 5.00E+01 | 0.00 | 1.00E-50 |
| 1.00E+02 | 2.19 | 6.13E+00 |
| 2.00E+02 | 21.69 | 1.22E+02 |
| 3.00E+02 | 30.40 | 2.56E+02 |
| 4.00E+02 | 35.33 | 3.96E+02 |
| 5.00E+02 | 38.62 | 5.42E+02 |
| 6.00E+02 | 40.93 | 6.89E+02 |
| 7.00E+02 | 42.93 | 8.43E+02 |
| 8.00E+02 | 44.66 | 1.00E+03 |
| 9.00E+02 | 46.08 | 1.16E+03 |
| 1.00E+03 | 47.27 | 1.33E+03 |
| 1.00E+00 | 0.00 | 1.00E-50 |
| 5.00E+00 | 0.00 | 1.00E-50 |
| 1.00E+01 | 0.00 | 1.00E-50 |
| 2.00E+01 | 0.00 | 1.00E-50 |
| 5.00E+01 | 0.00 | 1.00E-50 |
| 1.00E+02 | 8.54 | 2.39E+01 |

Table D-2. Portion of the EXCEL Spreadsheet *fig6-17_2*

| Q_p(mm/year) | Mean Seep (%) | Real.1 | Real.2 | Real.3 | Real.4 | Real.5 | Real.6 | Real.7 | Real.8 |
|-------------------------------|----------------------|---------------|---------------|---------------|---------------|---------------|---------------|---------------|---------------|
| 1.00E+00 | 0.00 | 1.00E-50 |
| 5.00E+00 | 0.00 | 1.00E-50 |
| 1.00E+01 | 0.00 | 1.00E-50 |
| 2.00E+01 | 0.00 | 1.00E-50 |
| 5.00E+01 | 2.62 | 1.00E-50 | 1.00E-50 | 6.17E+00 | 1.00E-50 | 2.29E+00 | 1.00E-50 | 1.00E-50 | 1.64E+01 |
| 1.00E+02 | 12.59 | 6.13E+00 | 2.39E+01 | 4.72E+01 | 1.73E+01 | 7.56E+01 | 3.11E+01 | 9.12E+00 | 7.03E+01 |
| 2.00E+02 | 31.75 | 1.22E+02 | 1.88E+02 | 1.63E+02 | 1.68E+02 | 2.34E+02 | 1.83E+02 | 1.09E+02 | 2.20E+02 |
| 3.00E+02 | 41.60 | 2.56E+02 | 4.05E+02 | 3.03E+02 | 3.66E+02 | 4.10E+02 | 3.39E+02 | 2.36E+02 | 4.14E+02 |
| 4.00E+02 | 48.09 | 3.96E+02 | 6.40E+02 | 4.66E+02 | 5.80E+02 | 6.11E+02 | 5.05E+02 | 3.78E+02 | 6.26E+02 |
| 5.00E+02 | 52.88 | 5.42E+02 | 9.03E+02 | 6.43E+02 | 8.07E+02 | 8.24E+02 | 6.88E+02 | 5.34E+02 | 8.46E+02 |
| 6.00E+02 | 56.77 | 6.89E+02 | 1.17E+03 | 8.30E+02 | 1.05E+03 | 1.06E+03 | 8.78E+02 | 7.05E+02 | 1.08E+03 |
| 7.00E+02 | 60.05 | 8.43E+02 | 1.44E+03 | 1.03E+03 | 1.31E+03 | 1.29E+03 | 1.08E+03 | 8.79E+02 | 1.33E+03 |
| 8.00E+02 | 62.80 | 1.00E+03 | 1.72E+03 | 1.23E+03 | 1.58E+03 | 1.53E+03 | 1.29E+03 | 1.07E+03 | 1.59E+03 |
| 9.00E+02 | 65.12 | 1.16E+03 | 2.00E+03 | 1.44E+03 | 1.86E+03 | 1.77E+03 | 1.50E+03 | 1.29E+03 | 1.85E+03 |
| 1.00E+03 | 67.12 | 1.33E+03 | 2.28E+03 | 1.65E+03 | 2.14E+03 | 2.02E+03 | 1.72E+03 | 1.51E+03 | 2.10E+03 |